DTU Library

Design and Evaluation of An Intranasal Carbohydrate-based Vaccine against Streptococcus pneumoniae Serotype 12F

Wei, Peng

Link back to DTU Orbit

Design and Evaluation of An Intranasal Carbohydrate-based Vaccine against *Streptococcus pneumoniae* Serotype 12F

A THESIS PRESENTED
BY
PENG WEI
魏朋 (CHINESE NAME)
TO
THE DEPARTMENT OF CHEMISTRY
FOR THE DEGREE OF
DOCTOR OF PHILOSOPHY

TECHNICAL UNIVERSITY OF DENMARK
KONGENS LYNGBY, DENMARK
SEPTEMBER 2023

Supervisor: Prof. Mads H. Clausen
Cosupervisor: Assoc. Prof. Jonas R. Henriksen

Peng Wei

Design and Evaluation of An Intranasal Carbohydrate-based Vaccine against *Streptococcus pneumoniae* Serotype 12F

ABSTRACT

Diseases caused by *S. pneumoniae* are the leading cause of child mortality, estimated to kill 1,000,000 children yearly. As antibiotic resistance of *S. pneumoniae* is rising, vaccination programs remain the most recommended solution. However, the existing pneumococcal polysaccharides vaccine (PPSV) proved only to induce T-independent immunity, and cold chain dependence of the protein conjugate vaccine (PCV) impedes its promotion in developing countries, where infections are most problematic. Affordable and efficient vaccines against pneumococcus are therefore in high demand. Here, we present an innovative intranasal vaccine Lipo$^+$CPS12F&αGC, containing the capsular polysaccharides of *S. pneumoniae* 12F and the iNKT agonist α-galactosylceramide in cationic liposomes. The vaccine effectively activated iNKTs and promoted B cell maturation, stimulated the production of affinity-matured IgA and IgG in both the respiratory tract and systemic blood, and displayed sufficient protection efficacy both *in vivo* and *in vitro*. The novel vaccine is a promising cost-effective solution against pneumococcus, which can potentially be applied to other carbohydrate antigens covering more serotypes and pathogens.

Vejleder: Prof. Mads H. Clausen
Medvejleder: Assoc. Prof. Jonas R. Henriksen

Peng Wei

Design og Evaluering af En Intranasal Kulhydratbaseret Vaccine mod *Streptococcus pneumoniae* Serotype 12F[*]

Resumé

Sygdomme forårsaget af *S. pneumoniae* er den største årsag til børnedødelighed, hvor det er estimeret til at dræbe 1.000.000 børn årligt. Som antibiotikaresistensen af *S. pneumoniae* stiger, er vaccinationsprogrammer fortsat den mest anbefalede løsning. Den eksisterende pneumokokpolysakkaridvaccine (PPSV) har imidlertid vist sig kun at inducere T-uafhængig immunitet og koldkædeafhængighed af proteinkonjugatvaccinen (PCV) hæmmer dens promovering i udviklingslande, hvor infektioner er mest problematiske. Billige og effektive vacciner mod pneumokokker er derfor meget efterspurgte. Vi præsenterer her en innovativ intranasal vaccine Lipo$^+$CPS12F&αGC, der indeholder kapselpolysakkarider af *S. pneumoniae* 12F og iNKT-agonisten α-galactosylceramid i kationiske liposomer. Vaccinen aktiverede effektivt iNKT og fremmede B-cellemodning, stimulerede produktionen af affinitetsmodnet IgA og IgG i både luftveje og systemisk blod og udviste tilstrækkelig beskyttelseseffektivitet både *in vivo* og *in vitro*. Den nye vaccine er en lovende omkostningseffektiv løsning mod pneumokokker, som potentielt kan anvendes på andre kulhydratantigener der dækker flere serotyper og patogener.

---

[*]Dr. Faranak Nami at DTU Chemistry helped with the Danish translation.

Contents

Listing of Abbreviations

Ab	antibody
ADCC	antigen-dependent cell cytotoxicity
ADCP	antigen-dependent cell phagocytosis
AF4	asymmetrical flow field-flow fractionation
ANOVA	analysis of variance
ATCC	The American Type Culture Collection
BALF	bronchoalveolar lavage fluids
BSA	bovine serum albumin
CBA	cytometric bead array
CDC	complement-dependent cytotoxicity
CDCP	complement-dependent cell phagocytosis
CFU	colony-forming units
CPS	capsular polysaccharide
CRM197	cross-reactive material 197

DAB	3,3'-diaminobenzidine
DF	degrees of freedom
DLS	dynamic light scattering
DMF	N,N-dimethylformamide
DMSO	dimethyl sulfoxide
DSPC	1,2-distearoyl-*sn*-glycero-3-phosphocholine
DT	diphtheria toxoid
DSTAP	1,2-stearoyl-3-trimethylammonium-propane
ELISA	enzyme-linked immunosorbent assay
eV	an electron volt
FBS	fetal bovine serum
FCM	flow cytometry
fg	femto-gram
FMO	fluorescence minus one
g	gram or gravitational constant
G	gauge
GDP	gross domestic product
GMP	good manufacturing practices
HBSS	Hanks' balanced salt solution
HEPES	4-(2-hydroxyethyl)-1-piperazineethanesulfonic acid
HI	heat-inactivated
HRP	horseradish peroxidase
iBALT	inducible bronchus-associated lymphoid tissue

ICP-MS	inductively coupled plasma mass spectrometry
ICP-OES	inductively coupled plasma optical emission spectroscopy
IFN	interferon
IgM/A/G/D	immunoglobulin M/A/G/D
IHC	immunohistochemistry
IL	interleukin
i.m.	intramuscular
i.n.	intranasal
iNKT cell	semi-invariant natural killer T cell
i.p.	intraparitoneal
IPD	invasive pneumococcal disease
K_d	binding kinetic
kDa	kilo-dalton
kg	kilo-gram
KLH	keyhole limpet hemocyanin
L	liter
LC	liquid chromatography
Log	logarithm
M	molar
MALDI-TOF MS	matrix-assisted laser desorption ionization time-of-flight mass spectrometry
MALS	multi-angle light scattering
mbar	milli-bar

MDR	multi-drug resistance
MFI	medium fluorescence intensity
MHC	major histocompatibility complex
min	minute
mL	milli-liter
mM	milli-molar
mOsm	milli-osmole
MRM	multiple reaction monitoring
mV	milli-volt
Mw	molecular weight
NALT	nasopharynx-associated lymphoid tissue
NICE	Nist's integrated colony enumerator
NKT_{FH} cell	NKT follicular helper cell
nm	nano-meter
OD	optical density
OMIP	optimized multi-color immunofluorescence panel
OPKA	opsonophagocytic killing assay
P	the probability for null hypothesis
PAMP	pathogen-associated molecular pattern
PBS	phosphate-buffered saline
PBST	phosphate-buffered saline with Tween™ 20
PCR	polymerase chain reaction
PCV	pneumococcal conjugate vaccine

PES	polyethersulfone
PNA	peanut agglutinin
PPSV	pneumococcal polysaccharides vaccine
PspA	pneumococcal surface protein A
PVDF	polyvinylidene fluoride
R^2	coefficient of determination
RBCs	red blood cells
rpm	revolutions per minute
RP-UPLC-MS/MS	reverse-phase ultra-performance liquid chromatography-tandem mass spectrometry
RPMI 1640 medium	Roswell Park Memorial Institute 1640 medium
s.c.	subcutaneous
SEC	size-exclusion chromatography
SEM	standard error of the mean
S. pneumoniae	*Streptococcus pneumoniae*
SSM	spillover spreading matrix
t-BuOH	*tert*-butanol
THYA plate	Todd-Hewitt broth with 0.5 % (w/v) yeast extract agar plate
THY broth	Todd-Hewitt broth with 0.5 % (w/v) yeast extract
TMB	3,3',5,5'-tetramethylbenzidine
TQMS	triple quadrupole mass spectrometer
TT	tetanus toxoid
T.T.C.	triphenyltetrazolium chloride

v/v	volume per volume
w/v	weight per volume
w/w	weight per weight
αGC	α-galactosylceramide
$\lambda_{ex,\ 535\ nm}$	excitation wavelength at 535 nm
$\lambda_{em,\ 587\ nm}$	emission wavelength at 587 nm
μL	micro-liter
°C	degree Celsius

Listing of figures

For those who believe in the power of science.

Acknowledgments

為天地立心，

為生民立命，

為往聖繼絕學，

為萬世開太平。

張載（北宋）

1

Introduction

Figure 1.1: Pneumococcus, from serotype to CPS type. a) Prince Valdemar of Denmark (1858 – 1939) died from pneumonia. The portrait was taken in 1936 and retrieved from the Agence de presse Meurisse[1]. **b)** The ineffectiveness of antiserum 9N and 9L treatment on Prince Valdemar led to the discovery of *S. pneumoniae* 9V, named after him. **c)** Techniques for identifying pneumococcus upgraded from seroreactivity to capsular polysaccharide structure and gene sequence. The illustration was created with BioRender.

In 1939, Prince Valdemar of Denmark (Figure 1.1 a) was diagnosed with pneumonia. By that time, researchers already knew *Streptococcus pneumoniae*, or pneumococcus, was the main pathogen responsible for this disease, and the bacteria virulence was closely related to the capsular polysaccharide (CPS, Figure 1.2 right). Also, pneumococcus was not homogeneous, as isolated cultures displayed different morphology after specific antiserum incubation (Figure 1.2 left). According to its seroreactivity, the bacteria was categorized into 32 serotypes at that time[2].

A further diagnosis determined the Prince was infected by the pneumococcus belonging to serotype 9. At that time, antiserum treatment was the most effective option available; therefore, the Prince re-

ceived the antiserum (Figure 1.1 b) 9L from the Lederle Lab (now part of Pfizer) and 9N from the New York State Lab (now the Wadsworth Center). Regrettably, neither antiserum proved effective, leading to the Prince's passing in that same year. Following studies discovered that the strain infected the Prince differed from the ones producing the antiserum. In memory of the Prince, the newly discovered strain was named "9V"[3].
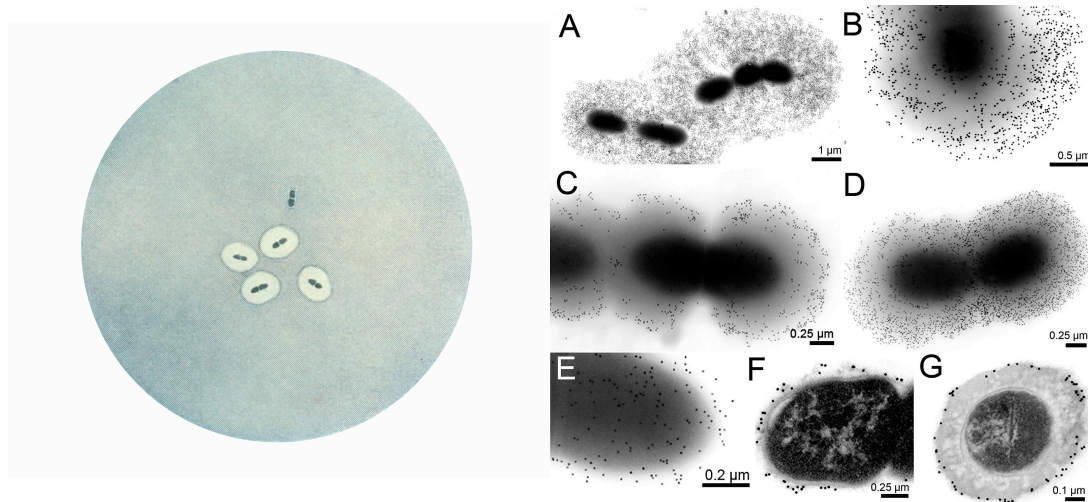
Figure 1.2: *Streptococcus pneumoniae* displayed positive (capsular swelling) and negative (no capsule) results in the Quellung test (left, retrieved from the Public Health Image Library #2113[4]) and visualization of pneumococcus capsular polysaccharides by gold nanoparticles under an electron microscope (right, retrieved from a published study[5]).

The case of the Prince highlighted the need for a more accurate method to identify pneumococcus. Later research revealed that the seroreactivity of pneumococcus was determined by the unique structure of the bacterial capsular polysaccharide repeat unit; thus, the classification system shifted from serotype to CPS type (Figure 1.1 c). Currently, gene sequencing using real-time PCR is a faster and more reliable method to identify pneumococcus in the laboratory[6].

By now, more than 100 CPS types of pneumococcus have been documented by the Global Pneumococcal Sequencing Project[7]. Sometimes, we still term them as serotypes by traditions. Based on their shared serum reactivity, some serotypes were combined as serogroup. While the cross-reactivity

is frequent, it cannot be presumed[8], which explains the therapy failure of the Prince. Studies from Denmark and the United States led to two different pneumococcus nomenclature systems[9]. Since the last century, the Danish system has been widely accepted by academics worldwide.

1.2 Carbohydrate Vaccines, Sweet Solutions to the Sticky Situation
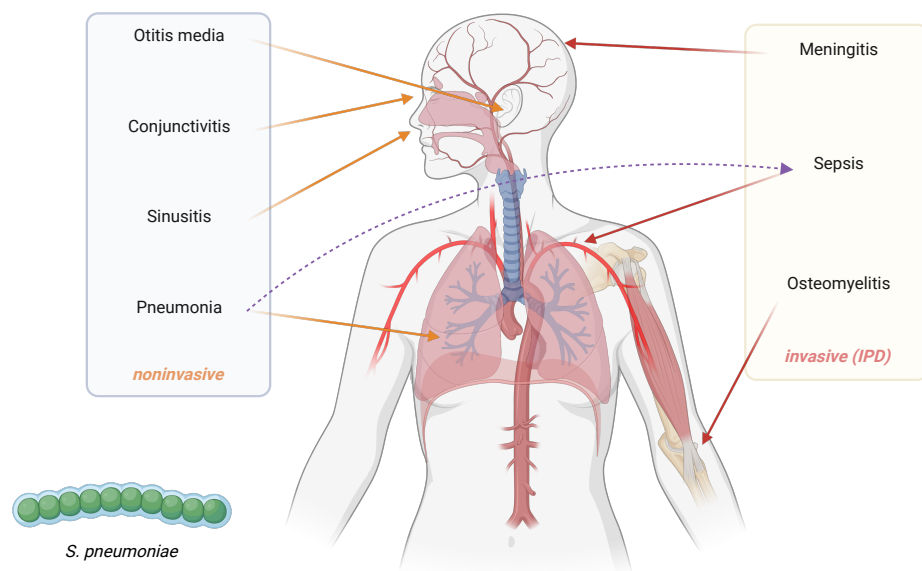
Figure 1.3: Pneumococcal diseases include noninvasive ones like otitis media, conjunctivitis, sinusitis, and pneumonia, as well as invasive ones like meningitis, sepsis, and osteomyelitis. The illustration was created with BioRender.

Pneumococcus is transmitted among the population by respiratory droplets and normally resides asymptomatically in the human upper respiratory tract, where it downregulates capsule production to assist its binding to the epithelium[10]. The carrying ratio of pneumococcus can be as high as 60 % in specific populations, such as school-aged children and the military[11]. In some hosts (Figure 1.3), primarily children, elderly, and immunity-compromised individuals, the pneumococcus will resume the capsule expression to form biofilm and escape phagocytosis clearance, expand into deeper places,

such as the lower respiratory tract and bloodstream, and finally causes both noninvasive (pneumonia, otitis media, sinusitis, and conjunctivitis) and invasive diseases (IPDs, such as meningitis, sepsis, and osteomyelitis)[12].

Figure 1.4: Pneumonia is the leading cause of child deaths. A comparison between the causes of child mortality on a global scale in 1990 and 2017, retrieved from Our World in Data[13].

Currently, pneumococcus-related diseases are a significant concern for global public health. Importantly, they are the leading causes of child mortality, estimated to kill 1,000,000 children per year by the World Health Organization[14], including 809,000 pneumonia deaths (Figure 1.4).

Death rate from pneumonia for children vs. GDP per capita, 2019

Death rate from pneumonia and other lower respiratory diseases in children under 5 per 100,000 children. Gross domestic product (GDP) per capita is measured in current international-$.
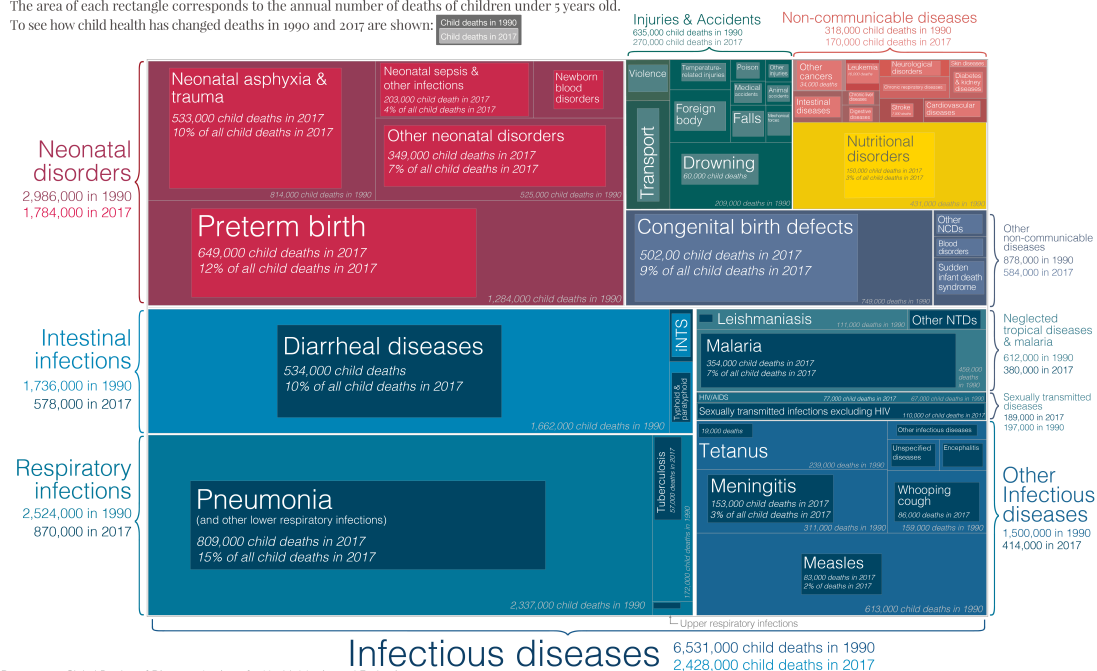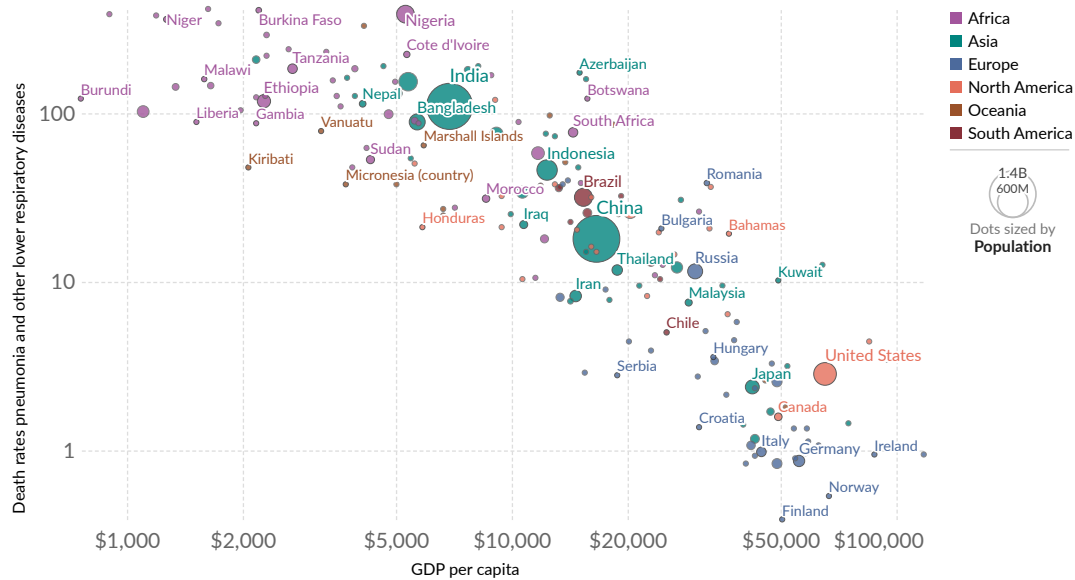
Source: IHME, Global Burden of Disease (2019); Data compiled from multiple sources by World Bank
OurWorldInData.org/pneumonia • CC BY

Figure 1.5: Negative correlation between children's pneumonia mortality and economic development degree. The death rate from pneumonia for children vs. GDP per capita, 2019, retrieved from Our World in Data[15].

The death rate from pneumonia for children negatively correlates with the economic development degree (Figure 1.5), highlighting the need for effective and affordable treatments.
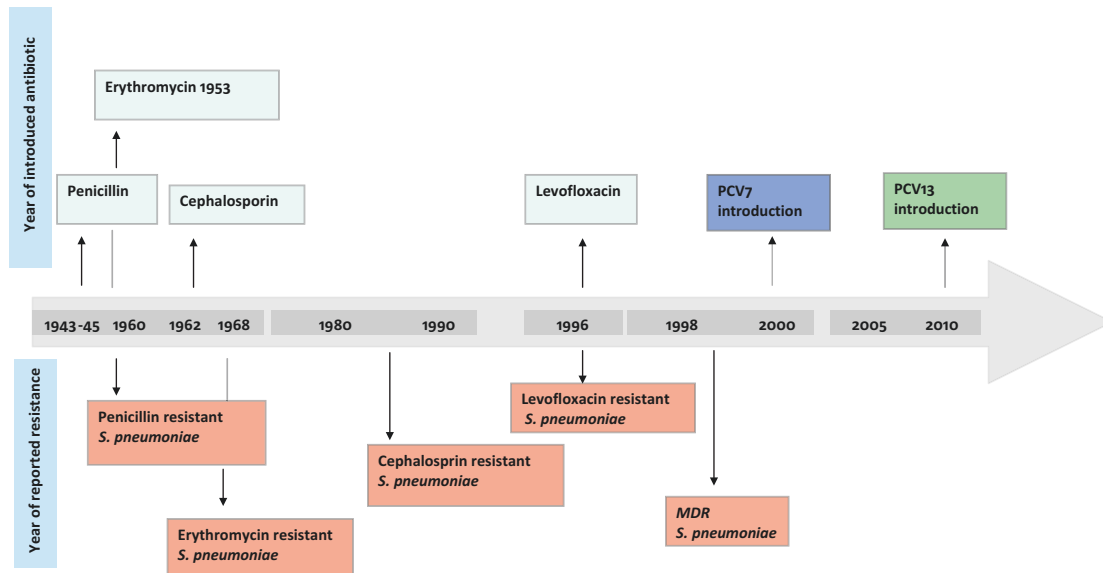
Figure 1.6: Timeline of antibiotic resistance of *Streptococcus pneumoniae*, retrieved from a published study [16].

The development of effective vaccines against pneumococcus commenced in the early 20th century, with the first clinical trial conducted in 1911 [17]. However, since the discovery of penicillin, antibiotic treatment has become the most commonly applied therapy against pneumococcal diseases, which led to the decline in efforts for pneumococcal vaccine development. Unfortunately, this bacteria has developed resistance against all antibiotics except vancomycin (Figure 1.6), and in many countries, macrolide antimicrobials, penicillins, and cephalosporins are no longer assumed effective [12]. The significant challenge of multi-drug resistance (MDR) has made developing effective vaccines reconsidered as the most promising method against pneumococcus.
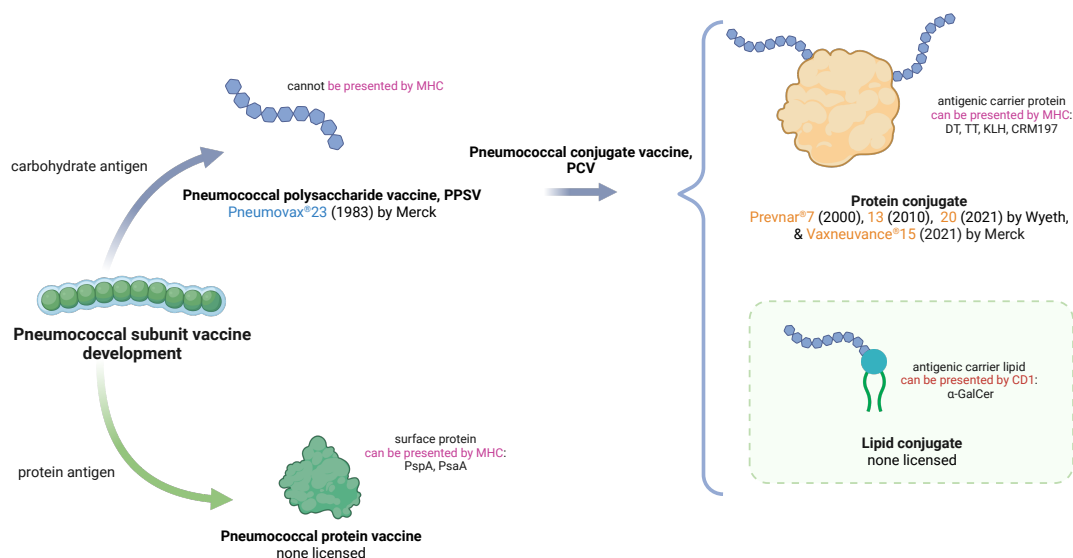
Figure 1.7: Strategies for developing pneumococcal subunit vaccines. The illustration was created with BioRender.

Pneumococcal subunit vaccines can be broadly divided into two categories based on the type of antigen used: protein and carbohydrate (Figure 1.7 left). Pneumococcal surface protein A (PspA) [18,19,20,21,22,23] is the most studied protein antigen candidate, but none has been licensed. In contrast, the capsular polysaccharide is believed to be a more promising antigen, as it is the most virulent component that covers the bacteria. Merck developed the first pneumococcal polysaccharide vaccine (PPSV), Pneumovax®23 [24], licensed in 1983. The vaccine comprised a mixture of capsular polysaccharides from 23 different serotypes of pneumococcus without adjuvant. However, the classical major histocompatibility complex (MHC) molecule cannot present carbohydrate-based antigens, which is essential for inducing T-dependent adaptive immunity. As a result, the vaccine was of low immunogenicity (56 % effectiveness [25]) and unable to bring immunological memory.

To break this restriction, the carbohydrate antigens can be conjugated to a carrier protein (e.g., CRM197, a detoxified variant of diphtheria toxin, Figure 1.7 top right) [26]. Based on this strategy,

Prevnar®s (7^{27}, 13^{28}, and 20^{29}, which was licensed in 2007, 2010, and 2021; developed by Wyeth, now part of Pfizer), Vaxneuvance™ 15^{30} (licensed in 2021, developed by Merck) and some preclinical vaccines [31,32,33,34,35,36] were developed. Clinical studies showed that Prevnar®13, the currently most widely applied one, had overall improved efficacy but still showed limitations in older individuals (46 % risk reduction [37]).

Characteristics of iNKT:

1. "one-size fits all": conserved CD1 (iNKT TCR ligand) vs. polymorphic MHC

2. faster response: iNKT proliferates and differentiates into functional phenotypes within hours (days for normal T); iNKT$_{FH}$ helps the germinal centers' formation by day 3 (10 days for normal T$_{FH}$)

3. bridge between innate ("PAMPs" like) and adaptive ("T$_H$" phenotype) immunities
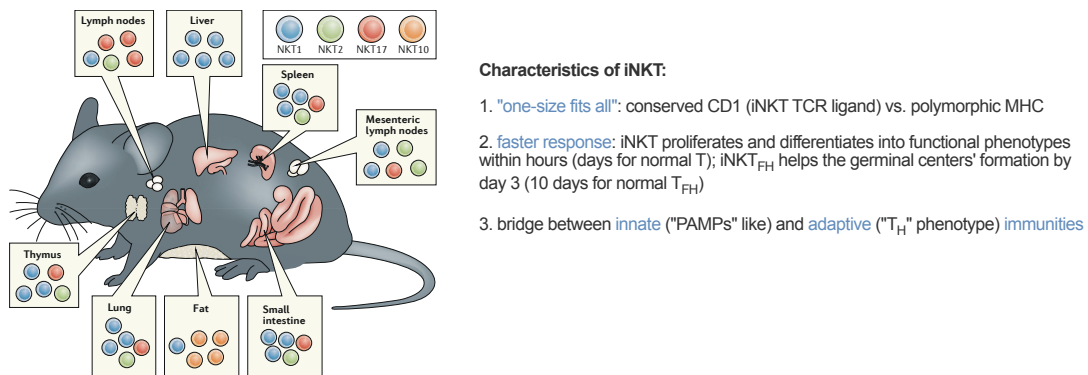
Figure 1.8: iNKTs' tissue distribution and immune characteristics in mice. The left illustration and right features were retrieved and summarized from the published studies[38,39,40].

Another approach is to link the carbohydrate antigen to an immunogenic lipid (Figure 1.7 bottom right), such as α-galactosylceramide (αGC), which can activate semi-invariant natural killer T (iNKT, Figure 1.8) cells and further initiate the iNKT-assisted adaptive immune responses. Compared with the classical T cell-dependent immune responses, targeting iNKT holds several advantages. Firstly, iNKTs are "pre-primed" and respond faster than normal T cells. While T$_{FH}$ helps form germinal centers in 10 days, NKT$_{FH}$ only takes 3 days[38]. Secondly, activating iNKTs will result in a universal effect, as its ligand CD1d (CD1a–e in humans) is more conserved in structure than the conventional MHC molecule[41]. Most importantly, iNKT cells are capable of activating innate immunities by the "pathogen-associated molecular patterns (PAMPs) like" functions and also contributing to adaptive immunities through differentiating into "T-helper" phenotypes. The bridging capability

between innate and adaptive immunity can result in a synergistic effect and improve bacterial clearance efficacy[40]. Several semisynthetic vaccines[42,43,44,45] based on this strategy have shown promising results. However, their fabrication processes contain chemical synthesis, which increases the cost and restricts availability to vulnerable populations in low-income areas.

Notably, all currently licensed pneumococcal vaccines require to be stored and delivered within a cold chain, which can account for as much as 50 % of the total cost[46]. This cost further presents a noticeable obstacle to their distribution in developing countries, where preventive vaccination is most important.

1.3   Intranasal Vaccination, activating NALT and iBALT
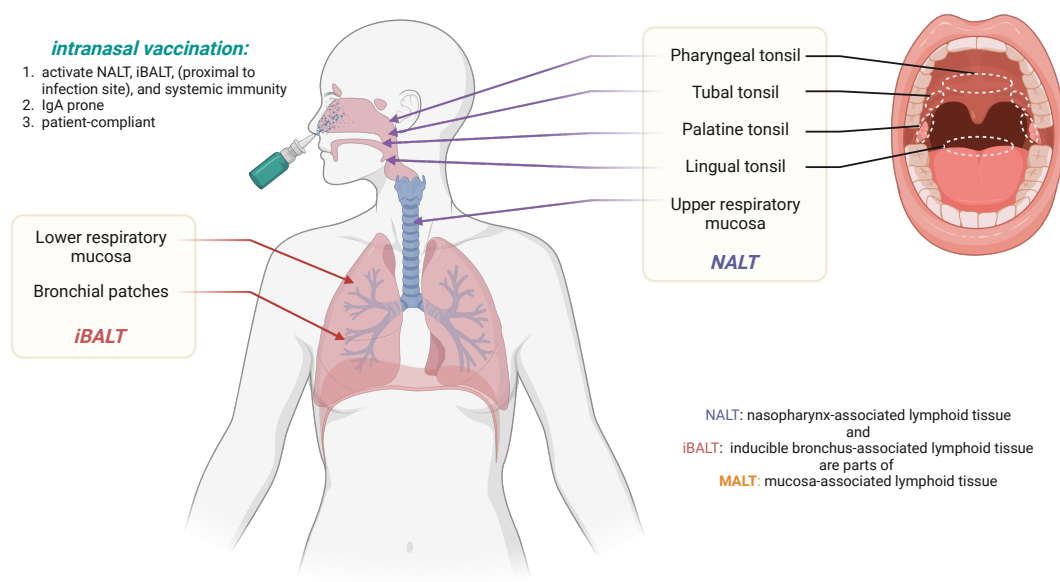
Figure 1.9: NALT, iBALT, and intranasal vaccination. The illustration was created with BioRender.

The currently licensed Pneumovax® and Prevnar®s are administered through parenteral ways, such as intramuscular (*i.m.*) or subcutaneous (*s.c.*) injection, which predominantly elicit systemic immune

responses. However, it is mucosal immunity that serves as the first line to block pathogen infection. Mucosa-associated lymphoid tissue (MALT) can be classified into several segments based on location, with nasopharynx- and inducible bronchus-associated lymphoid tissues (NALT and iBALT) closely related to pneumococcus respiratory infections (Figure 1.9). In systemic immunity, IgG plays a pivotal role by mediating complement-dependent cytotoxicity (CDC) and antigen-dependent cell cytotoxicity (ADCC), which can release toxins such as pneumolysin, resulting in inflammation and damage. In contrast, mucosal immunity mainly functions with IgA, which neutralizes and agglutinates the pathogen and clears it through ciliary motion, making it a safer and more suitable target to combat pneumococcus. Intranasal (*i.n.*) vaccination is an effective localized immunization approach to activate the NALT and iBALT. Compared with *i.m.* and *s.c.* routes, it is also more compliant with patients. To date, there are a lot of studies for pneumococcal intranasal vaccines [47,48,49,50,51,52,53,54,55]; almost all used protein-based antigens, but none has been authorized.

1.4 STUDY DESIGN

This study presents proof of principle for a cost-effective vaccine, Lipo⁺CPS12F&αGC, comprising the capsular polysaccharide of *S. pneumoniae* 12F as antigen and the iNKT agonist αGC as "adjuvant" in cationic liposomes. The antigen was extracted from cultured bacteria without additional chemical synthesis, the two components were co-delivered in easily fabricated cationic liposomes (different from the glycolipids conjugate strategy in Figure 1.7 bottom right), and the working formulation can be stored safely at room temperature for a minimum of 3 weeks. These features help reduce costs and simplify logistics. Moreover, our vaccine can be intranasally (*i.n.*) applied with the help of the cationic liposome formulation. This immunization route is more patient-compliant and effective in stimulating the local respiratory mucosal immune systems, which are proximal to infection sites.

Lipo⁺CPS12F&αGC successfully initiated the iNKT-mediated B cell maturation and produced

antigen-specific high-affinity IgA and IgG antibodies in both the mucosal and systemic immune systems. Importantly, in both *in vitro* and *in vivo* studies, the vaccine demonstrated efficient protection potential against the pathogen. Our study used capsular polysaccharides from serotype 12F as the prototype, since this strain can cause invasive pneumococcal diseases (IPDs) and cases broke out in many countries [56,57,58,59]. We believe our design holds promise for expansion to more serotypes.

凡事豫則立，

不豫則廢。

言前定則不跲，

事前定則不困，

行前定則不疚，

道前定則不窮。

《禮記‧中庸》

2

Vaccine Design and Preparation

2.1 Materials and Methods

2.1.1 Capsular Polysaccharides Molecular Weight Characterization

The CPS12F's molecular weight was characterized via asymmetrical flow field-flow fractionation coupled with multi-angle light scattering (AF4-MALS).

The protocols for AF4-MALS were developed with help from Dr. Mariusz Kubus and Dr. Chengxin Li at DTU Chemistry.

Table 2.1: Optimized program of cross-flow for separating CPS12F. Detector flow was constant at 0.50 mL/min.

Mode	Duration (min)	Cross-flow Start (mL/min)	Cross-flow Stop (mL/min)	Flow Profile
elution	3.0	2.00	2.00	constant
elution inject	5.0	2.00	2.00	constant
elution inject	22.0	2.00	0.70	linear
elution inject	25.0	0.70	0.05	exponential
elution inject	3.0	0.05	0.00	linear
elution	5.0	0.00	0.00	constant
elution	2.0	0.00	0.00	constant
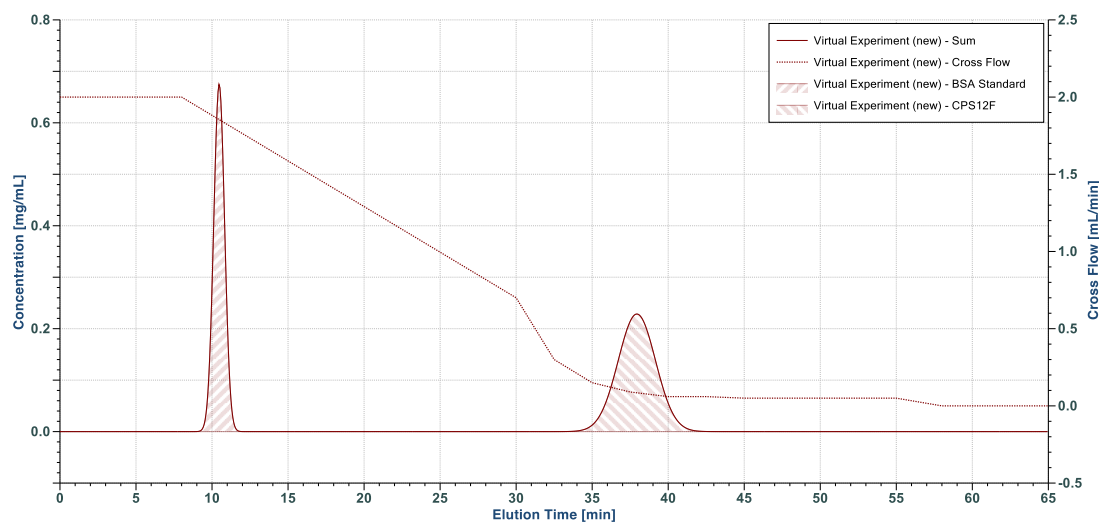
Figure 2.1: Simulated elution spectrum by the manufacturer's software SCOUT DPS. With the developed elution program (Table 2.1), the 66.5 kDa BSA standard comes at 10 min and assumed 500 kDa CPS comes at 35–40 min.

The machine method (the program of cross flow and detection flow, Table 2.1) was developed in the manufacturer's simulation software SCOUT DPS v2.0.2.9 (Figure 2.1) and optimized with actual results.

Phosphate buffer (38 mM $Na_2HPO_4 \cdot 2\,H_2O$ and 12 mM $NaH_2PO_4 \cdot 2\,H_2O$, Sigma-Aldrich® 71643 & 71505) was freshly prepared, filtered through 0.1 µm PVDF membranes (Durapore® VVLP04700), and used as the flush solution. Bovine serum albumin (BSA, Mw 66.5 kDa, Sigma-Aldrich® 05470) was used as the standard control. 100 µL of each sample (dissolved in the flush buffer at 2 mg/mL, filtered through a 0.2 µm PVDF syringe filters, Thermo Scientific™ 4-SF-02(PV)) was injected into the system with a pump (Agilent 1260 Infinity II), separated in the AF4 channel (350 µm spacer, PES 10 kDa MWCO, 17.5 cm long channel, Wyatt 1899), and measured by a differential refractive index detector (Optilab T-rEX from Wyatt) and a MALS detector (TREOS II from Wyatt). Results were analyzed using the manufacturer's software ASTRA v7.3, in which the refractive index increments for BSA and CPS12F were set as 0.185 mL/g and 0.150 mL/g, according to the published studies[60].

2.1.2 Liposomal Vaccines Preparation

The liposomal vaccines were prepared by the extrusion method.

The protocols were modified from the manufacturer's instructions[61,62]:

Table 2.2: Molar ratios of liposome compositions before fabrication. **a)** The molecular weight of CPS12F single repeat unit (1127.39) was used for calculation. **b)** The DSTAP ratio of 15 % was determined by stepwise increasing its proportion until the surface charge of the liposome reached 25 – 30 mV[63]. **c)** The sum of lipophilic components equals 1, and the molar amount of αGC equals CPS12F in Group 4, 5, & 6.

Group	Abbreviation	Lipophilic (molar ratio)				Hydrophilic (molar ratio)
		DSPC	DSTAP	cholesterol	αGC	CPS12F[a]
1	Lipo$^+$	55 %	15 %[b]	30 %	-	-
2	Lipo$^+$αGC	53.5 %	15 %	30 %	1.5 %	-
3	Lipo$^+$CPS12F	55 %	15 %	30 %	-	1.5 %[c]
4	LipoCPS12F&αGC	68.5 %	-	30 %	1.5 %	1.5 %
5 & 6	Lipo$^+$CPS12F&αGC	53.5 %	15 %	30 %	1.5 %	1.5 %

Table 2.3: List of materials, reagents, and equipment used in liposome fabrications.

Product	Producer	Code
tert-butanol (*t*-BuOH)	Sigma-Aldrich®	24127, 75-65-0
1,2-distearoyl-*sn*-glycero-3-phosphocholine (DSPC)	Avanti Polar Lipids®	850365P, 816-94-4
1,2-stearoyl-3-trimethylammonium-propane (18:0 TAP, DSTAP)	Avanti Polar Lipids®	890880P, 220609-41-6
cholesterol	Sigma-Aldrich®	C8667, 57-88-5
α-galactosylceramide (αGC)	Biosynth®	MG15978, 158021-47-7
vessel rack (heating block)	SiliCycle MiniBlock®	13260546
magnetic stirrer with hotplate	Heidolph	MR Hei Standard
4 mL 13 mm screw neck glass vials	Fisherbrand™	10571013
13 mm caps	Fisherbrand™	11506044
18 G injection needles	HSW FINE-JECT®	4710012050
liquid nitrogen	-	-
Dewar flask	KGW ISOTHERM	SCH 20 CAL
freeze dryer	LaboGene™	ScanVac CoolSafe
polysaccharide, purified type 12F	SSI Diagnostica	76939
4-(2-hydroxyethyl)-1-piperazineethanesulfonic acid (HEPES) buffer	Fisher Bioreagents™	BP299-500
sodium chloride (NaCl)	Fisher Bioreagents™	BP3581, 7647-14-5
pH/ion meter	METTLER TOLEDO	SevenCompact™ S220
0.2 μm sterile syringe filter	Fisherbrand™	15206869
extruder	Avanti Polar Lipids®	610020
1000 μL extruder syringe	Avanti Polar Lipids®	610017
extruder holder/heating block	Avanti Polar Lipids®	61002
filter support	Avanti Polar Lipids®	610014
0.2 μm hydrophilic membrane	Cytiva Whatman™ Nuclepore™	10417004

Prepare lipid film:

- Prepare *t*-BuOH/H$_2$O mixture (9/1, v/v, Sigma-Aldrich® 24127) mixture.

- Calculate, weigh, and dissolve all lipophilic components with *t*-BuOH/H$_2$O mixture in glass vials (Fisherbrand™ 10571013 & 11506044) inserted in a vessel rack (SiliCycle MiniBlock® 13260546) at 70 °C with magnetic stirring (Heidolph MR Hei Standard): DSPC (20 mg/mL, Avanti Polar Lipids® 850365P), DSTAP (3 mg/mL, Avanti Polar Lipids® 890880P), cholesterol (8 mg/mL, Sigma-Aldrich® C8667), αGC (1 mg/mL, Biosynth® MG15978). The temperature should be above the phase transition temperatures of DSPC (55 °C[64]) and DSTAP (62.9 °C[65]).

- Once fully dissolved, mix the lipophilic components according to formulations (Table 2.2) and further magnetic stir the mixture at 70 °C for 5 min.

- Insert the glass vials containing the lipids mixture into liquid nitrogen in a Dewar flask (KGW ISOTHERM SCH 20 CAL) until fully frozen. Make holes on the caps of glass vials with 18 G injection needles (HSW FINE-JECT® 4710012050), and lyophilize the lipids mixture on a freeze dryer (-55 °C, -1 mbar, LaboGene™ ScanVac CoolSafe) to remove the solvent.

Hydrate lipophilic and hydrophilic components:

- Prepare the HEPES saline solution (10 mM HEPES, 150 mM NaCl, pH = 7.4, isotonic, ~300 mOsm/kg): add 5 mL 1M HEPES (Fisher Bioreagents™ BP299-500), 4.383 g NaCl (Fisher Bioreagents™ 10316943) to 495 mL ultra-pure water, adjust pH to 7.4 (METTLER TOLEDO SevenCompact™ S220), filter through 0.2 μm PES membrane (Fisherbrand™ 15206869) for sterilization.

- Hydrate lyophilized lipid film with HEPES saline solution at 40 mM and 70 °C with magnetic stirring until fully dissolved. Dissolve hydrophilic CPS12F in HEPES saline solution at

10 mg/mL, mix it with the lipid solution according to formulation (Table 2.2), and further magnetic stir the mixture at 70 °C for 5 min.

Extrude the mixture:

- Wet the filter support (Avanti Polar Lipids® 610014) and 0.2 μm hydrophilic membrane (Cytiva Whatman™ Nuclepore™ 10417004) with HEPES saline solution.
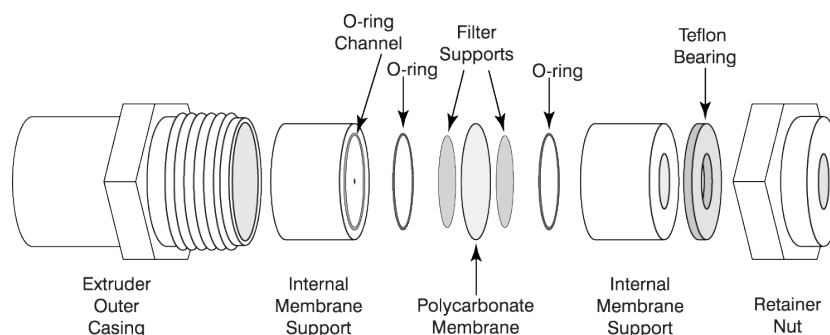
Figure 2.2: **Assembly of the extruder,** recaptured from the manufacturer's website [66].

- Assemble the extruder (Avanti Polar Lipids® 610020) according to the manufacturer's instruction (Figure 2.2). Heat the extruder to 70 °C with the extruder holder (Avanti Polar Lipids® 61002) on a hotplate.

- Take two of 1000 μL extruder syringes (Avanti Polar Lipids® 610017). Use one of them to take 1 mL of HEPES saline solution. Insert the two into the assembled extruder. When the temperature stabilizes at 70 °C, push the solution repeatedly through the membrane 10 times to check the tightness and reduce the dead volume. Then, discard the HEPES saline solution in the syringes.

- Use one of the 1000 μL extruder syringes to take 1 mL of formulation mixture solution and insert them into the extruder. When the temperature stabilizes at 70 °C again, push the solution repeatedly through the membrane 21 times. After extrusion, the liposome solution should go

into the alternative extruder syringe to prevent unfiltered larger aggregates. The prepared liposome solution should be transparent, in which the remaining large particles will cause light scattering and make it a little cloudy.

2.1.3 DSPC and DSTAP Quantification

The retained DSPC and DSTAP in liposomal vaccines were measured by determining the phosphorus concentration through the malachite green phosphate assay (Sigma-Aldrich® MAK307)*, assuming the retaining ratios of the two compounds were the same.

The protocols were modified from the published research[67] and the manufacturer's instructions[68].

Table 2.4: List of materials, reagents, equipment, and software used in DSPC and DSTAP quantifications.

Product	Producer	Code
95.0-98.0 % (w/w) sulfuric acid (H_2SO_4)	Alfa Aesar	33273, 7664-93-9
70 % (w/w) perchloric acid ($HClO_4$)	Alfa Aesar	L13298, 7601-90-3
vessel rack (heating block)	SiliCycle MiniBlock®	13260546
magnetic stirrer with hotplate	Heidolph	MR Hei Standard
malachite green phosphate assay kit	Sigma-Aldrich®	MAK307
96-well clear flat bottom plate	Corning®	3591
microplate reader	TECAN	Spark® Cyto
GraphPad Prism	GraphPad Software, LLC.	9.5.0

Release the organic phosphate in phospholipids:

- Prepare 1 M H_2SO_4: dilute 0.54 mL 98 % (w/w) H_2SO_4 (Alfa Aesar 33273) to 10 mL with ultra-pure water.

- Prepare 14 % (w/v) $HClO_4$: dilute 1.20 mL 70 % (w/w, ρ= 1.67 g/cm³) perchloric acid $HClO_4$ (Alfa Aesar L13298) to 10 mL with ultra-pure water.

- Prepare the ashing solution: mix 9 mL 1 M H_2SO_4 with 1 mL 14 % (w/v) $HClO_4$.

- Add 0.7 mL ashing solution to testing tubes containing 0.5 mL diluted samples. Heat the mixture tubes in a heating block (SiliCycle MiniBlock® 13260546) at 230 °C (Heidolph MR Hei Standard) for 1 hour. During the process, the $HClO_4$ will be removed by evaporation,

---

*ICP-OES or ICP-MS is the more convenient and reliable method to do it. But unfortunately, the machine at DTU Health Tech was down, so we used this kit as an alternative.

the H_2SO_4 will concentrate into a clear liquid, and the organic phosphate will be transformed into free orthophosphate.

- When the temperature returns to 18-24 °C, dilute the mixture to 1 mL with ultra-pure water.

Develop the color complex:

- Serially dilute the phosphate standard as calibration controls.

- In a 96-well clear flat bottom plate (Corning® 3591), mix 80 μL of testing samples or calibration standards with 20 μL of malachite green and molybdate working solution (Sigma-Aldrich® MAK307).

- Incubate the plate at 18-24 °C for 30 minutes to allow the complex formation and color development.

Data acquisition and analysis

- Acquire the OD_{620} values of each testing well with a microplate reader (TECAN Spark® Cyto).

- Draw the Log-Log calibration curve in a data analysis software (GraphPad Prism 9) and interpolate the testing samples concentration.

2.1.4 Cholesterol Quantification

The retained cholesterol was measured by coupled enzyme reactions and a fluorometric assay (Sigma-Aldrich® CS0005).

The protocols were modified from the manufacturer's instructions[69].

Table 2.5: List of materials, reagents, equipment, and software used in cholesterol quantifications.

Product	Producer	Code
cholesterol quantification assay kit	Sigma-Aldrich®	CS0005
96-well black well clear flat bottom plate	Corning®	3631
aluminum foil	ABENA	-
shaker	IKA®	VXR basic Vibrax®
microplate reader	TECAN	Spark® Cyto
GraphPad Prism	GraphPad Software, LLC.	9.5.0

Develop the coupled enzyme reactions

- Thaw all assay components of the kit (Sigma-Aldrich® CS0005). Take the volume to use and store at 2-8 °C. Aliquote the left and store at -20 °C.

- Serially dilute the cholesterol standard as calibration controls.

- In a 96-well black well clear flat bottom plate (Corning® 3631), mix 49 µL of diluted testing samples or calibration standards with 0.5 µL of the enzyme and 0.5 µL of the probe.

- Wrap the plate with aluminum foil (ABENA) to protect it from light.

- Place the plate on a shaker (IKA® VXR basic Vibrax®) at 300 rpm for 1 minute to homogenize the mixture.

- Incubate the plate at 37 °C for 30 minutes to develop coupled enzyme reactions.

Data acquisition and analysis

- Acquire the $\lambda_{ex,\ 535\ nm}/\lambda_{em,\ 587\ nm}$ values of each testing well with a microplate reader (TECAN Spark® Cyto).

- Draw the Log-Log calibration curve in a data analysis software (GraphPad Prism 9) and interpolate the testing samples concentration.

2.1.5 αGC Quantification

The retained αGC was quantified by RP-UPLC-MS/MS (reverse-phase ultra-performance liquid chromatography-tandem mass spectrometry) via multiple reaction monitoring (MRM) using a 2.6 μm C8 column.

The protocols were developed by Dr. Ulrik Keiding, Dr. Sahar Tahvili, Charlie Johansen, and Dr. Faranak Nami at DTU Chemistry.

Table 2.6: List of materials, reagents, equipment, and software used in αGC quantifications.

Product	Producer	Code
dimethyl sulfoxide (DMSO)	Sigma-Aldrich®	D8418, 67-68-5
water (H_2O)	VWR Chemicals®	83645, 7732-18-5
acetonitrile (CH_3CN)	VWR Chemicals®	83640, 75-05-8
isopropyl alcohol ((CH_3)$_2$CHOH)	VWR Chemicals®	84881, 67-63-0
formic acid (HCOOH)	VWR Chemicals®	84865, 64-18-6
liquid chromatograph (LC machine)	SHIMADZU	Nexera-i LC-2040C
2.6 μm C8 100 Å 150 × 2.1 mm LC column	Kinetex®	00F-4497-AN
triple quadrupole mass spectrometer (TQMS)	SHIMADZU	LCMS-8045
GraphPad Prism	GraphPad Software, LLC.	9.5.0

- Dissolve standards in DMSO (Sigma-Aldrich® D8418), and further dilute standards and testing samples in H_2O/CH_3CN (v/v, 1/1) mixture.

- Separate the compounds using a 2.6 μm C8 column (Kinetex® 00F-4497-AN) via reverse-phase ultra-performance liquid chromatography (RP-UPLC, SHIMADZU Nexera-i LC-2040C) with the following eluents program (Table 2.7):

Table 2.7: Eluents program: **eluent A**: CH_3CN/H_2O/HCOOH (v/v/v, 49.5 %/49.5 %/1 %, VWR Chemicals® 83645, 83640 & 84865); **eluent B**: (CH_3)$_2$CHOH/HCOOH (v/v, 99 %/1 %, VWR Chemicals® 84881)

Time (min)	1	5	8	10	12
% B	30	100	100	30	30

- Characterize the αGC through a tandem mass spectrometer (SHIMADZU LCMS-8045) via multiple reaction monitoring (mass/charge: 859→679, collision energy: -30 eV, mode: positive) and record its integrated signal area.

- Draw the Log-Log calibration curve in a data analysis software (GraphPad Prism 9) and interpolate the testing samples concentration.

2.1.6 CPS12F Quantification

The retained CPS12F was determined by the phenol sulfuric acid method.

The protocols were modified from the published research[70,71].

Table 2.8: List of materials, reagents, equipment, and software used in CPS12F quantifications.

Product	Producer	Code
polysaccharide, purified type 12F	SSI Diagnostica	76939
phenol	Alfa Aesar	A15760, 108-95-2
95.0-98.0 % (w/w) sulfuric acid (H_2SO_4)	Alfa Aesar	033273A1, 7664-93-9
96-well clear flat bottom plate	Corning®	3591
microplate reader	TECAN	Spark® Cyto
GraphPad Prism	GraphPad Software, LLC.	9.5.0

Develop the reaction

- Dissolve CPS12F (SSI Diagnostica 76939) in ultra-pure water and serially dilute it as calibration controls.

- Dilute testing samples with ultra-pure water to the linear concentration range of standards.

- Prepare 5 % (w/v) phenol solution: dissolve 1 g of phenol (Alfa Aesar A15760) in 20 mL of ultra-pure water.

- In each testing tube, add 200 μL of control or testing sample, 100 μL of 5 % (w/v) phenol solution, and 500 μL of 98 % (w/w) concentrated sulfuric acid (Alfa Aesar 033273A1).

- Vortex the testing tubes to mix well.

- Place the mixture at 18-24 °C for 30 minutes to develop the color. During this process, the polysaccharide will first be broken down and dehydrated by concentrated sulfuric acid into 5-hydroxymethylfurfural; then, the furfural derivative will react with phenol and give an orange color, which has a maximum absorbance of 490 nm.

- Transfer 200 µL of each control or testing sample to a 96-well clear flat bottom plate (Corning® 3591).

Data acquisition and analysis

- Acquire the OD_{490} values of each testing well with a microplate reader (TECAN Spark® Cyto).

- Draw the Log-Log calibration curve in a data analysis software (GraphPad Prism 9) and interpolate the testing samples concentration.

2.1.7 Size Distribution, Surface Charge, and Stability Evaluation

The hydrodynamic size distribution and surface charge were characterized in a zetasizer (Malvern NanoZS). To evaluate their stability under room temperature (18 – 24 °C) and in the fridge (2 – 8 °C), the changes in size distribution and surface charge were monitored.

The protocols were developed with Dr. Gael Veiga at DTU Health Tech:

Table 2.9: List of materials, reagents, equipment, and software used in liposome characterizations with a zetasizer.

Product	Producer	Code
4-(2-hydroxyethyl)-1-piperazineethanesulfonic acid (HEPES) buffer	Fisher Bioreagents™	BP299-500, 7365-45-9
sodium chloride (NaCl)	Fisher Bioreagents™	10316943, 7647-14-5
calcium chloride dihydrate (CaCl$_2$ · 2 H$_2$O)	Fisher Bioreagents™	10306313, 10035-04-8
glucose solution	Gibco™	A2494001
pH/ion meter	METTLER TOLEDO	SevenCompact™ S220
0.2 µm sterile syringe filter	Fisherbrand™	15206869
disposable polystyrene cuvette	SARSTEDT	67.754
folded capillary zeta cell	Malvern Panalytical	DTS1070
zetasizer	Malvern Panalytical	Nano ZS
zetasizer software	Malvern Panalytical	8.02
GraphPad Prism	GraphPad Software, LLC.	9.5.0
OriginPro 2023	OriginLab Co.	10.0.0.154

- Prepare the HEPES saline solution (10 mM HEPES, 150 mM NaCl, pH = 7.4, isotonic ~300 mOsm/kg) as described before.

- Prepare the HEPES-glucose solution (10 mM HEPES, 5 % (w/v) glucose, 1 mM CaCl$_2$, pH = 7.4, isotonic ~300 mOsm/kg): add 2 mL 1 M HEPES (Fisher Bioreagents™ BP299-500), 50 mL 0.2 g/mL glucose solution (Gibco™ A2494001), 29.404 mg CaCl$_2$ · 2 H$_2$O (Fisher Bioreagents™ 10306313) to 148 mL ultra-pure water, adjust pH to 7.4 (METTLER TOLEDO SevenCompact™ S220), filter through 0.2 µm PES membrane (Fisherbrand™ 15206869) to remove undissolved particles.

- To characterize the hydrodynamic size, 2.5 µL (depending on the concentration) of each testing sample was diluted with 1 mL HEPES saline solution in a polystyrene cuvette (SARST-

EDT 67.754) and inserted in a zetasizer (Malvern Panalytical Nano ZS) for dynamic light scattering (DLS) measurement.

- To characterize the surface charge, 2.5 μL (depending on the concentration) of each testing sample was diluted with 1 mL HEPES glucose solution, transferred to a zeta cell (Malvern Panalytical DTS1070), and inserted in a zetasizer for ζ-potential measurement.

- Each sample was characterized three times, data were fitted by the manufacturer's software (zetasizer software 8.02), and the final result was displayed as a mean $\pm$ standard deviation.

- To evaluate the stability, liposomal vaccines were stored in a fridge (2-8 °C) or under room temperature (18-24 °C), and their size and surface charge were measured every week for 2 months.

- Data was plotted in GraphPad Prism. The ridgeline plot was created with OriginPro 2023.

2.2 Vaccine Formulation Design
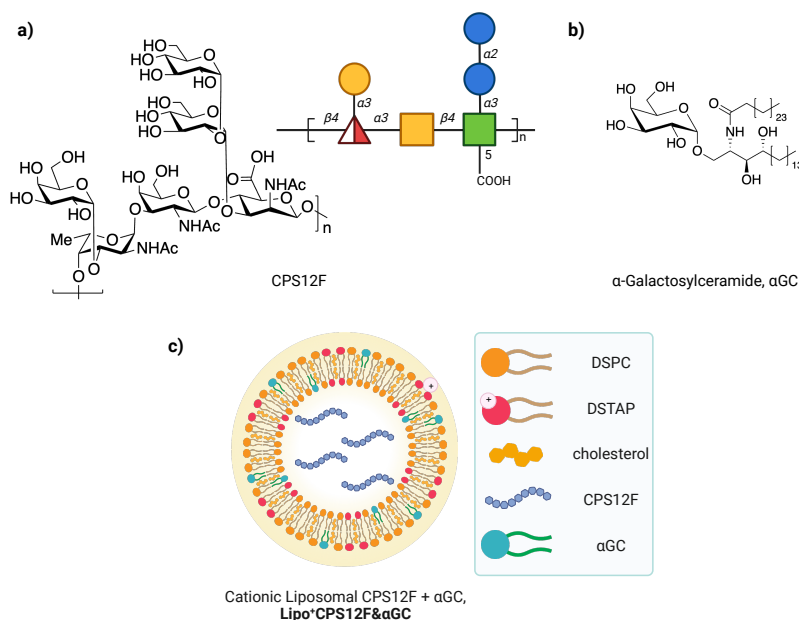
Figure 2.3: Designed vaccine formulation. Chemical structures of **a)** the capsular polysaccharide repeating unit of the *S. pneumoniae* serotype 12F and **b)** the iNKT agonist α-galactosylceramide. **c)** Formulation of the liposomal vaccine Lipo$^+$CPS12F&αGC. The illustration was created with ChemDraw and BioRender.

The complete formulation was cationic liposomal CPS12F with αGC, abbreviated as Lipo$^+$CPS12F&αGC. CPS12F (Figure 2.3 a) was the naturally extracted antigen from *S. pneumoniae* 12F, and αGC (Figure 2.3 b) was co-formulated to induce iNKT-mediated immune responses. In the liposome recipe (Figure 2.3 c), DSPC was used as the backbone lipid, cholesterol was added to improve the stability, and DSTAP was included to introduce positive charges on the liposome surface. The vaccine was designed to be administered through the intranasal (*i.n.*) route.

2.3   Capsular Polysaccharides Molecular Weight Characterization

Before incorporating the CPS12F into liposomes, we needed to determine its molecular weight (Mw) range. For large biomolecules like polysaccharides with Mw over 100 kDa, it's challenging to use traditional methods like MALDI-TOF MS to characterize their absolute molecular weights, particularly when they are mixtures with different polymerization degrees.

Fortunately, asymmetrical flow field-flow fractionation coupled with multi-angle light scattering (AF4-MALS, protocols: subsection 2.1.1) is an easier way to achieve this goal.
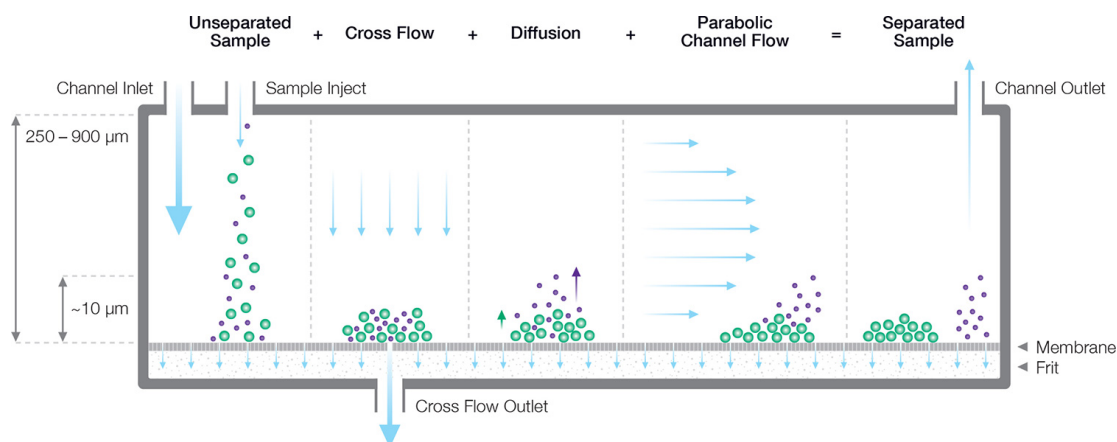
Figure 2.4: Asymmetrical flow field-flow fractionation (AF4) separates samples by size. The illustration was retrieved from the manufacturer's website [72].

In the AF4 channel (Figure 2.4), there are two kinds of flow that separate the mixture: cross-flow (vertical in the scheme) and detector flow (horizontal in the scheme). After being injected into the channel, the sample mixture will first be concentrated on the semi-permeable membrane by the cross flow. Then, the sample will diffuse back into the channel and further be carried by the detector flow into coupled detectors. The diffusion speed is negatively correlated with the sample size, and samples are thus separated. In AF4, contrary to the size-exclusion chromatography (SEC), smaller particles are flushed out of the channel early.
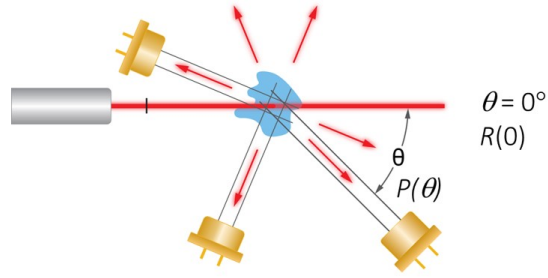
Figure 2.5: Multi-angle light scattering (MALS) measures the scattered light intensities. The illustration was retrieved from the manufacturer's website[73].

Then, the MALS detectors will measure the scattered light intensities (Figure 2.5), and the signal is directly proportional to the sample component's molecular weight and concentration with its refractive index known or measured (Equation 2.1).

$$I(\theta)_{scattered} \propto Mc \left(\frac{dn}{dc}\right)^2 \tag{2.1}$$

In Equation 2.1, the $I(\theta)_{scattered}$ is the light intensities measured by detectors; M is the sample's molecular weight; c is the sample's concentration; dn/dc is the sample's refractive index increment.
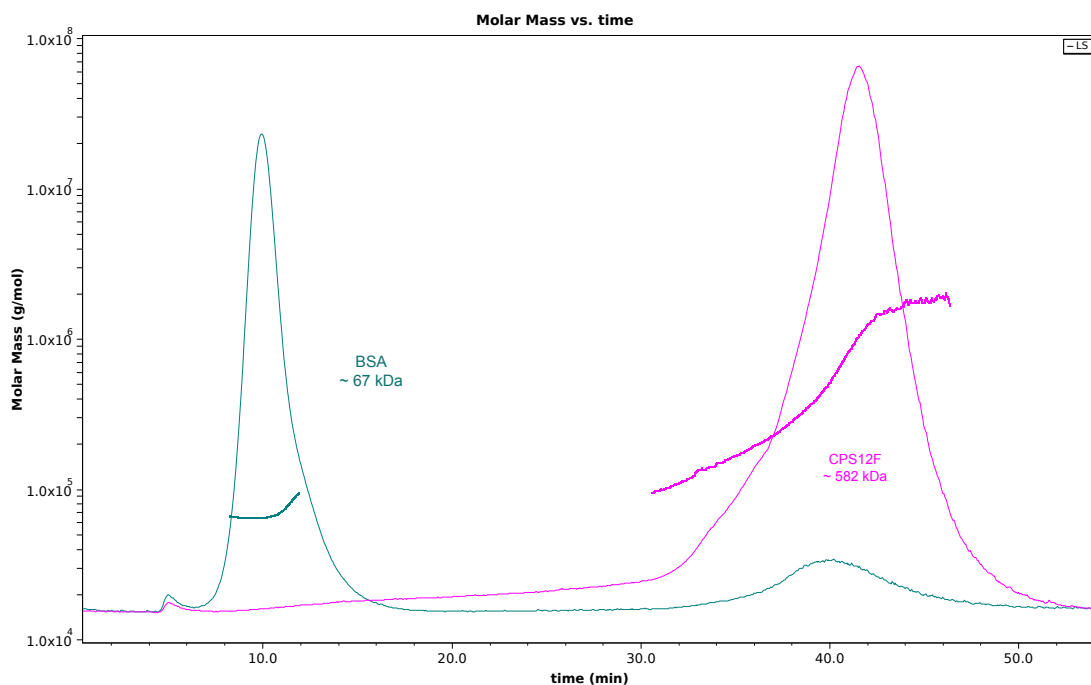
Figure 2.6: Elution spectrum and calculated Mw analyzed by the manufacturer's software ASTRA v7.3.

In Figure 2.6, it can be seen that the calculated molecular weight of BSA was 67 kDa, which matches the manufacturer's provided profile of 66.5 kDa. Furthermore, the BSA and CPS12F were well separated in the AF4 channel, and the actual spectrum was in agreement with the predicted spectrum (Figure 2.1). Finally, the average molecular weight of CPS12F was calculated to be 582 kDa.

2.4 Liposomal Vaccines Fabrication and Components Quantification
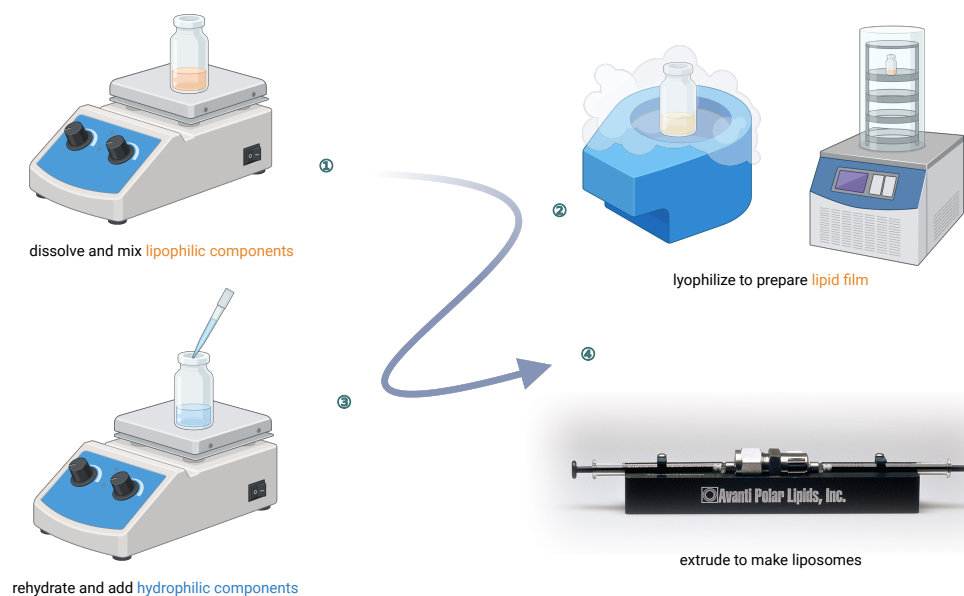
Figure 2.7: Liposomal vaccines fabrication. Photo 4 was recaptured from the manufacturer's website[61]. The illustration was created with BioRender.

We fabricated the liposomal vaccines by the extrusion method (Figure 2.7, protocols: subsection 2.1.2).
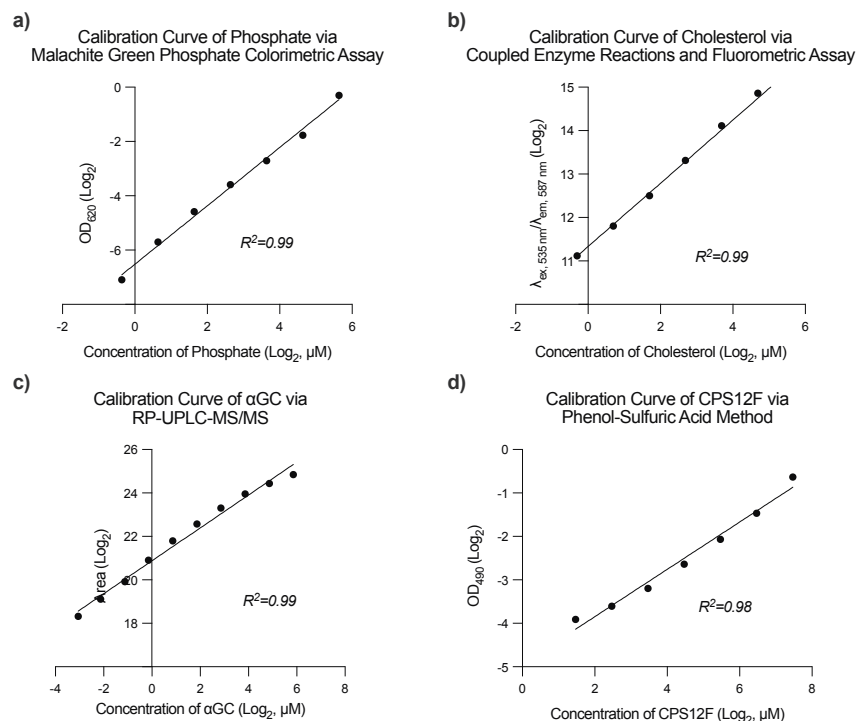
Figure 2.8: Calibration curves of liposome components.

Then, we quantified the retained DSPC and DSTAP by the malachite green phosphate colorimetric assay (protocols: subsection 2.1.3), cholesterol by the coupled enzyme reactions and fluorometric assay (protocols: subsection 2.1.4), αGC by RP-UPLC-MS/MS (protocols: subsection 2.1.5), and CPS12F by the phenol sulfuric acid method (protocols: subsection 2.1.6).

Table 2.10: Liposome compositions after fabrication: molar ratio/retained ratio.

Group	Abbreviation	Lipophilic				Hydrophilic
		DSPC	DSTAP	cholesterol	αGC	CPS12F
1	Lipo⁺	59.7 %/46.3 %	16.3 %/46.3 %	24 %/34.0 %	-/-	-/-
2	Lipo⁺αGC	63.5 %/61.5 %	17.8 %/61.5 %	18.7 %/32.2 %	1.4 %/48.1 %	-/-
3	Lipo⁺CPS12F	62.7 %/41.6 %	17.1 %/41.6 %	20.2 %/24.6 %	-/-	2.5 %/59.7 %
4	LipoCPS12F&αGC	75.7 %/55.6 %	-/-	22.4 %/37.5 %	1.9 %/64.3 %	1.7 %/58.1 %
5 & 6	Lipo⁺CPS12F&αGC	42.0 %/38.9 %	11.8 %/38.9 %	43.5 %/75.1 %	0.7 %/23.5 %	1.2 %/39.7 %

All calibration curves (Figure 2.8) had an R^2 value of at least 0.98, demonstrating the robustness

of the quantification methods. The molar ratios of fabricated liposome compositions (Table 2.10) were close to the designed formulation (Table 2.2), and the encapsulation ratios of the polysaccharide antigen ranged from 39.7 % to 59.7 %, which were acceptable.

2.5   Size Distribution, Surface Charge, and Stability Evaluation

After that, we assessed the hydrodynamic size distribution of the prepared liposomal vaccines by dynamic light scattering (DLS) in a zetasizer (Malvern NanoZS). We measured the surface charge as ζ-potential in the same zetasizer. Moreover, we stored the samples separately at room temperature (18–24 °C) or in the fridge (2–8 °C) and repeated the characterization to evaluate their stability (protocols: subsection 2.1.7).
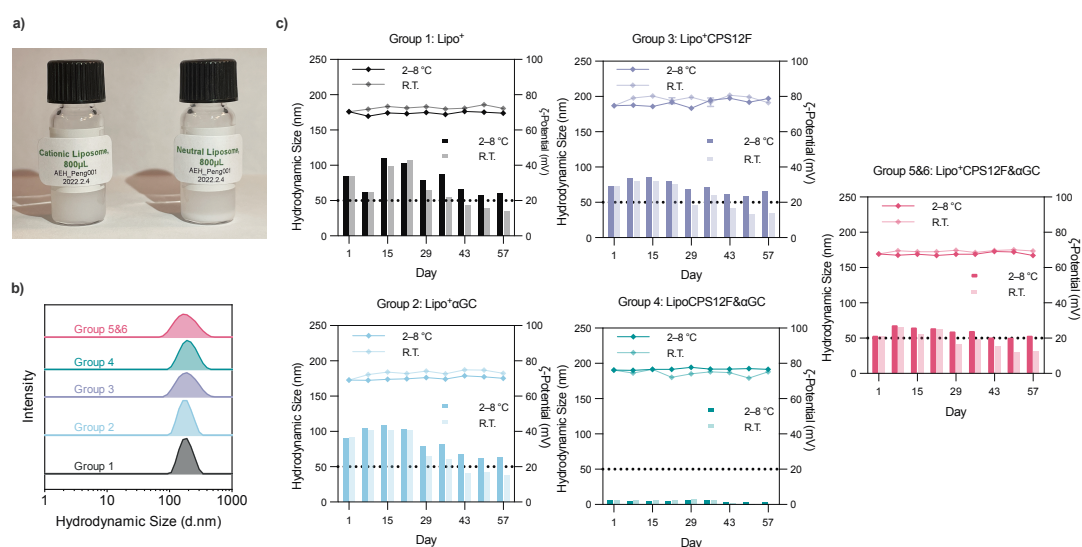
Figure 2.9: Size distribution, surface charge, and stability of liposomal vaccines. a) Photo of cationic and neutral liposomal vaccine solution after static placement. **b)** Hydrodynamic size distribution of liposomal vaccines characterized via DLS with a zetasizer. **c)** Liposomal vaccines were stored at 2 – 8 °C (in a fridge) or 18 – 24 °C (at room temperature). The hydrodynamic size (left axis, curves above) and surface charge (right axis, bars below) were measured weekly for 2 months with a zetasizer.

After static placement (Figure 2.9 a), the neutral liposomes were deposited to the bottom; in contrast, the cationic liposomes remained stable in the suspension, presumably because their positive surface charge prevented aggregation due to electrostatic repulsion. However, this didn't prove the cationic liposome was more stable than the neutral liposome, as the homogeneity could be restored

to the neutral liposome suspension by simple vortexing or pipetting.

Liposomal vaccines of all groups displayed homogeneous hydrodynamic size distribution ranging from 150 to 200 nm (Figure 2.9 b). Figure 2.9 c demonstrated that the hydrodynamic size of all liposomal vaccines did not undergo changes after storage at either room temperature (18–24 °C) or in the fridge (2–8 °C). The surface charge tended to decrease over time under both conditions. However, they remained above 20 mV for at least 2 months in the fridge and 3 weeks at room temperature. The storage length was superior to both the widely applied liposomal vaccine (12 hours at room temperature) for COVID-19 and the non-liposomal vaccine PCV20 (96 hours at room temperature) for pneumonia by Pfizer[74,29].

權，然後知輕重；

度，然後知長短。

物皆然，心為甚。

《孟子・梁惠王上》

3
Mouse Study

3.1 Materials and Methods

3.1.1 Mouse Strain, Vaccination Route, and Sampling Method
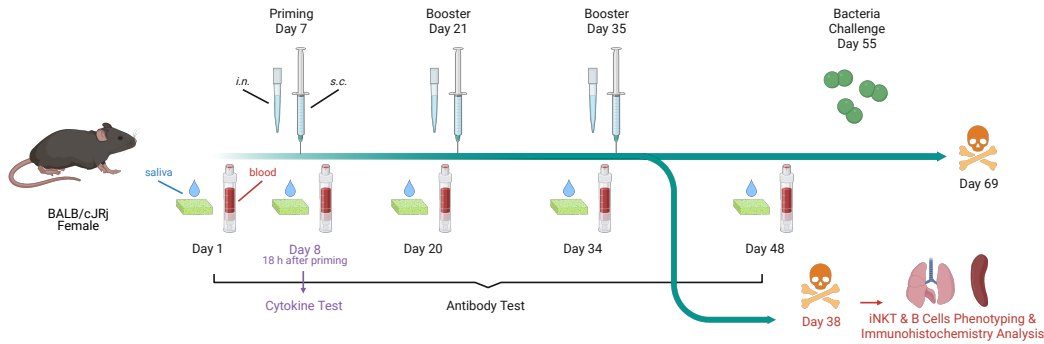
Figure 3.1: Scheme of the mouse study. The illustration was created with BioRender.

All animal experiments in this study were approved by the Danish Animal Experiments Inspectorate (2020-15-0201-00482-C1 and 2022-15-0201-01249) and complied with Directive 2010/63/EU. 6–8 weeks old BALB/cJRj female mice (JANVIER LABS®), after 1 week of acclimation, were randomized into treatment groups and bred in IVC cages. The vaccinations were carried out via subcutaneous (*s.c.*) injections at 50 μL or intranasal (*i.n.*) installations[75] at 25 μL for each nostril, to provide enough exposure to NALT and iBALT[76].

For cytokine and antibody quantification, at defined time points (Figure 3.1), blood samples were collected (sublingual bleeding) and processed into the serum to evaluate the systemic immune responses; saliva samples were collected with sampling sponges (Nasco® B01245WA) after pilocarpine injection (Medchem Express HY-B0726, saliva secretion stimulator, *i.p.*, 0.36 μg/g of body weight) to evaluate mucosal immune responses[77]. Samples were stored at 2–8 °C for the short term ($\leq$ 7 days) and -80 °C for the long term ($>$ 7 days).

For organ examination and cell phenotyping, 3 days after the final vaccination, half of the mice

were sacrificed by cervical dislocation, and their lungs and spleens were cryopreserved with OCT (Cell-Path KMA-0100-00A) for immunohistochemistry analysis or prepared into single-cell suspensions for multi-color flow cytometry analysis. Another half of the mice were challenged with bacteria 1 week after the final serum and saliva sampling to evaluate the efficacy of protection *in vivo*.

At the end of the study, all remaining mice were euthanized by cervical dislocation.

Below are the detailed protocols for mice experiments:

Table 3.1: List of materials, reagents, equipment, and software used in mice experiments.

Product	Producer	Code
BALB/cJRj	JANVIER LABS®	-
0.5 mL syringe with a 30 G needle	BD Micro-Fine™	324525
50 mL centrifuge tube	CELLSTAR™	277261
blood sampling tube with coagulation activators	SARSTEDT Microvette®	200
96-well conical-bottom plate	Thermo Scientific™	232698
torch	Rothenberger Industrial	MT-820
0.6 mL microcentrifuge tubes	Thermo Scientific™	3449
2 mL microcentrifuge tubes	Thermo Scientific™	3453
pilocarpine hydrochloride	Medchem Express	HY-B0726
phosphate-buffered saline (PBS)	Gibco™	10010015
sampling sponge	Nasco®	B01245WA
aluminum sealing tape	Thermo Scientific™	232698

Subcutaneous injection:

• Restrain the mouse appropriately with a hand.

• Use a 0.5 mL syringe with a 30 G needle (BD Micro-Fine™ 324525) to carefully puncture into the skin fold between the leg and abdomen. Slightly lift the needle to ensure it is only under the skin and not inside a muscle or perforating the abdominal wall.

• After confirmation, inject 50 μL of the vaccine solution.

Intranasal instillation:

• The protocol was modified from the public materials[75].

- Restrain the mouse appropriately with a hand and position its nose upward. Alternatively, cut a hole in the bottom of a 50 mL centrifuge tube (CELLSTAR™ 277261), use it to restrain the mouse, and let its nose emerge from the hole[78].

- Use a 100 μL pipette tip to carefully apply half of the vaccine dose (25 μL) to each mouse nostril drop by drop slowly to allow the mouse to inhale (~1 minute for each nostril). An intranasal instillation volume at 50 μL will give enough exposure to NALT and iBALT[76].

- Monitor the mice after intranasal instillation to ensure they breathe normally. If the mouse showed labored respiration with increased respiratory rate, effort, or intense abdominal breathing, euthanize immediately.

Serum sampling:

- The total blood volume of a 25 g mouse is approximately 25 g × 58.5 μL/g=1462.5 μL[79]. According to Danish Animal Experiments Inspectorate[80], the mice should have 1, 2, and 4 weeks for recovery if 7.5 %, 10 %, and 15 % of the total blood was taken. Collect maximally one blood sample per day.

- Restrain the mouse appropriately with a hand and use the thumb to push out its tongue. Use a 21 G needle to puncture the thick caudal part of the *V. sublingualis*. Collect ~120 μL of the blood into sampling tubes with coagulation activators (SARSTEDT Microvette® 200).

- Leave tubes undisturbed at room temperature for 30 minutes to allow the blood to clot. Centrifuge the sampling tubes at 10000 × g for 5 minutes at 18–24 °C[81]. The isolated serum (supernatant) should look light yellow. The light red indicates hemolysis, which has been tested not to interfere with cytokine quantification and antibody measurement results.

- Aliquot the serum at 10 μL for 2 copies and at 2 μL for 6 copies into 96-well conical-bottom plates (Thermo Scientific™ 249662), and seal the plates with aluminum sealing tapes (Thermo

Scientific™ 232698). Store samples at 2–8 °C for the short term ($\leq$ 7 days) and -80 °C for the long term ($>$ 7 days).

Saliva sampling:
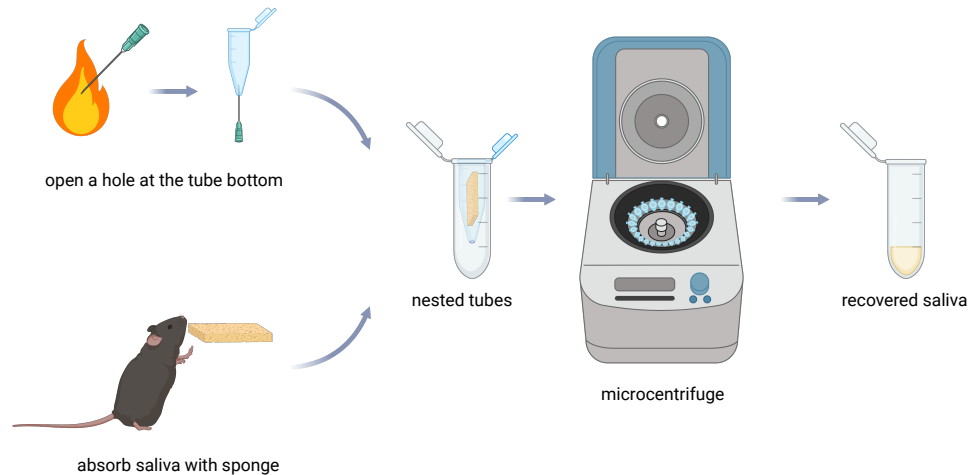
Figure 3.2: Saliva collection. The illustration was created with BioRender.

- The protocol was modified from the published research[77].

- Burn a 21 G needle red with a torch (Rothenberger Industrial MT-820), and immediately use it to punch the bottom of a 0.6 mL microcentrifuge tube (Thermo Scientific™ 3449) to open a hole. Nest the processed 0.6 mL microcentrifuge tube into a 2 mL microcentrifuge tube (Thermo Scientific™ 3453).

- Prepare pilocarpine stock solution (6 mg/mL, 100 $\times$): dissolve 12 mg of pilocarpine hydrochloride (Medchem Express HY-B0726) in 2 mL of PBS (Gibco™ 10010015). Aliquote it at 0.125 mL into 0.6 mL centrifuge tubes, and store it at -80 °C. On the day of use, dilute 0.125 mL

of the stock solution (0.06 mg/mL, 1 ×) to 12.5 mL working solution with PBS. 12.5 mL is enough for 100 injections.

- Intraperitoneally (*i.p.*) inject the mice with pilocarpine working solution at 5 μL/g of body weight to stimulate saliva secretion. After 4 minutes, insert a pre-cut (2 mm × 18 mm) sampling sponge (Nasco® B01245WA) into the mouse's mouth for 3 minutes of saliva absorbance. Transfer the sampling sponges to the nested tubes, and centrifuge them with their cap off at 8000 × g for 5 minutes at 18–24 °C. With the following timetable (unit: min), 20 minutes is enough to collect saliva from 4 mice.

Mouse 1	Mouse 2	Mouse 3	Mouse 4
0–1 (*i.p.* injection)	-	-	-
-	4–5	-	-
5-8 (saliva collection)	-	-	-
-	-	8–9	-
-	9–12	-	-
-	-	-	12–13
-	-	13–16	-
-	-	-	17–20

- Aliquot the saliva at 5 μL for 1 copy and at 2 μL for 3 copies into 96-well conical-bottom plates, and seal the plates with aluminum sealing tapes (Thermo Scientific™ 232698). Store samples at 2–8 °C for the short term (≤ 7 days) and -80 °C for the long term (> 7 days).

3.1.2 Cytokine Quantification

Cytokines (IL-12, IL-4, IFN-γ, and IL-17) were quantified with BD™ cytometric bead array (CBA) assay kits (BD Biosciences 562264, 562272, 562233, 562261) via flow cytometry.

The protocols were modified from the manufacturer's instructions[82].

Table 3.2: List of materials, reagents, equipment, and software used in CBA FCM.

Product	Producer	Code
mouse IL-12p70 enhanced sensitivity flex set	BD Biosciences™	562264
mouse IL-4 enhanced sensitivity flex set	BD Biosciences™	562272
mouse IFN-γ enhanced sensitivity flex set	BD Biosciences™	562233
mouse IL-17A enhanced sensitivity flex set	BD Biosciences™	562261
mouse enhanced sensitivity master buffer kit	BD Biosciences™	562246
96-well round-bottom plates	Corning®	3365
flow cytometer	BD©	LSRFortessa™
FlowJo	BD©	10.8.2
GraphPad Prism	GraphPad Software, LLC.	9.5.0

Prepare standards and testing samples:

- 50 μL of sample is needed for each test.

- Separately reconstitute the IL-12p70, IL-4, IFN-γ, and IL-17A standards with 2 mL of assay diluent and further dilute 5 μL of each in 120 μL assay diluent to get 200000 fg/mL standards.

- Serially dilutes the standards by 3 folds at 75 μL (50 μL left) for 7 levels with assay diluent in a round-bottom 96-well plate (CorningCorning® 7007); use assay diluent as the blank control in the 8th well (200000, 66667, 22222, 7407, 2469, 823, 274, 0 fg/mL).

- Dilute 10 μL of each serum sample by 5 folds to 50 μL and 5 μL of each saliva sample by 10 folds to 50 μL with assay diluent.

Prepare testing reagents:

- 20 μL of working capture beads solution is needed for each test. Prepare working capture beads solution, for 96 testing samples with 4 cytokines to evaluate and 8-level standards for each cytokine:

    for testing samples: mix 96+5=101 μL of each capture bead with 101×(20-4)=1616 μL of capture bead diluent;

    for standards, dilute 8+1=9 μL of each capture bead with 9×(20-1)=171 μL of capture bead diluent.

- 20 μL of working detection reagent Part A is needed for each test. Prepare working detection reagent Part A, for 96 testing samples with 4 cytokines to evaluate and 8-level standards for each cytokine:

    for testing samples: mix 96+5=101 μL of each detection reagent Part A with $101 \times (20 - 4) = 1616$ of detection reagent Part A diluent;

    for standards, dilute 8+1=9 μL of each detection reagent Part A with $9 \times (20 - 1) = 171$ μL of detection reagent Part A diluent.

- 100 μL of working detection reagent Part B is needed for each test. Prepare working detection reagent Part B, for 96 testing samples with 4 cytokines to evaluate and 8-level standards for each cytokine:

    Reconstitute 2 vials of the detection reagent Part B in $(96 + 8 \times 4 + 5) \times 100 = 13300$ μL of detection reagent Part B diluent.

Develop detection structure:

- In round-bottom plates, add 50 μL of each diluted standard and testing sample.

- Vortex and add 20 μL of the prepared working capture beads solution to corresponding wells.

- Mix the solution by shaking the plate at 500 rpm for 5 minutes; then, incubate for 2 hours at 18–24 °C.

- Add 20 μL of the prepared working detection reagent Part A to corresponding wells.

- Mix the solution by shaking the plate at 500 rpm for 5 minutes; then, incubate for 2 hours at 18–24 °C.

- Wash the plates 2 times with 200 μL of wash buffer by centrifugation at 400 × g and 18–24 °C for 5 minutes and dumping to discard the supernatant.

- Add 100 μL of the prepared working detection reagent Part B to each well.

- Mix the solution by shaking the plate at 500 rpm for 5 minutes; then, incubate for 1 hour at 18–24 °C.

- Wash the plates 1 time with 200 μL of wash buffer by centrifugation at 400 × g and 18–24 °C for 5 minutes and dumping to discard the supernatant.

- Resuspend the beads with 150 μL of wash buffer in each well.

Acquire and analyze data:

- Set up the flow cytometer (BD LSRFortessa™) according to the manufacturer's guide[83].

- Run the prepared samples as soon as possible.

- Import the acquired data into FlowJo, calculate the MFI_{PE}, and execute statistical tests for further conclusion.

3.1.3 Cell Phenotyping

iNKTs and B cells in the spleen and lung were phenotyped by multi-color flow cytometry.

a)

Marker	Fluorophore
FVS520	FITC
CD3 epsilon	Brilliant Violet 605
mCD1d tetramer	PE
CD1d	PE/Dazzle
CD69	APC
CD25	Brilliant Violet 480
CD45R	APC-Cy7
CD27	BB700
CD138	Brilliant Violet 421
CD185 (CXCR5)	Brilliant Violet 711

b)

SSM	APC-A	APC-Cy7-A	BB700-A	BV421-A	BV480-A	BV605-A	BV711-A	FITC-A	PE-A	PE-CF594-A
APC-A	0.00	0.56	0.04	0.00	0.00	0.00	0.05	0.00	0.00	0.00
APC-Cy7-A	0.11	0.00	0.00	0.00	0.00	0.00	0.00	0.01	0.00	0.00
BB700-A	3.72	3.63	0.00	0.31	0.07	0.25	3.62	2.78	0.03	0.04
BV421-A	0.00	0.02	0.00	0.00	0.64	0.02	0.01	0.02	0.00	0.00
BV480-A	0.00	0.01	0.01	0.03	0.00	0.06	0.04	0.56	0.00	0.00
BV605-A	0.07	0.19	0.11	0.70	0.09	0.00	0.77	0.03	0.09	0.80
BV711-A	0.41	2.47	0.35	0.80	0.12	0.01	0.00	0.07	0.00	0.00
FITC-A	0.01	0.01	0.02	0.00	0.13	0.00	0.01	0.00	0.01	0.00
PE-A	0.03	0.00	0.05	0.00	0.00	0.06	0.08	1.28	0.00	0.16
PE-CF594-A	0.28	0.05	0.39	0.01	0.00	0.19	0.38	0.54	0.30	0.00

c)

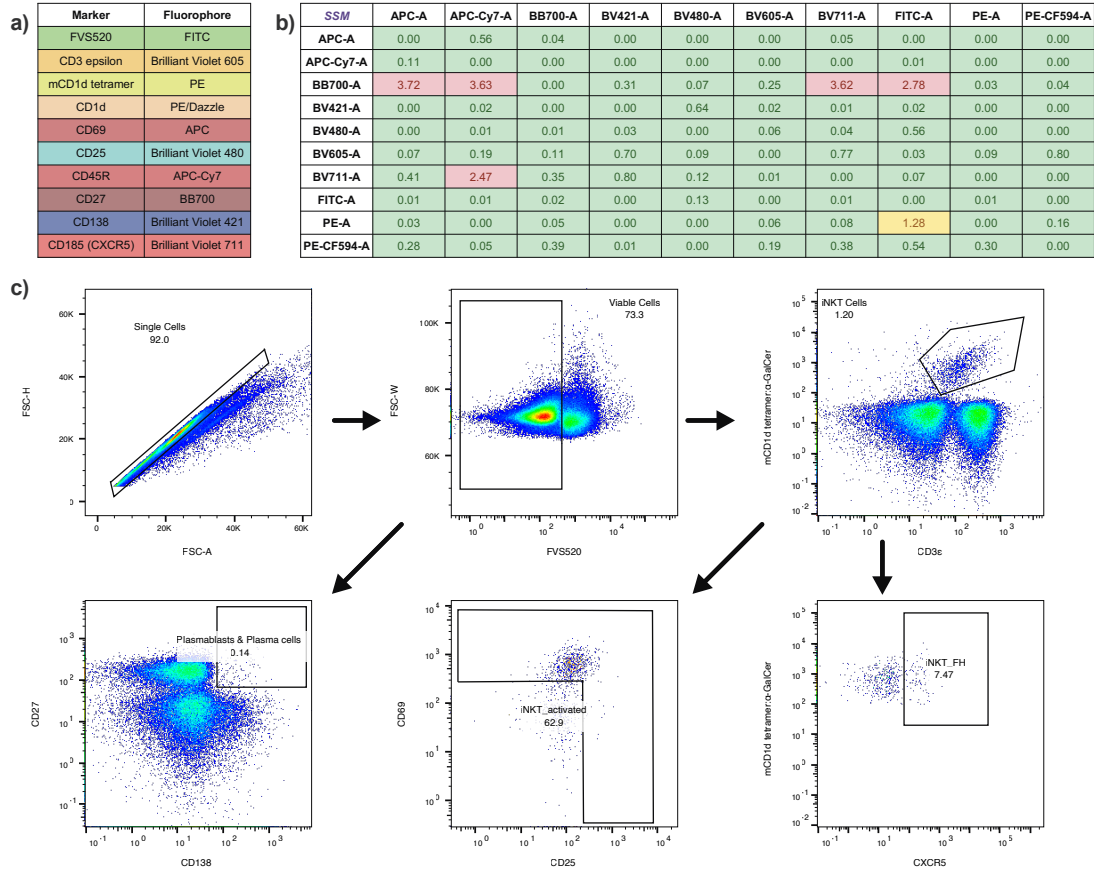**Figure 3.3: Technical information for the multi-color flow cytometry. a)** antibodies panel, **b)** spillover spreading matrix (SSM) calculated by FlowJo, and **c)** gating strategies for iNKT and B cells subclasses.

The antibody panel (Figure 3.3 a) and gating strategy (Figure 3.3 c) were developed based on phenotyping markers[84] and published optimized multi-color immunofluorescence panels (OMIP 076)[85].

Table 3.3: List of materials, reagents, equipment, and software used in multi-color flow cytometry.

Product	Producer	Code
base molds	Epredia™	58951
OCT embedding matrix	CellPath	KMA-0100-00A
70 μm cell strainer	Falcon®	352350
50 mL centrifuge tube	CELLSTAR™	277261
phosphate-buffered saline (PBS)	Gibco™	10010015
centrifuge	Thermo Scientific™	Multifuge™ X1R 75004250
lysing buffer	BD Biosciences™	555899
stain buffer	BD Biosciences™	554656
automated cell counter	Invitrogen™	Countless II
cell counting chamber slides	Invitrogen™	C10228
compensation beads	Invitrogen™	01-333-41
rat anti-mouse CD16/32 (Fc block, 2.4G2)	BD Biosciences™	553141
96-well round-bottom plates	Corning®	3365
fixable viability stain 520	BD Biosciences™	564407
BV605 hamster anti-mouse CD3ε (145-2C11)	BD Biosciences™	563004
mCD1d, α-galactosylceramide, PE	Tetramer Shop	MCD1d-001
PE/Dazzle 594 rat anti-mouse CD1d (1B1)	BioLegend®	123519
APC hamster anti-mouse CD69 (H1.2F3)	BD Biosciences™	560689
BV480 rat anti-mouse CD25 (PC61)	BD Biosciences™	566202
APC-Cy7 rat anti-mouse CD45R (RA3-6B2)	BD Biosciences™	561102
BB700 hamster anti-mouse CD27 (LG.3A10)	BD Biosciences™	742135
BUV395 rat anti-mouse IgD (11-26c.2a)	BD Biosciences™	565988
BV421 rat anti-mouse CD138 (281-2)	BD Biosciences™	562610
BV711 rat anti-mouse CD185 (L138D7)	BioLegend®	145529
96-well round-bottom plates	Corning®	3365
flow cytometer	BD©	LSRFortessa™
FlowJo	BD©	10.8.2
GraphPad Prism	GraphPad Software, LLC.	9.5.0

Prepare single-cell suspensions:

- Operations were modified from the public materials[86].

- Euthanize mice by cervical dislocation, disinfect them with 70 % ethanol, and open them with scissors.

- Dissect the spleen and lung, cut and transfer half of the samples to base molds (Epredia™ 58951), cover them with OCT (CellPath KMA-0100-00A), freeze them by placing them on dry ice, and store them at -80 °C for further immunohistochemistry analysis.

- To prepare single-cell suspensions: mince the left spleen and lung into pieces, use syringe plunges to smash them through 70 μm cell strainers (Falcon™ 352350) into 50 mL centrifuge tubes (CELLSTAR™ 277261) inserted in ice, and use ice-cold PBS (Gibco™ 10010015) to help the remained cells on the sieve flow into tubes.

- To remove red blood cells (RBCs): centrifuge (Thermo Scientific™ Multifuge™ X1R 75004250) the cell suspension at 400 × g and 2–8 °C for 5 minutes and discard the supernatant, re-suspend the cell pellet with 2 mL of lysing buffer (BD Biosciences™ 555899) for 5 minutes incubation at 18–24 °C, add 10 mL of ice-cold PBS and centrifuge the cell suspension at 400 × g and 2–8 °C for 5 minutes and discard the supernatant, resuspend the cell pellet with 1 mL of stain buffer (DPBS+FBS+NaN$_3$, BD Biosciences™ 554656).

- Count (Invitrogen™ Countless II & C10228) and dilute live cells to 2×10^7 cells/mL. Keep them at 2–8 °C.

Stain cells:

- The optimal working concentration for each antibody was titrated in advance with protocols modified from public materials[87].

- Prepare the Fc block (BD Biosciences™ 553141) working solution (5 μg/mL), single stain solution, FMO stain solution, and the full stain cocktail (50 μL for each test, viability stain should be included) according to the previous titration results.

- Transfer 50 μL (1×10^6 cells) of each sample, unstained control, compensation control (1 drop of compensation beads, Invitrogen™ 01-333-41), FMO control (fluorescence minus one) in duplicate to the wells of 96-well round-bottom plates (Corning® 3365).

- Add 50 μL (0.25 μg) of Fc block working solution to each well (except for the compensation control) for 10 minutes of incubation at 2–8 °C in the dark.

- Add 50 μL of stain solution to each corresponding well for 60 minutes of incubation at 2–8 °C in the dark.

- Centrifuge the stained cells at 400 × g and 2–8 °C for 5 minutes and discard the supernatant. Repeat 2 times to remove unbounded antibodies.

- Resuspend the stained cells with 200 μL stain buffer and place it at 2–8 °C in the dark until analysis.

Acquire and analyze data:

- Set up the flow cytometer (BD© LSRFortessa™) according to the manufacturer's guide[83].

- Run the prepared samples as soon as possible.

- Import the acquired data into the analysis software (FlowJo, BD© 10.8.2), calculate the compensation matrix (Figure 3.3 b) with compensation control results, determine the gating boundary with FMO control results, calculate the ratio of the population of interest, and finally execute statistical tests for further conclusion.

3.1.4 Organ Examination

Spleens and lungs were examined by immunohistochemistry.

The protocols were developed with help from Susanne Primdahl at DTU Health Tech.

Cryopreserved spleens and lungs were fixed with 4 % (w/v) formaldehyde (Histolab® 02178), dehydrated with a series of ethanol solutions of increasing concentration and Histolab Clear solution (Histolab® 14250) in a tissue processor (Epredia™ Excelsior AS), embedded in paraffin wax (Histology Wax 0587), cut into 3 μm sections with a rotary microtome (Shandon Finesse AS325), and mounted on adhesion slides (Epreida™ J1810AMNZ). Then, the sections were deparaffinized with xylene (Sigma-Aldrich® 534056) and a series of ethanol solutions of decreasing concentration and water rinse, boiled in sodium citrate buffer (10 mM citrate, pH adjusted to 6.0) for 20 minutes for epitope retrieval, treated with streptavidin and biotin blocking reagents (VectorLabs SP-2002) to block endogenous biotin, treated with 2 % (w/v) BSA (Invitrogen™ DS98200) in 0.3 % (v/v) Triton X-100 (Sigma-Aldrich® X100) to reduce unspecific binding. After that, the sections were sequentially incubated with the biotinylated peanut agglutinin (PNA, VectorLabs B-1075-5) for germinal center detection, 3 % (w/v) hydrogen peroxide (Millipore® 88597) to quench endogenous peroxidase activity, streptavidin-HRP conjugate (Agilent Dako P0397), and developed color with DAB (abcam ab64238). To better visualize the tissue morphology, the slides were counterstained with Mayer's hematoxylin (lab-made) for 10 seconds. Unbounded components were washed away with Tris-buffered saline + 0.025 % (w/v) Tween 20 (lab-made) between each step. Afterward, the stained sections were again dehydrated with a series of ethanol solutions of increasing concentration, air dried, and preserved with the mounting medium (Histolab® 00801) and coverslips (Hounisen 2422.2560). Finally, the slides were observed and photoed under a pathology microscope (Leica DMRB and MC170 HD).

3.1.5 ANTIBODY QUANTIFICATION

At the start of the study and 2 weeks after each vaccination, serum and saliva were collected from the mice and stored at -80 °C. CPS12F-specific antibodies in the samples were measured by indirect ELISA.

Table 3.4: List of materials, reagents, equipment, and software used in indirect ELISA.

Product	Producer	Code
384-well clear flat-bottom immuno plate	Thermo Scientific™ Nunc™ MaxiSorp™	464718
96-well conical-bottom plate	Thermo Scientific™ Nunc™ Microwell™	249662
polysaccharide, purified type 12F	SSI Diagnostica	76939
phosphate-buffered saline (PBS)	Gibco™	10010015
sealing tape	Thermo Scientific™	15036
20 × PBS Tween™ 20 buffer	Thermo Scientific™ Pierce™	28352
ELISA assay buffer (5 ×)	Invitrogen™	DS98200
goat anti-mouse IgM μ chain (HRP)	abcam	ab97230
goat anti-mouse IgA α chain (HRP)	abcam	ab97235
goat anti-mouse IgG H&L (HRP)	abcam	ab6789
goat anti-rabbit IgG H&L (HRP)	abcam	ab6721
goat anti-mouse IgG_3 heavy chain (HRP)	abcam	ab97260
goat anti-mouse IgG_1 (HRP)	abcam	ab97240
goat anti-mouse IgG_{2b} heavy chain (HRP)	abcam	ab97250
goat anti-mouse IgG_{2a} heavy chain (HRP)	abcam	ab97245
pneumococcus antiserum type 12b	SSI Diagnostica	16947
ELISA TMB stabilized chromogen	Invitrogen™	SB02
aluminum foil	ABENA	-
ELISA stop solution	Invitrogen™	SS04
shaker	IKA®	VXR basic Vibrax®
microplate reader	TECAN	Spark® Cyto
GraphPad Prism	GraphPad Software, LLC.	9.5.0

Before formal experiments, coating concentration, sample dilution folds, and detecting antibody concentration were optimized with the manufacturer's protocols[88]. To improve hydrophilic coating efficiency, MaxiSorp™ plates were chosen.

Coat and block plates:

- Prepare the CPS12F coating stock solution (100 ×, 1 mg/mL) by dissolving 0.1 mg of CPS12F (SSI Diagnostica 76939) in 100 μL of PBS (Gibco™ 10010015). Prepare the coating working

solution (1 ×, 10 µg/mL) by diluting 100 µL of CPS12F coating stock solution to 10 mL with PBS; 10 mL is enough for two 384-well plates of the assay. Add 10 µL of coating solution (100 ng of CPS12F) to each well of the 384-well immunoassay plates (Nunc™ MaxiSorp™ 464718). Seal the plates with sealing tape (Thermo Scientific™ 15036) and incubate them at 2–8 °C for 18 hours.

- Prepare PBST working solution (1 ×, PBS + 0.05 % (w/v) Tween 20) by diluting 25 mL of PBST stock solution (20 ×, Thermo Scientific™ Pierce™ 28352) to 500 mL with ultra-pure water; 500 mL is enough for two 384-well plates assay.

- Prepare BSA working solution (1 ×, buffered solution with bovine protein): dilute 20 mL of assay buffer stock solution (5 ×, Invitrogen™ DS98200) to 100 mL with ultra-pure water; 100 mL is enough for two 384-well plates of the assay, including sample and antibody dilution.

- Dump the plate to discard the solution in the well and tap it on tissues. Add 50 µL of PBST per well and let the plates soak for 1 minute with 100 rpm shaking (IKA® VXR basic Vibrax®). Repeat 3 times to remove unbounded components in the well.

- Add 50 µL of BSA working solution to each well of the 384-well plates for 1 hour of incubation at 37 °C to block the uncoated area in the well.

Add samples and develop reactions:

- During the blocking, take out the sample from -80 °C and let the sample melt at room temperature. Use commercial antiserum (SSI Diagnostica 16947) as a positive and normalizing control. In a conical-bottom 96-well plate (Thermo Scientific™ Nunc™ Microwell™ 249662), dilute testing samples by 100 folds with BSA working solution.

- Dump the plate to discard the solution in the well and tap it on tissues. Add 10 µL of the diluted testing sample to each well of the 384-well plate for 1 hour of incubation at 37 °C.

- Dump the plate to discard the solution in the well and tap it on tissues. Add 50 μL of PBST per well and let the plates soak for 1 minute with 100 rpm shaking. Repeat 3 times to remove unbounded components in the well.

- Prepare the detecting antibody stock solution (100 ×) by diluting antibodies with BSA working solution: HRP-conjugated goat anti-mouse IgM (20 μg/mL, abcam ab97230), IgA (20 μg/mL, abcam ab97235), IgG$_{poly}$ (40 μg/mL, abcam, ab6789), IgG$_3$ (40 μg/mL, abcam ab97260), IgG$_1$ (40 μg/mL, abcam ab97240), IgG$_{2b}$ (40 μg/mL, abcam ab97250), IgG$_{2a}$ (40 μg/mL, abcam ab97255), and goat anti-rabbit IgG$_{poly}$ (2 μg/mL, abcam, ab6721). Prepare the detecting antibody working solution (1 ×) by diluting 12 μL of the detecting antibody stock solution to 1200 μL with assay buffer; 1000 μL is enough for 96 wells of assay.

- Add 10 μL of the detecting antibody working solution to each corresponding well of the 384-well plate for 1 hour of incubation at 37 °C.

- Dump the plate to discard the solution in the well and tap it on tissues. Add 50 μL of PBST per well and let the plates soak for 1 minute with 100 rpm shaking. Repeat 4 times to remove unbounded components in the well.

- Add 10 μL of the TMB working solution (Invitrogen™ SB02) to each well of the 384-well plates for 30 minutes of incubation at 37 °C with protection from light by aluminum foil (ABENA).

- Add 10 μL of the 0.16 M sulfuric acid (Invitrogen™ SS04) to each well of the 384-well plates to stop the reaction.

Acquire and analyze data:

- Acquire the absorbance at 450 nm with 650 nm as the reference within 30 minutes in a microplate reader (TECAN Spark® Cyto).

- In the data analysis software (GraphPad Prism 9), execute statistical tests to verify the beginning hypothesis of the experiment.

3.1.6 Antibody Affinity Measurement

The affinities of antibodies in the samples to CPS12F were determined by competitive ELISA, in which the binding kinetics K_d equals the half-binding concentration of CPS12F.

The protocols were modified from the published study[89].

Table 3.5: List of materials, reagents, equipment, and software used in competitive ELISA.

Product	Producer	Code
384-well clear flat-bottom immuno plate	Thermo Scientific™ Nunc™ MaxiSorp™	464718
96-well conical-bottom plate	Thermo Scientific™ Nunc™ Microwell™	249662
polysaccharide, purified type 12F	SSI Diagnostica	76939
phosphate-buffered saline (PBS)	Gibco™	10010015
sealing tape	Thermo Scientific™	15036
20 × PBS Tween™ 20 buffer	Thermo Scientific™ Pierce™	28352
ELISA assay buffer (5 ×)	Invitrogen™	DS98200
goat anti-mouse IgG H&L (HRP)	abcam	ab6789
goat anti-rabbit IgG H&L (HRP)	abcam	ab6721
pneumococcus antiserum type 12b	SSI Diagnostica	16947
ELISA TMB stabilized chromogen	Invitrogen™	SB02
aluminum foil	ABENA	-
ELISA stop solution	Invitrogen™	SS04
shaker	IKA®	VXR basic Vibrax®
microplate reader	TECAN	Spark® Cyto
GraphPad Prism	GraphPad Software, LLC.	9.5.0

Note: The coating concentration should be low enough not to interfere significantly with the binding equilibrium in the solution, which was determined in advance.

Coat and block plates:

- Prepare the CPS12F coating solution (200 ng/mL) in PBS (Gibco™ 10010015). 10 mL is enough for two 384-well plates of the assay. Add 10 µL of coating solution (2 ng of CPS12F) to each well of the 384-well immunoassay plates (Nunc™ MaxiSorp™ 464718). Seal the plates with sealing tape (Thermo Scientific™ 15036) and incubate them at 2–8 °C for 18 hours.

- Prepare PBST working solution (1 ×, PBS + 0.05 % (w/v) Tween 20) by diluting 25 mL of

PBST stock solution ($20 \times$, Thermo Scientific™ Pierce™ 28352) to 500 mL with ultra-pure water; 500 mL is enough for two 384-well plates assay.

- Prepare BSA working solution ($1 \times$, buffered solution with bovine protein): dilute 20 mL of assay buffer stock solution ($5 \times$, Invitrogen™ DS98200) to 100 mL with ultra-pure water; 100 mL is enough for two 384-well plates of the assay, including sample and antibody dilution.

- Dump the plate to discard the solution in the well and tap it on tissues. Add 50 μL of PBST per well and let the plates soak for 1 minute with 100 rpm shaking (IKA® VXR basic Vibrax®). Repeat 3 times to remove unbounded components in the well.

- Add 50 μL of BSA working solution to each well of the 384-well plates for 1 hour of incubation at 37 °C to block the uncoated area in the well.

Add samples and develop reactions:

- During the blocking, take out the sample from -80 °C and let the sample melt at room temperature. Use commercial antiserum (SSI Diagnostica 16947) as a positive and normalizing control. Dilute testing samples by 500 folds with BSA working solution.

- In a conical-bottom 96-well plate (Thermo Scientific™ Nunc™ Microwell™ 249662), serially dilute the CPS12F by 5 folds at 25 μL (20 μL left), add 20 μL of the diluted testing samples for 1 hour of incubation at 37 °C.

- Dump the blocked plate to discard the solution in the well and tap it on tissues. Add 10 μL of the testing mixture to each well of the 384-well plate for 1 hour of incubation at 37 °C.

- Dump the plate to discard the solution in the well and tap it on tissues. Add 50 μL of PBST per well and let the plates soak for 1 minute with 100 rpm shaking. Repeat 3 times to remove unbounded components in the well.

- Prepare the detecting antibody stock solution ($100 \times$) by diluting antibodies with BSA working solution: HRP-conjugated goat anti-mouse IgG$_{poly}$ (40 µg/mL, abcam, ab6789) and goat anti-rabbit IgG$_{poly}$ (2 µg/mL, abcam, ab6721). Prepare the detecting antibody working solution ($1 \times$) by diluting 100 µL of the detecting antibody stock solution to 10 mL with assay buffer; 10 mL is enough for two 384-well plates assay.

- Add 10 µL of the detecting antibody working solution to each corresponding well of the 384-well plate for 1 hour of incubation at 37 °C.

- Dump the plate to discard the solution in the well and tap it on tissues. Add 50 µL of PBST per well and let the plates soak for 1 minute with 100 rpm shaking. Repeat 4 times to remove unbounded components in the well.

- Add 10 µL of the TMB working solution (Invitrogen™ SB02) to each well of the 384-well plates for 30 minutes of incubation at 37 °C with protection from light by aluminum foil (ABENA).

- Add 10 µL of the 0.16 M sulfuric acid (Invitrogen™ SS04) to each well of the 384-well plates to stop the reaction.

Acquire and analyze data:

- Acquire the absorbance at 450 nm with 650 nm as the reference within 30 minutes in a microplate reader (TECAN Spark® Cyto).

- In the data analysis software (GraphPad Prism 9), calculate binding rates, fit them with CPS12F concentrations into binding curves via one-site total binding model, interpolate the half-binding concentration of CPS12F as the equilibrium dissociation constant K_d, and execute statistical tests for further conclusions.

3.1.7 Protection Efficacy Evaluation *In Vitro*

The vaccine's protective efficacy was evaluated *in vitro* via the opsonophagocytic killing assay (OPKA).

The protocols were modified based on the public materials[90].

Table 3.6: List of materials, reagents, equipment, and software used in OPKA.

Product	Producer	Code
pneumococcus strain serotype 12F	SSI Diagnostica	82201
Todd-Hewitt broth	OXOID™	CM0189B
yeast extract	Fisher BioReagents™	BP1422
autoclavor	HICLAVE™	HV-50
culture tube	Falcon®	352001
CO_2 incubator	BINDER	CB-S 170
cell density meter	biochrom	Ultrospec® 10
dehydrated blood agar base	OXOID™	CM0854B
defibrinated sheep blood	OXOID™	SR0051B
Petri dish	SARSTEDT	82.1472.001
sealed box	IKEA®	803.931.31 & 303.930.63
anaerobic gas-generating sachet	Thermo Scientific™	AN0025A
resazurin anaerobic indicator	Thermo Scientific™	BR0055B
glycerol	Invitrogen™	15514011
cryogenic vial	SARSTEDT	72.379
dehydrated agar	BD BACTO™	214010
square 12 cm × 12 cm Petri dish	Gosselin™	BP124-05
triphenyltetrazolium chloride (T.T.C.)	OXOID™	SR0148A
class II biosafety cabinet	Ninolab	ninoSAFE class II
96-well conical-bottom plate	Thermo Scientific™	249662
phosphate buffered saline	Gibco™	10010015
multichannel pipette	SARTORIUS	LH-929230
HL-60	ATCC®	CCL-240™
fetal bovine serum	Gibco™	A3160802
RPMI 1640 with GlutaMAX™	Gibco™	61870010
15 mL centrifuge tube	greiner BIO-ONE	CELLSTAR™ 188271
centrifuge	Thermo Scientific™	Multifuge™ X1R 75004250
automated cell counter	Invitrogen™	Countless II
cell counting chamber slides	Invitrogen™	C10228
25 cm^2 cell culture flask	Nunc™ EasYFlask™	156367
75 cm^2 cell culture flask	Nunc™ EasYFlask™	156499
dimethyl sulfoxide (DMSO)	Sigma-Aldrich®	D8418
controlled-rate freezing container	Corning®	CoolCell®
-152 °C freezer	PHCbi	MDF-1156
N,N-dimethylformamide (DMF)	Thermo Scientific™	210585000
baby rabbit complement	MP Biomedicals	08642961
water bath	VWR®	VWB2 26 462-0559
1.5 mL microcentrifuge tubes	Thermo Scientific™	3451
gelatin	Thermo Scientific™	410875000
Hanks' balanced salt solution (HBSS)	Gibco™	24020091
pneumococcus antiserum type 12b	SSI Diagnostica	12947
microcentrifuge	VWR®	Micro Star 17
HBSS ($-Ca^{2+}-Mg^{2+}$)	Gibco™	14175095
Nist's integrated colony enumerator (NICE)	National Institute of Standards and Technology	doi:10.18434/M32073
GraphPad Prism	GraphPad Software, LLC.	9.5.0

S. pneumoniae 12F strain (SSI Diagnostica 82201) recovery:

- Prepare THY broth (Todd-Hewitt broth with 0.5 % (w/v) yeast extract): add 15 g of dehy-

drated Todd-Hewitt broth (OXOID™ CM0189B) and 2.5 g of yeast extract (Fisher BioRe-agents™ BP1422) to 500 mL of ultra-pure water in a 1 L glass media bottle; mix well; sterilize it by autoclaving at 121 °C for 35 minutes (HICLAVE™ HV-50); store it at 2–8 °C.

- For lyophilized strain in an ampoule: scratch the narrow part with an ampoule file; decon-taminate and wrap the ampoule outer surface with ethanol-sprayed tissues; carefully break the scratched point to open the ampoule; add 1 mL of THY broth to reconstitute the bacteria solution.

- For cryopreserved strain in a vial: immerse the bacteria cryogenic vial into a 37 °C water bath with its cap above the water until only a few ice crystals remain (approximate 2 minutes); ster-ilize the vial outer surface with 70 % ethanol spray.

- Transfer the bacteria suspension to a 14 mL culture tube (Falcon® 352001) containing 6 mL of THY broth. Keep the tube cap vented and incubate it in a 5 % (v/v) CO_2 (recommended but not mandatory) 37 °C incubator (BINDER CB-S 170) until its OD_{600} (biochrom Ultrospec ® 10) reaches 0.8 ($\sim$ 8 hours).

S. pneumoniae 12F colony isolation and α-hemolytic test:

- Prepare blood agar plates: add 8 g of dehydrated blood agar base (OXOID™ CM0854B) to 200 mL of ultra-pure water in a 500 mL glass media bottle; mix well; sterilize it by autoclaving at 121 °C for 35 minutes and cool it to 45 °C; supplement it with 15 mL of defibrinated sheep blood (OXOID™ SR0051B); transfer 15 mL of it to each 92 mm Petri dish (SARSTEDT 82.1472.001) with serological pipettes; wait for $\sim$ 20 minutes for it to solidify and prevent later moisture condensing; label the plates; seal the plates with parafilm to avoid dehydration and contamination; store them upside down at 2–8 °C.

- Streak 100 μL of bacteria solution to a blood agar plate with a pipette tip. Incubate it in a 5 % (v/v) CO_2 37 °C incubator for 18 hours to obtain isolated colonies.

- For the α-hemolytic test, the inoculated blood agar plate was incubated anaerobically in a sealed box (IKEA® 803.931.31 & 303.930.63) with an anaerobic gas generating sachet (Thermo Scientific™ AN0025A) and a resazurin anaerobic indicator (Thermo Scientific™ BR0055B) in a 37 °C incubator for ∼ 18 hours. The α-hemolytic property was indicated by a green halo surrounding the colony.

S. pneumoniae 12F propagation and cryopreservation of the assay stock:

- Prepare 80 % (v/v) glycerol solution: add 80 mL of glycerol (Invitrogen™ 15514011) to 20 mL of ultra-pure water in a 250 mL glass media bottle; mix well; sterilize it by autoclaving at 121 °C for 35 minutes; store it at room temperature.

- Transfer 1 isolated colony to a 15 mL culture tube containing 7 mL of THY broth by a pipette tip. Incubate it in a 5 % (v/v) CO_2 37 °C incubator until its OD_{600} reaches 0.8 (∼ 8 hours).

- Mix bacteria solution (OD_{600} = 0.8), fresh THY broth, and 80 % (v/v) glycerol solution by 2:2:1. Aliquot 0.5 mL of the mixture to each cryogenic vials (SARSTEDT 72.379). Freeze and store the vials at -80 °C.

CFU quantification of the assay stock:

- Prepare THYA plates (Todd-Hewitt broth with 0.5 % (w/v) yeast extract agar plates): dissolve 12 g of dehydrated Todd-Hewitt broth, 2 g of yeast extract and 6 g of dehydrated agar (BD BACTO™ 214010) in 400 mL of ultra-pure water in a 500 mL glass media bottle; sterilize it by autoclaving at 121 °C for 35 minutes; cool it to 56 °C in a water bath; transfer 25 mL of it to each square 12 cm × 12 cm Petri dish (Gosselin™ BP124-05) with serological pipettes;

wait for $\sim$ 20 minutes for it to solidify; label the plates; seal the plates with parafilm to prevent dehydration and contamination; store them upside down at 2 – 8 °C. 400 mL of the agar is enough for producing 16 plates.

- Prepare overlay agar: add 3 g of dehydrated Todd-Hewitt broth, 0.5 g of yeast extract, and 1.5 g of dehydrated agar to 100 mL of ultra-pure water in a 250 mL glass media bottle; sterilize it by autoclaving at 121 °C for 35 minutes; cool and keep it at 56 °C; add 2 mL 50 × (1.25 mg/mL) T.T.C. solution (OXOID™ SR0148A) before use. 100 mL of the agar is enough for 4 plates assay.

- Dry the THYA plates by placing them in a class II biosafety cabinet (Ninolab ninoSAFE class II) with lids off for $\sim$ 30 minutes, which can homogenize the colony distribution.

- Thaw a cryopreserved assay stock. Serially dilute the bacteria suspension by 5 folds at 50 μL (40 μL left) for 12 levels in quadruplicate in a 96-well conical-bottom plate (Thermo Scientific™ 249662) with PBS (Gibco™ 10010015).

- Spot 10 μL of each suspension on a THYA plate with a multichannel pipette (SARTORIUS LH-929230); after each spotting, tilt the plate immediately to shape the spots into $\sim$ 2 cm strips. Dry the plates in the biosafety hood with the lid off for 5 minutes. Pour 25 mL of the overlay agar into each plate, and wait for $\sim$ 15 minutes for the medium to solidify.

- Invert the plates and incubate them at 37 °C for 18 hours.

- Photo the plates; count the colonies with NICE (NIST's Integrated Colony Enumerator); calculate the CFU in each vial.

HL-60 thaw and passaging:

- Prepare cell culture medium: add 50 mL ($\sim$ 10 %, v/v) of HIFBS (Gibco™ A3160802) to 500 mL RPMI 1640 with GlutaMAX™ (Gibco™ 61870010); mix well; store it at 2–8 °C.

- Immerse the HL-60 cryogenic vial (ATCC® CCL-240™) into a 37 °C water bath with its cap above the water until only a few ice crystals remain (approximately 2 minutes). Sterilize the vial's outer surface with 70 % ethanol. Transfer the cell suspension to a 15 mL centrifuge tube (greiner BIO-ONE CELLSTAR™ 188271) containing 9 mL cell culture medium for 5 minutes of centrifugation (Thermo Scientific™ Multifuge™ X1R 75004250) at 400 $\times$ g and room temperature to remove DMSO. Resuspend the cells in the cell culture medium at $\sim 2 \times 10^5$ cells/mL (Invitrogen™ Countless II & C10228). Transfer the cell suspension to a 25 cm² cell culture flask (Nunc™ EasYFlask™ 156367) and incubate it in a 5 % (v/v) CO_2 37 °C incubator (about 5 days).

- When the cell density reaches $\sim 8 \times 10^5$ cells/mL, transfer 10 mL of the cell solution to a 75 cm² cell culture flask (Nunc™ EasYFlask™ 156499) and supplement it with 40 mL of cell culture medium.

- Don't let the cell density lower than 1×10^5 or higher than 1×10^7 cells/mL.

HL-60 cryopreservation:

- Prepare fresh cryopreservation medium: add 1 mL (10 %, v/v) of DMSO (Sigma-Aldrich® D8418) to 9 mL of cell culture medium; mix well.

- Centrifuge HL-60 cells at 400 $\times$ g for 5 minutes at room temperature. Resuspend cells in the cryopreservation medium at 1×10^7 cells/mL. Aliquot 1 mL of the cell suspension to each 1.5 mL cryogenic vial. Freeze the vials to -80 °C at -1 °C/min with a controlled-rate freezing container (Corning® CoolCell®). Store them in a -152 °C freezer (PHCbi MDF-1156)。Two 75

cm^2 cell culture flask containing 100 mL 8×10^5 cells/mL of HL-60 produces approximately 8 vials.

HL-60 differentiation (two weeks after the thaw):

- Prepare differentiation medium: add 10 mL (~10 %, v/v) of HIFBS and 0.8 mL (~0.8 %, v/v) of DMF (Thermo Scientific™ 210585000) to 100 mL of RPMI 1640 with GlutaMAX™; mix well, store it at 2–8 °C.

- Centrifuge HL-60 cells at $400 \times g$ for 5 minutes at room temperature; Resuspend cells in the differentiation medium at 4×10^5 cells/mL. Transfer 50 mL cell suspension to a 75 cm^2 cell culture flask and incubate them in a 5 % (v/v) CO$_2$ 37 °C incubator for 5 days. One 75 cm^2 cell culture flask containing 50 mL of HL-60 is enough for four 96-well plates assay.

Complement preparation:

- Prepare the baby rabbit complement working stock: thaw the baby rabbit complement (MP Biomedicals 08642961) under room temperature; aliquot 1 mL of it into 1.5 mL microcentrifuge tubes and store it at -80 °C.

- Prepare the heat-inactivated baby rabbit complement working stock: incubate 1 mL of the thawed baby rabbit complement in a 56 °C water bath for 30 minutes (VWR® VWB2 26 462-0559); aliquot 100 μL of it into 1.5 mL microcentrifuge tubes (Thermo Scientific™ 3451) and store it at -80 °C.

- Avoid repeated freeze-thaw cycles of the complement. One working stock is enough for one 96-well plate assay.

Coculture:

- Prepare THYA plates and overlay agar as described in "CFU quantification of assay stocks".

- Prepare 1 % (w/v) gelatin solution: add 1 g of gelatin (Thermo Scientific™ 410875000) to 100 mL of ultra-pure water in a 100 mL glass media bottle; mix well; sterilize it by autoclaving at 121 °C for 35 minutes; store it at room temperature.

- Prepare fresh opsonization buffer: add 10 mL of 1 % (w/v) gelatin solution and 5.3 mL of HIFBS to 90 mL of HBSS (Gibco™ 24020091); mix well.

- Use pneumococcus antiserum type 12b (SSI Diagnostica 12947) treated with baby rabbit complement as the positive control and treated with heat-inactivated baby rabbit complement as the negative control. Deactivate endogenous complement by incubating samples and controls in a 56 °C water bath for 30 minutes; transfer 30 µL of each to a 96-well conical-bottom plate and serially dilute them by 3 folds at 30 µL (20 µL left) for 11 levels with opsonization buffer.

- Thaw a cryopreserved bacteria assay stock by immersing the bacteria cryogenic vial into a 37 °C water bath with its cap above the water until only a few ice crystals remain ($\sim$ 2 minutes). Sterilize the vial's outer surface with 70 % ethanol. Transfer the bacteria suspension to a 1.5 mL microcentrifuge tube containing 0.5 mL of the opsonization buffer for 5 minutes of centrifugation (VWR® Micro Star 17) at 12000 $\times$ g and room temperature. Resuspend the bacteria in the opsonization buffer at 50000 CFU/mL. 1 mL of the bacteria suspension is enough for 1 96-well plate assay, and prepare 1 mL more if using a multichannel pipette. Add 10 µL of the bacteria suspension to each well of the 96-well plate for 30 minutes of incubation at room temperature.

- Centrifuge HL-60 cells at 400 $\times$ g for 5 minutes at room temperature. Resuspend cells in HBSS (-Ca^{2+}-Mg^{2+}, Gibco™ 14175095) at 1×10^7 cells/mL. Centrifuge cells at 400 $\times$ g for 5 minutes at room temperature. Resuspend cells in HBSS (Gibco™ 24020091) at 1×10^7 cells/mL. Mix 4 mL of HL-60 with 1 mL of complement for samples and positive control

assay. 4.2 mL of the mixture is enough for 1 96-well assay, but prepare 1 mL more if using a multichannel pipette. Mix 0.8 mL of HL-60 with 0.2 mL of HI complement for negative control assay.

- Add 50 μL of the mixture to each well of the 96-well plate for 45 minutes of incubation in a 5 % (v/v) CO_2 37 °C incubator. The HL-60 is sensitive to the CO_2 concentration; therefore, don ' t open the cabinet during incubation. After incubation, place the 96-well plate at 2–8 °C in the fridge for 20 minutes to stop phagocytosis.

- Dry the THYA plates in a biosafety hood with lids off for 30 minutes, which can homogenize the colony distribution.

- Add 10 μL of each final mixture by row to the THYA plates with a multichannel pipette. After each addition, tilt the plate immediately to shape the samples into ∼ 2 cm strips. Dry the plates in the biosafety hood with the lid off for 20 minutes. Pour 25 mL of the overlay agar into each plate, and wait for ∼ 20 minutes for the medium to solidify.

- Invert the plates and incubate them at 37 °C for 18 hours.

Survival bacteria colony counting and half-killing dilution fold interpolation:

- Photo the plates and count the colonies with the software NICE[91].

- In GraphPad Prism 9, fit the data in sigmoidal & 4 parameters logistical curves, interpolate the half-killing dilution folds, and execute Dunnett's T3 multiple comparisons tests to assess statistical differences.

3.1.8 Protection Efficacy Evaluation *In Vivo*

The vaccine's protective efficacy was evaluated *in vivo* through the bacteria challenge study.

Table 3.7: List of materials, reagents, equipment, and software used in bacteria challenge.

Product	Producer	Code
pneumococcus strain serotype 12F	SSI Diagnostica	82201
phosphate-buffered saline (PBS)	Gibco™	10010015
GraphPad Prism	GraphPad Software, LLC.	9.5.0

Challenge mice:

- Thaw a vial of cryopreserved *S. pneumoniae* 12F (SSI Diagnostica 82201) and dilute it to 2×10^7 CFU/mL with PBS (Gibco™ 10010015).

- Challenge vaccinated mice with 50 µL of bacteria suspension containing 1×10^6 CFU of *S. pneumoniae* 12F by intranasal instillation.

- Observe the challenged mice twice daily for the following 2 weeks. At the end of the study, euthanize all survived mice by cervical dislocation.

Humane endpoint:

- This bacteria challenge study generally only causes mild to moderate adverse effects, pain, or distress to the mice. To secure animal welfare, we set the criteria below as the experiment's humane endpoint.

- Weight loss > 20 %.

- Labored respiration with increased respiratory rate, effort, or strong abdominal breathing.

- Rough hair coat, unkempt appearance, hunched posture.

- Lethargy or persistent recumbency.

- Loss of righting reflex or failure to maintain equilibrium.

Acquire and analyze data:

- Record the death of mice during the study.

- In the data analysis software (GraphPad Prism 9), draw survival curves and execute Gehan-Breslow-Wilcoxon tests to assess statistical differences.
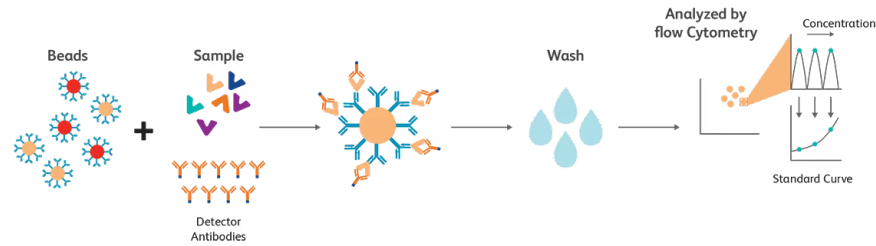
3.2 Cytokine Quantification

Figure 3.4: Cytometric bead array (CBA) flow cytometry (FCM) assay, retrieved from BD Biosciences[92].

We first investigated if Lipo$^+$CPS12F&αGC can invoke cells to secrete pro-inflammatory cytokines, including IL-12, IFN-γ, IL-4, and IL-17 by BD$^{\text{TM}}$ cytometric bead array (CBA) flow cytometry (FCM) assays (Figure 3.4, protocols: subsection 3.1.2).
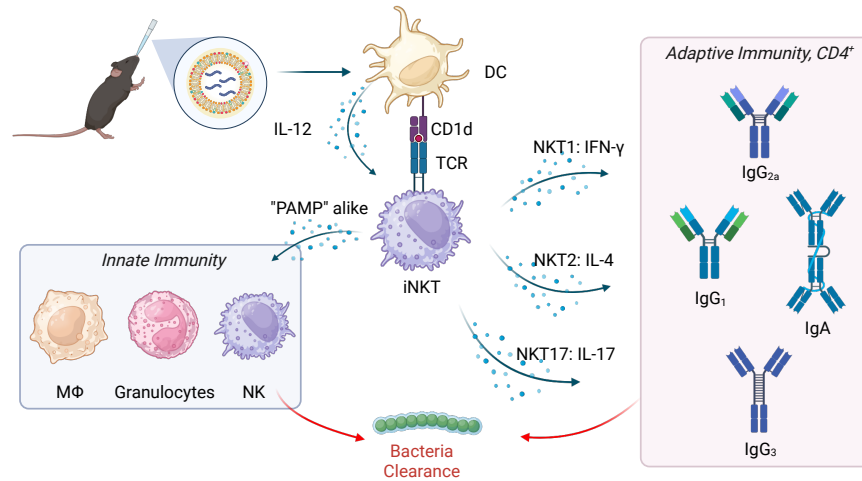

Figure 3.5: Cytokines secretion after vaccination. The illustration was created with BioRender.

As depicted in Figure 3.5, antigen-presenting cells (e.g., dendritic cells) secrete IL-12, which helps iNKT cells activate and proliferate; iNKT cells further secrete IFN-γ, IL-4, and IL-17, which sepa-

rately promote their differentiation into NKT1, NKT2, and NKT17. Combinations of the cytokines will create different cytokine milieus, which will steer the final immune responses[93].
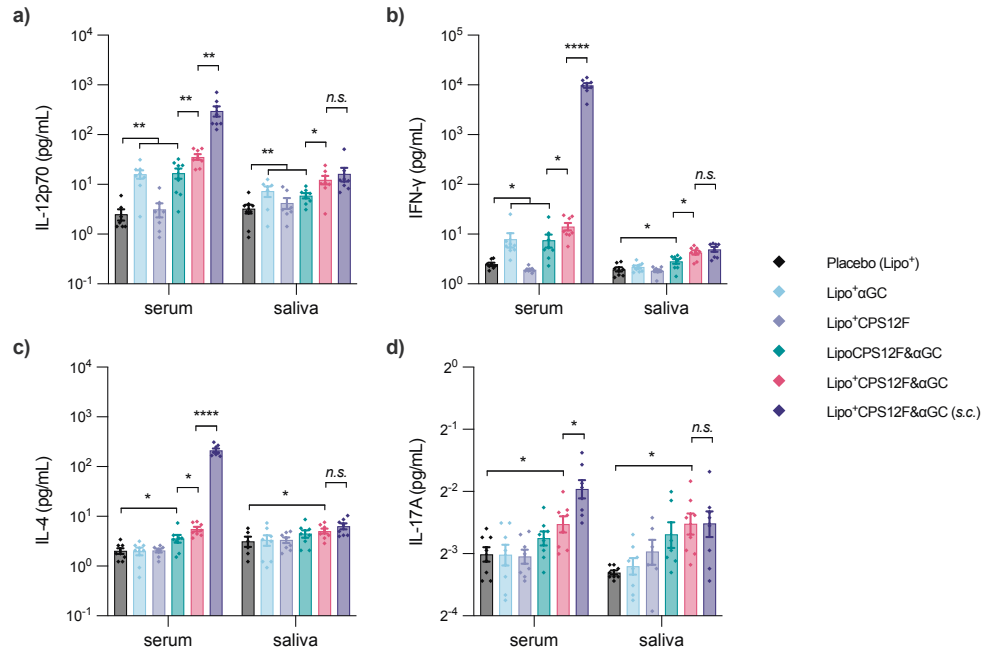

Figure 3.6: Lipo⁺CPS12F&αGC stimulated elevated pro-inflammatory cytokines secretion compared with other formulations. Concentrations of **a)** IL-12p70, **b)** IFN-γ, **c)** IL-4, and **d)** IL-17A in serum and saliva. BALB/cJRj mice were immunized with Lipo⁺ (group 1, blank cationic liposomes as placebo), Lipo⁺αGC (group 2), or 3 nmol antigen (repeat units of the polysaccharides) in Lipo⁺CPS12F (group 3), LipoCPS12F&αGC (group 4), or Lipo⁺CPS12F&αGC (group 5 & 6) via intranasal instillation (*i.n.*, group 1 − 5) or subcutaneous injection (*s.c.*, group 6). Serum and saliva were collected 18 hours after the priming vaccination, and IL-12p70, IFN-γ, IL-4, and IL-17A inside were quantified via cytometric bead array flow cytometry. Data were plotted as mean ± SEM (*n*=8). Welch's ANOVA tests and multiple comparisons were executed to assess statistical significance. *, **, ***, **** represent P<0.1, P<0.01, P<0.001, P<0.0001.

Lipo⁺CPS12F&αGC, when delivered intranasally (group 5) or subcutaneously (group 6), both induced the elevation of IL-12, IFN-γ, IL-4, and IL-17 levels (Figure 3.6 a − d). Compared with the *s.c.* route, the *i.n.* route raised comparable cytokines in the saliva but fewer in the serum, which represents the respiratory mucosal (nasal- and inducible bronchus-associated lymphoid tissue, NALT and iBALT, see Figure 1.9) and systemic immune responses separately. It indicated the *i.n.* route is suitable

for inducing localized airway mucosal immune responses. Still, the *s.c.* route remained a safe option as the mice thrived after receiving it. The cationic formulation (group 5) presented more potential in cytokine stimulation than the neutral formulation (group 4), although the differences were slight. The secretion of IL-12 and IFN-γ displayed a strong correlation with iNKT agonist αGC, as the cationic liposomal αGC (group 2) independently induced the production of IL-12 and IFN-γ.

Overall, these results showed that Lipo$^+$CPS12F&αGC successfully stimulated the secretion of pro-inflammatory cytokines. The liposome surface charge, αGC, and immunization route all played a role in this effect. The combination of these cytokines could further activate immune cells and enhance both innate and adaptive immune responses.

3.3 CELL PHENOTYPING

We then assessed whether Lipo⁺CPS12F&αGC could activate iNKT and B cells in the systemic and mucosal immune systems by multi-color flow cytometry (protocols: subsection 3.1.3).
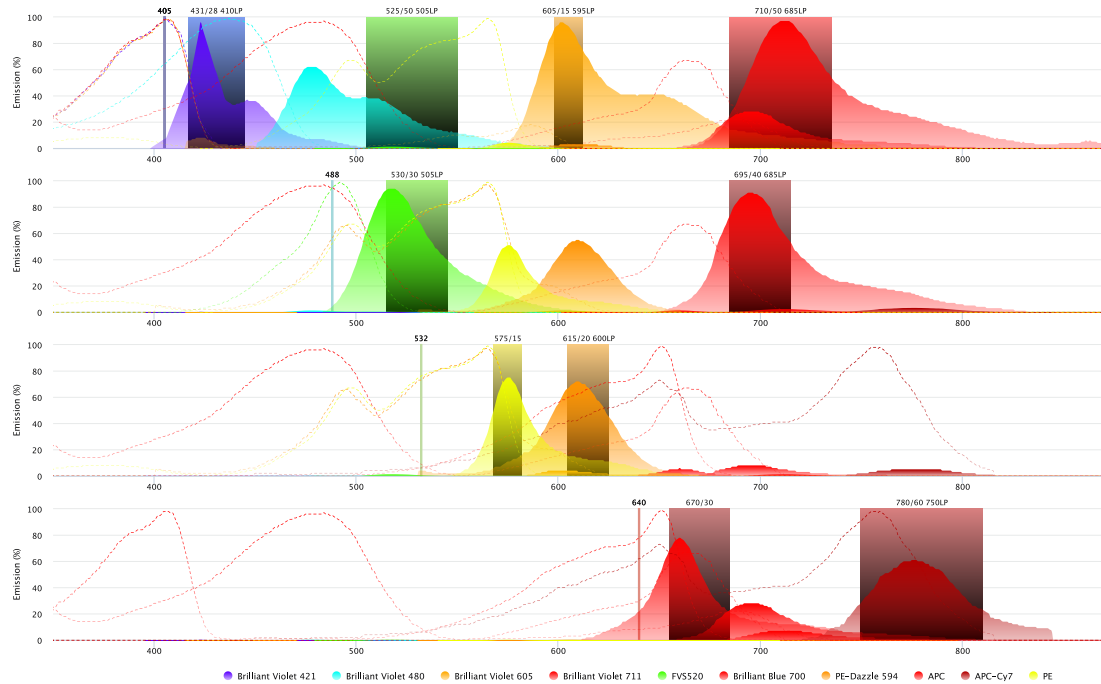

Figure 3.7: Fluorescence panel for cell phenotyping. The dashed and area curves show the excitation and emission of fluorophores. The bold lines represent the lasers, and the rectangles are filters. The illustration was created with **Spectra**Viewer™ from FluoroFinder[94].

The fluorescence panel (Figure 3.7) was established based on the instrument (BD© LSRFortessa™) configuration and the fluorophore spillover spreading matrix (SSM, provided by Dr. Morten Løbner[95] at BD Biosciences™).

Similar to conventional T_{FH} cells, activation of iNKTs (CD69/25⁺[84]) and their differentiation into NKT_{FH} (CXCR5⁺) provided critical and prolonged support[38] of B cells during its somatic hypermutation into mature plasma cells (CD27⁺CD138⁺), which produce and secrete high-affinity IgA
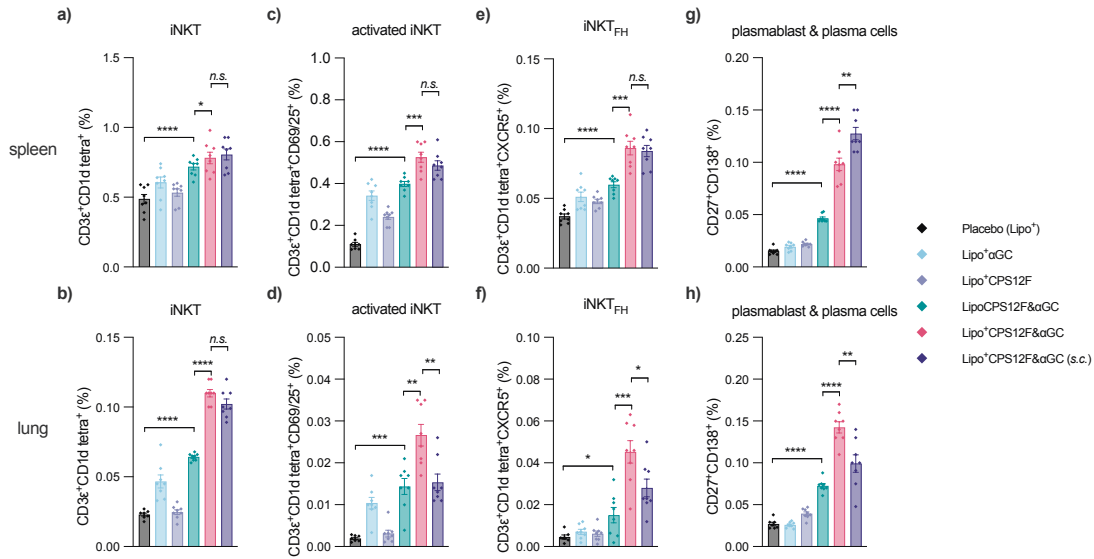
and IgG antibodies.

Figure 3.8: Lipo$^+$CPS12F&αGC initiated a higher level of iNKT cell activation and B cell maturation compared with other formulations. Percentage of **a & b)** iNKT cells (CD3ε$^+$CD1d tetra:αGC$^+$), **c & d)** activated iNKT cells (CD3ε$^+$CD1d tetra:αGC$^+$CD69/25$^+$), **e & f)** follicular helper iNKT cells (CD3ε$^+$CD1d tetra:αGC$^+$CXCR5$^+$), and **g & h)** plasmablast and plasma cells (CD27$^+$CD138$^+$) to total viable cells in the spleen and lung, separately. BALB/cJRj mice were immunized with Lipo$^+$ (group 1, blank cationic liposomes as placebo), Lipo$^+$αGC (group 2), or 3 nmol antigen (repeat units of the polysaccharides) in Lipo$^+$CPS12F (group 3), LipoCPS12F&αGC (group 4), or Lipo$^+$CPS12F&αGC (group 5 & 6) via intranasal instillation (*i.n.*, group 1–5) or subcutaneous injection (*s.c.*, group 6) for 3 times at 2 weeks intervals. Spleen and lung were isolated 3 days after the final vaccination and analyzed via multi-color flow cytometry. Data were plotted as mean $\pm$ SEM (*n*=8). Welch and Brown-Forsythe ANOVA with Dunnett's T3 multiple comparisons tests were done to assess statistical significance. *, **, ***, **** represent P<0.1, P<0.01, P<0.001, P<0.0001.

Compared with mice that received the placebo formulation (group 1), mice vaccinated with Lipo$^+$CPS12F&αGC (group 5 & 6) exhibited increased levels of iNKTs proliferation (Figure 3.8 a & b), activation (Figure 3.8 c & d), differentiation into the follicular helper phenotype (Figure 3.8 e & f), and B cells maturation into plasmablast and plasma cells (Figure 3.8 g & h). For iNKTs, in the spleen, the effect between the intranasally (group 5) and subcutaneously (group 6) vaccinated group was comparable since no statistically significant difference was observed; in contrast, in the lung, results showed that *i.n.* vaccination tended to be more effective than *s.c.* vaccination. For B cells, the correlation between

the vaccination route and response location was more evident, as the *s.c.* and *i.n.* vaccination generated more plasma cells in the spleen and lung respectively. Also, results revealed that the cationic liposomal formulation (group 5) displayed a significantly higher efficiency in both iNKT and B cells stimulation than the neutral liposomal formulation (group 4), which might be due to its help in the attachment to the negatively charged airway mucosal. It's noticeable that the antigen alone group (group 3) elicited small iNKT and B cells responses, which verified that carbohydrate antigen is poorly immunogenic and hardly activates adaptive immunity as the classical MHC molecule cannot present it.
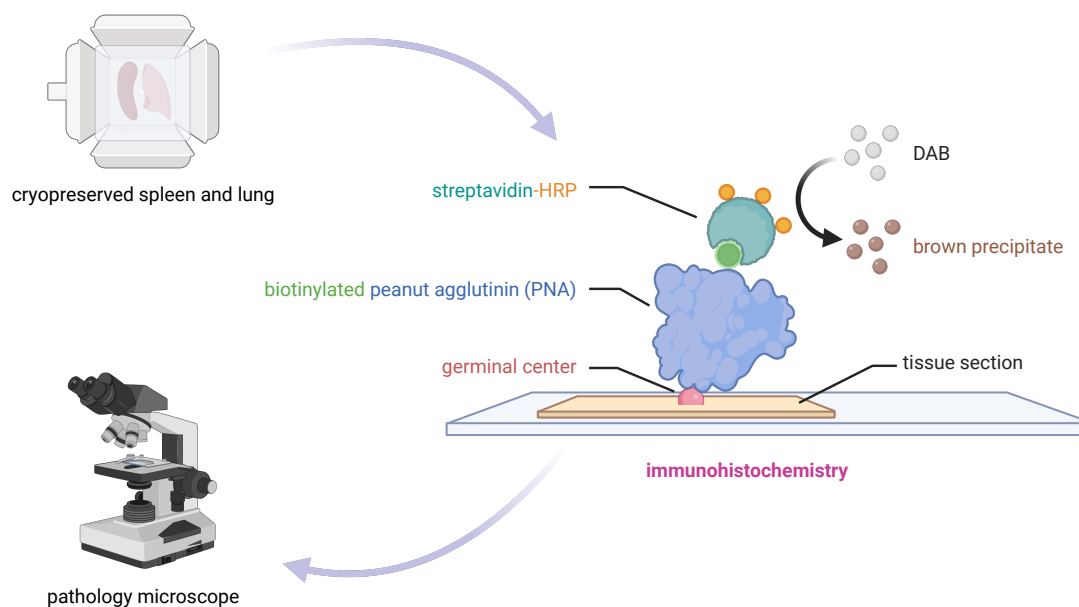
3.4 Organ Examination

Figure 3.9: Germinal centers examination by immunohistochemistry. The illustration was created with BioRender.

We also examined the spleens and lungs of vaccinated mice by immunohistochemistry (IHC, Figure 3.9, protocols: subsection 3.1.4) with help from Susanne Primdahl at DTU Health Tech.
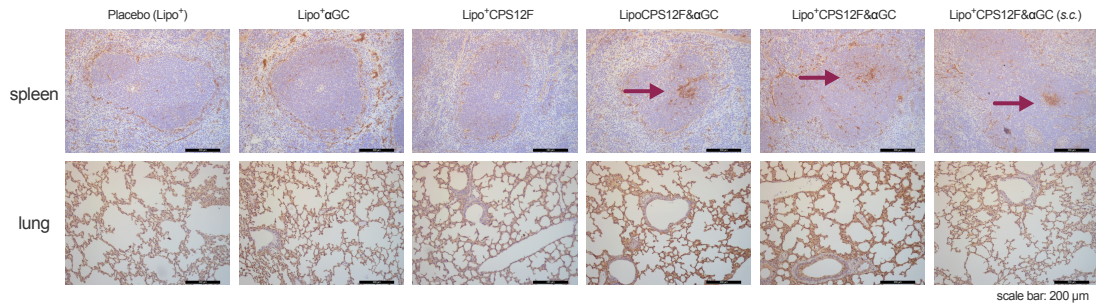
Figure 3.10: Lipo⁺CPS12F&αGC activated the formation of germinal centers. Germinal centers (marked by arrows) formed in spleens and morphology of lung tissues after vaccinations. BALB/cJRj mice were immunized with Lipo⁺ (group 1, blank cationic liposomes as placebo), Lipo⁺αGC (group 2), or 3 nmol antigen (repeat units of the polysaccharides) in Lipo⁺CPS12F (group 3), LipoCPS12F&αGC (group 4), or Lipo⁺CPS12F&αGC (group 5 & 6) via intranasal instillation (*i.n.*, group 1 – 5) or subcutaneous injection (*s.c.*, group 6) for 3 times at 2 weeks intervals. Spleen and lung were isolated 3 days after the final vaccination and examined via immunohistochemistry.

Germinal centers, where B cells mature into plasma cells, were detected in the spleens of mice from group 4–6, proving the effectiveness of the vaccine formulations and that applying them intranasally triggered systemic immune responses similar to the subcutaneous injection. The lung sections displayed an intact morphology, suggesting the intranasal delivery of the vaccine components was safe. Although the flow cytometry result showed the activation of mucosal immunity, we didn't find the inducible bronchus-associated lymphoid tissue (iBALT) in the lung sections. It was likely due to the fact that iBALT is a rare, inducible, and temporary structure which only presents during immune responses and disappears afterward[96].

To conclude, Lipo⁺CPS12F&αGC effectively initiated iNKT-dependent adaptive immune responses and B cell maturation into plasma cells in both the mucosal and systemic immunity. Similar to the results of cytokine analysis, the contributions from liposome surface charge, αGC, and immunization route were also observed here.
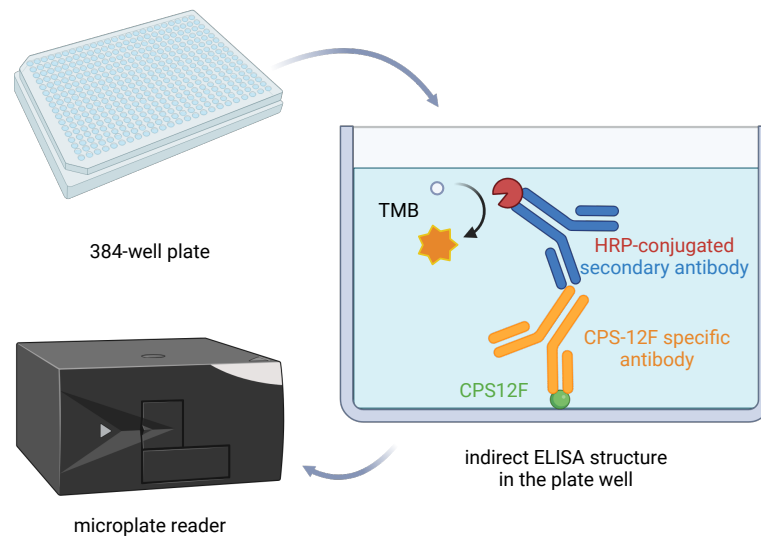
Figure 3.11: Antibody quantification via indirect ELISA. The illustration was created with BioRender.

We next checked the change of antibody levels after priming-booster vaccinations and their isotype composition 2 weeks after being fully immunized by indirect ELISA (Figure 3.11, protocols: subsection 3.1.5).
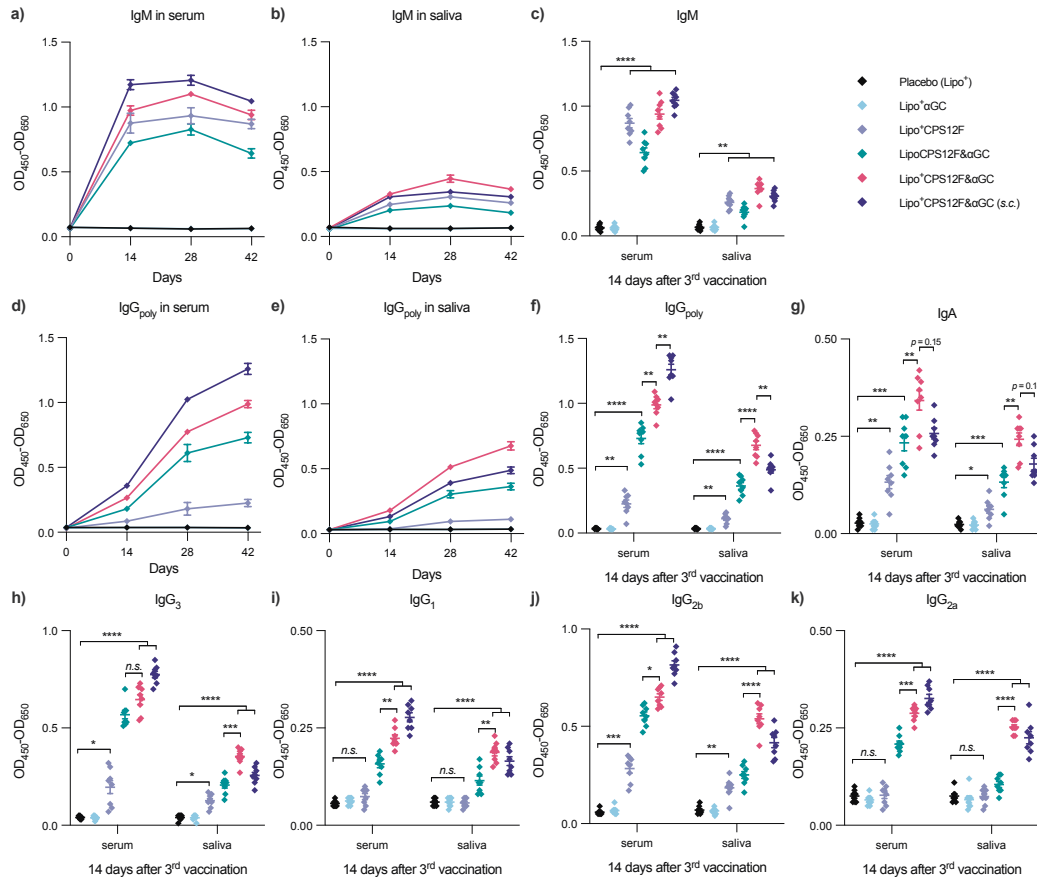
Figure 3.12: Lipo+CPS12F&αGC induces superior CPS12F-specific antibody production compared with other formulations. Change of CPS12F-specific **a & b)** IgM and **d & e)** IgG_{poly} in serum and saliva after immunization. Levels of CPS12F-specific **c)** IgM, **f)** IgG_{poly}, **g)** IgA, **h)** IgG_3, **i)** IgG_1, **j)** IgG_{2b}, **k)** IgG_{2a} in serum and saliva 2 weeks after the final vaccination. BALB/cJRj mice were immunized with Lipo+ (group 1, blank cationic liposomes as placebo), Lipo+αGC (group 2), or 3 nmol antigen (repeat units of the polysaccharides) in Lipo+CPS12F (group 3), LipoCPS12F&αGC (group 4), or Lipo+CPS12F&αGC (group 5 & 6) via intranasal instillation (*i.n.*, group 1−5) or subcutaneous injection (*s.c.*, group 6) for 3 times at 2 weeks intervals. Serum and saliva were collected at the start of the study and 2 weeks after each vaccination. Antibodies inside were quantified via indirect ELISA. Data were plotted as mean $\pm$ SEM (*n* = 8). Welch and Brown-Forsythe ANOVA with Dunnett's T3 multiple comparisons tests were done to assess statistical significance. *, **, ***, **** represent P<0.1, P<0.01, P<0.001, P<0.0001.

All antigen-containing formulations (group 3–6) provoked the secretion of IgM (Figure 3.12 a–c) and IgG_{poly} (Figure 3.12 d–f), which were observed in both the systemic and mucosal immune systems. Different from IgM, which peaked 2 weeks after the 1st booster vaccination, IgG_{poly} level

continued to rise following the priming and booster vaccinations. It validated that IgM is the first responding antibody after stimulation, which can switch into more mature IgG or IgA after B cells go through somatic hypermutation in germinal centers.
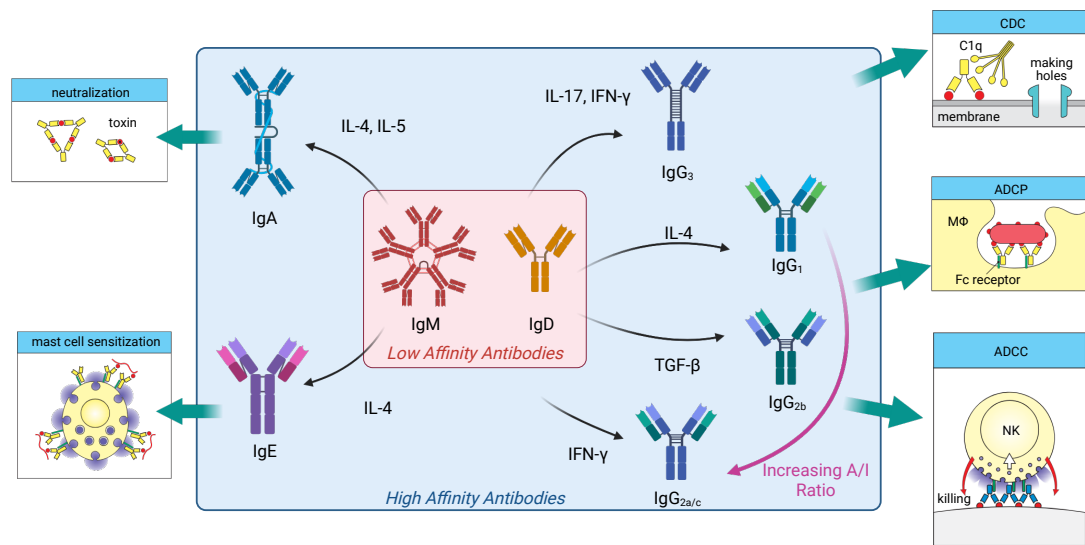

Figure 3.13: The main pathways for antibody functions. CDC: complement-dependent cytotoxicity. ADCP: antibody-dependent cellular phagocytosis. ADCC: antibody-dependent cellular cytotoxicity. The five small pictures were retrieved from the public materials[97]. The illustration was created with BioRender.

IgA is better than IgG in clearing pneumococcus in the respiratory mucosal system (Figure 3.13). Because IgG mainly functions via complement fixation, opsonization, and their mediated phagocytosis and cytotoxicity (CDC, CDCP, ADCC, and ADCP). During these processes, toxins inside, such as pneumolysin, might be released and cause inflammation. In contrast, IgA is safer as it acts by neutralizing and agglutinating the bacteria, which will finally be removed by ciliary motion[98].

Vaccination with Lipo$^+$CPS12F&αGC (group 5 & 6) effectively helped mice produce IgG$_{poly}$ (Figure 3.12 f) and IgA (Figure 3.12 g). While the local-distant effect (e.g., *i.n.* tends to bring stronger immune response in MALT) appeared again in the result of IgG$_{poly}$, it is remarkable that mice vacci-

nated intranasally displayed higher IgA levels in both serum and saliva. Although the differences were not statistically significant, the p-value at 0.14 in saliva suggested the trend. Both results proved that the *i.n.* route was more promising since it produced more IgG and IgA in the mucosal system. Similar to the results above, the positive surface charge also increased the secretion of IgG_{poly} and IgA, further confirming the cationic liposome platform's capability to deliver mucosal vaccine components.

BALB/c mice have four IgG subclasses (3, 1, 2b, and 2a) determined by the heavy chain constant region gene expression on chromosome 12. Interestingly, although the antigen-only formulation (group 3) stimulated the secretion of IgG_{poly}, the subclasses were T-help-limited early-stage IgG_3 (complement fixation only) and IgG_{2b} (FcγR mediated function), not later-stage IgG_1 (amplified power of the FcγR mediated function) and IgG_{2a} (limited inflammation)[93,99]. In contrast, Lipo$^+$CPS12F&αGC induced the production of all four IgG subclasses. These results further confirmed the essential role of αGC in antibody maturation.

3.6   Antibody Affinity Measurement

$$K_D = \frac{[\text{free Ab}][\text{free CPS12F}]}{[\text{Ab-CPS12F complex}]} = [\text{free CPS12F}] \approx [\text{total CPS12F}]$$

when [free Ab]
equals [bound Ab]
(half-binding)

when [bound CPS12F]
is much less than
[total CPS12F]

determine [total CPS12F] when ELISA
has half-maximum readout

quantification of unbound Ab
via competitive ELISA

microplate reader

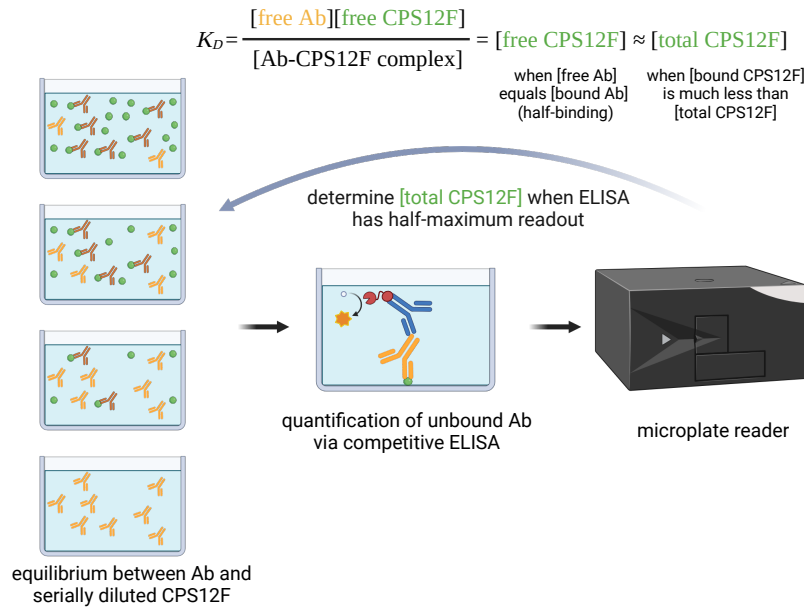equilibrium between Ab and
serially diluted CPS12F

Figure 3.14: Antibody affinity measurement via competitive ELISA. The illustration was created with BioRender.

We further measured the affinity of the antibody in collected samples against CPS12F by competitive ELISA (Figure 3.14, protocols: subsection 3.1.6).
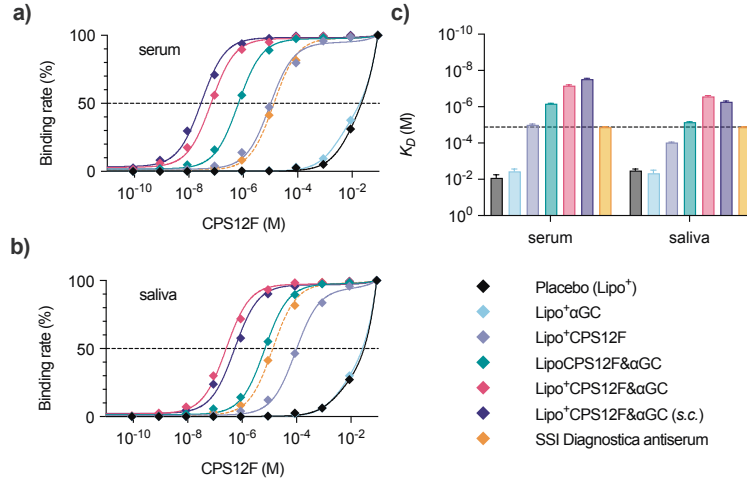
Figure 3.15: Lipo⁺CPS12F&αGC induces high-affinity antibodies against CPS12F both in the systemic and mucosal immune systems. Binding rate curve for CPS12F against **a)** serum antibody and **b)** saliva antibody. **c)** Dissociation constants (K_D) of antibodies in serum and saliva. BALB/cJRj mice were immunized with Lipo⁺ (group 1, blank cationic liposomes as placebo), Lipo⁺αGC (group 2), or 3 nmol antigen (repeat units of the polysaccharides) in Lipo⁺CPS12F (group 3), LipoCPS12F&αGC (group 4), or Lipo⁺CPS12F&αGC (group 5 & 6) via intranasal instillation (*i.n.*, group $1-5$) or subcutaneous injection (*s.c.*, group 6) for 3 times at 2 weeks intervals. Serum and saliva were collected 2 weeks after the final vaccination. Rabbit antiserum against CPS12F from SSI Diagnostica was used as an external control. The antibody affinities were evaluated via competitive ELISA, in which the binding rate refers to the ratio of [Ab bound with suspension CPS12F]/[Ab bound with bottom CPS12F] and the K_D equals the half-binding concentration of CPS12F. Data were plotted as mean $\pm$ SEM (DF=29), and curves were fitted using the one-site total binding model.

Lipo⁺CPS12F&αGC provoked the production of antibodies with higher affinities (Figure 3.15 c: *i.n.* vaccination: $K_{D\_serum} = 66.9 \pm 4.7 \times 10^{-9}M$, $K_{D\_saliva} = 259.5 \pm 19.4 \times 10^{-9}M$; *s.c.* vaccination: $K_{D\_serum} = 29.3 \pm 2.3 \times 10^{-9}M$, $K_{D\_saliva} = 530.9 \pm 49.2 \times 10^{-9}M$) than the commercial high-affinity rabbit antiserum ($K_D = 132.5 \pm 6.4 \times 10^{-7}M$) from SSI Diagnostica. The results indirectly proved that the designed carbohydrate vaccine successfully activated the adaptive immune responses, in which the B cells went through the somatic hypermutation and finally secreted the mature high-affinity antibodies. Similar to the results in the experiments above, iNKT agonist αGC and the cationic liposome both played roles in generating high-affinity antibodies. Furthermore, while *s.c.* injection generated higher affinity antibodies in serum, *i.n.* instillation produced higher

affinity antibodies in saliva. This feature indicated the superiority of *i.n.* vaccination in combating respiratory pathogens.

To sum up, Lipo$^+$CPS12F&αGC efficiently induced the secretion of isotype-switched and affinity-matured CPS12F-specific IgG and IgA both in systemic and mucosal immune systems, which was enhanced by the iNKT agonist αGC and cationic liposome design. The results also suggested that *i.n.* vaccination was more capable of eliciting local airway immune responses.
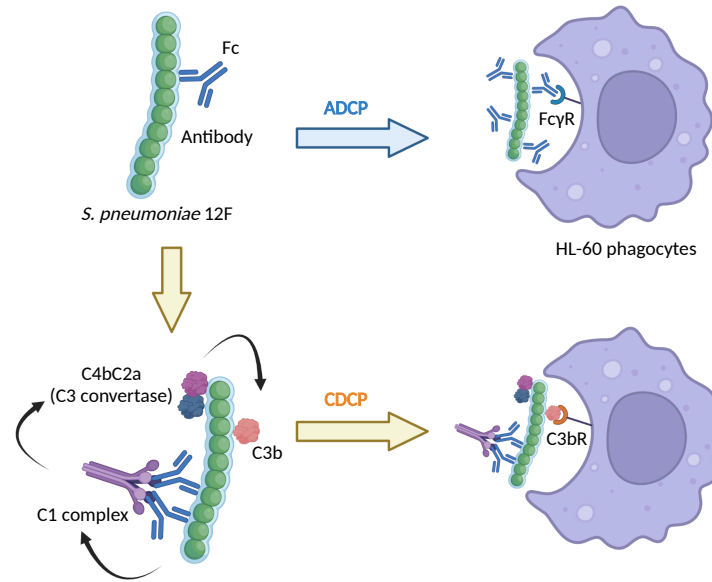
Figure 3.16: Bacteria-killing mechanisms in the opsonophagocytic killing assay (OPKA). ADCP: antibody-dependent cell phagocytosis. CDCP: complement-dependent cell phagocytosis. The illustration was created with BioRender.

We then examined the protective efficacy of the generated antibodies against *S. pneumoniae in vitro* through the opsonophagocytic killing assay (OPKA, protocols: subsection 3.1.7).

The antibody contributed to bacteria clearance (Figure 3.16) mainly by attaching to the pneumococcus surface and mediating phagocytosis by Fc and FcγR recognition (antibody-dependent cellular phagocytosis, ADCP) or contributing to the formation of complement C3b and mediating phagocytosis by C3b and C3bR recognition (complement-dependent cellular phagocytosis, CDCP).
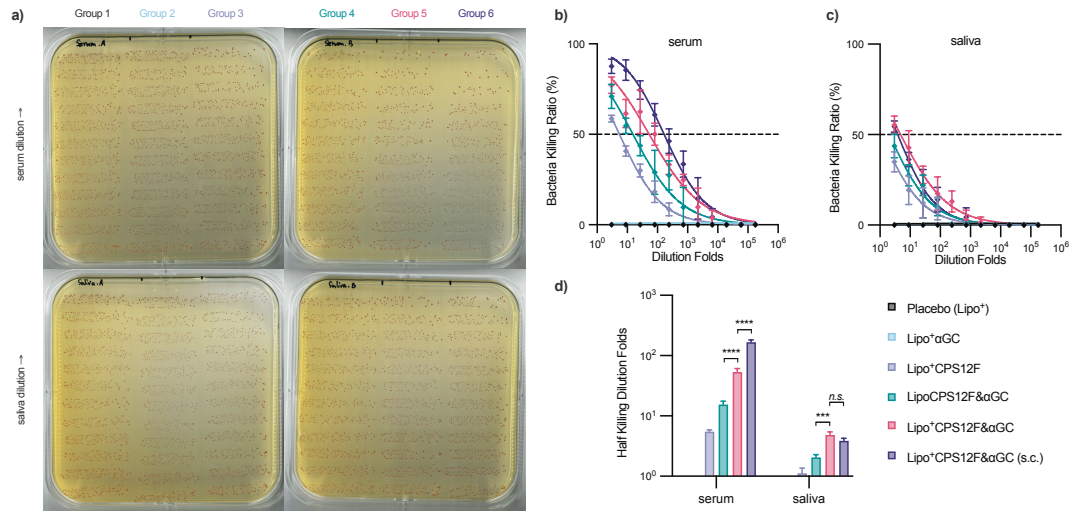
Figure 3.17: Lipo$^+$CPS12F&αGC generates antibodies with improved anti-*S. pneumoniae* 12F activity compared with other formulations. a) Colony dots formed by survived *S. pneumoniae* 12F after opsonophagocytosis. The ratio of bacteria killed by serum **b)** and saliva **c)** antibodies mediated opsonization and phagocytosis at different dilution folds. **d)** Half-killing dilution folds of the antibodies in serum and saliva samples. BALB/cJRj mice were immunized with Lipo$^+$ (group 1, blank cationic liposomes as placebo), Lipo$^+$αGC (group 2), or 3 nmol antigen (repeat units of the polysaccharides) in Lipo$^+$CPS12F (group 3), LipoCPS12F&αGC (group 4), or Lipo$^+$CPS12F&αGC (group 5 & 6) via intranasal instillation (*i.n.*, group 1−5) or subcutaneous injection (*s.c.*, group 6) for 3 times at 2 weeks intervals. Serum and saliva collected 2 weeks after the final vaccination were pooled-assessed via opsonophagocytic killing assay (OPKA). Data were fitted in the nonlinear dose-response model. Half-killing dilution folds were interpolated and plotted as mean ± SEM (DF≥38). Dunnett's T3 multiple comparisons tests were done to assess statistical differences. *, **, ***, **** represent P<0.1, P<0.01, P<0.001, P<0.0001.

The bacteria-killing efficiencies of antibodies were quantified as their half-killing dilution folds (Figure 3.17). The serum and saliva induced by Lipo$^+$CPS12F&αGC (group 5 & 6) both displayed elevated anti-*S. pneumoniae* 12F activity compared with the αGC-lacking (group 3) and neutral liposomal (group 4) formulation, suggesting the significance of iNKT agonist αGC and the cationic liposome in improving the immune responses. It's remarkable that, with the same formulation of Lipo$^+$CPS12F&αGC, while the *s.c.* route (group 6) produced more effective serum, the *i.n.* administration (group 5) tended to produce more effective saliva. However, the difference in saliva tests was not statistically significant.

The result verified the anti-*S. pneumoniae* efficiency of the serum and saliva collected from mice

immunized with Lipo$^+$CPS12F&αGC. The *i.n.* route was more promising, as it mainly stimulated the respiratory mucosal immune system, which was proximal to the infection and disease site.

3.8 PROTECTION EFFICACY EVALUATION *IN VIVO*

We finally performed the bacteria challenge study (protocols: subsection 3.1.8) to evaluate the protective potential of Lipo⁺CPS12F&αGC.
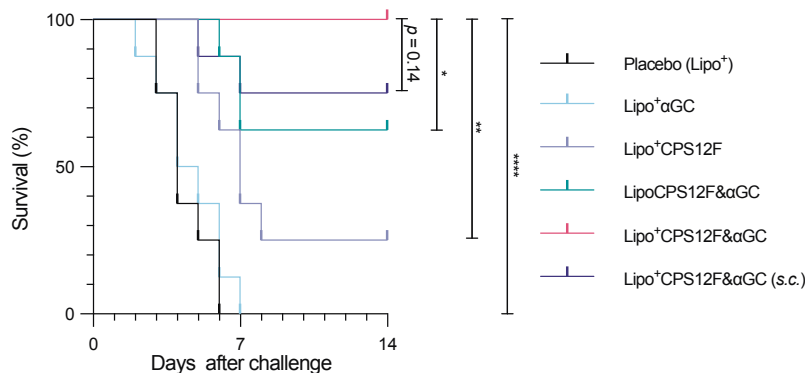

Figure 3.18: Lipo⁺CPS12F&αGC vaccination protects mice from *S. pneumonia* 12F challenge. Survival curves of vaccinated mice after bacteria challenge. BALB/cJRj mice were immunized with Lipo⁺ (group 1, blank cationic liposomes as placebo), Lipo⁺αGC (group 2), or 3 nmol antigen (repeat units of the polysaccharides) in Lipo⁺CPS12F (group 3), LipoCPS12F&αGC (group 4), or Lipo⁺CPS12F&αGC (group 5 & 6) via intranasal instillation (*i.n.*, group 1 – 5) or subcutaneous injection (*s.c.*, group 6) for 3 times at 2 weeks intervals. Three weeks after the final vaccination, mice were challenged with 1×10^6 CFU *S. pneumoniae* 12F via intranasal instillation and carefully monitored for the next 14 days. Results were plotted as survival curves. Gehan-Breslow-Wilcoxon tests were done to assess statistical differences. *, **, ***, **** represent P<0.1, P<0.01, P<0.001, P<0.0001.

In Figure 3.18, it is notable that mice intranasally vaccinated with Lipo⁺CPS12F&αGC (group 5) all survived the 2 weeks after infection; on the contrary, mice vaccinated with blank cationic liposome (group 1) or cationic liposomal αGC (group 2) were all sacrificed within the first week. It demonstrated the significant (P<0.0001) protection rendered by Lipo⁺CPS12F&αGC when applied intranasally. Meanwhile, only 2 of 8 (25 %) mice survived after receiving the formulation without αGC (group 3), and 5 of 8 (62.5 %) mice survived after receiving the neutral surface charge formulation (group 4), validating the important roles of the iNKT agonist αGC and nasal mucosa attachment facilitating positive surface charge.

Notably, 6 of 8 (75 %) mice survived after receiving the whole formulation via *s.c.* injection (group 6); compared with group 5, although the difference was not statistically significant, the P value of 0.14 indicated the route of vaccination played a role in the final protection strength. *S. pneumoniae* 12F mainly colonizes and causes disease in the respiratory system. Applying the vaccines intranasally can activate the NALT and iBALT, which is proximal to the infection site and more robust than the remote immune responses elicited by systemic *s.c.* vaccination.

These results confirmed that Lipo$^+$CPS12F&αGC, when immunized intranasally, can efficiently protect mice from *S. pneumoniae* 12F challenge.

取法於上，僅得為中；

取法於中，故為其下。

《李世民·帝範》

4

Conclusion

The effort to develop pneumococcal vaccines has continued for over 100 years, which weakened after the introduction of penicillin in the 1940s, but resurged as the problem of antibiotic resistance increased. Capsular polysaccharide is the most virulent component of *S. pneumoniae*; hence it is the most direct and promising target for vaccine development. However, developing carbohydrate-based vaccines is challenging as carbohydrate antigens cannot be presented by classical MHC molecules and were proven to have weak immunogenicity.

To break this limitation, we utilized the iNKT agonist αGC and co-deliver it with the capsular polysaccharide antigen in cationic liposomes. Compared with the carrier protein conjugation strategy, which activates normal T cells, the designed vaccine in this study targeting iNKTs holds several advantages. First, the iNKT-mediated adaptive immune responses are universal among individuals. The classical polymorphic MHC (human leukocyte antigen, HLA in humans) has many alleles, and their frequency distributions vary significantly among different populations[100]. In contrast, the ligand of TCRs on iNKTs, the CD1d (CD1a–e in humans) molecule, is highly structurally conserved, which helps bring a more predictable and consistent immunization efficacy[41]. Second, iNKTs respond faster after stimulation. Upon activation, iNKTs immediately proliferate and differentiate into functional phenotypes within hours, while it takes days for conventional T cells[39]. Moreover, iNKT$_{FH}$ helped the germinal centers' formation by day 3, which generally takes 10 days for conventional T$_{FH}$ cells[38]. Third, the vaccine cost is relatively low, making it more accessible to at-risk populations in low-income areas. The capsular polysaccharide is extracted from the bacteria culture instead of being produced by chemical synthesis. The liposome is fabricated by simple extrusion. The whole formulation can be stored safely at room temperature for at least 3 weeks; as a result, the cold chain can be avoided during transportation.

In conclusion, Lipo$^+$CPS12F&αGC, when immunized intranasally, initiated iNKT-helped B cells maturation and elicited the production of antigen-specific high-affinity isotype-switched antibodies both in mucosal and systemic immune systems, which were confirmed to be capable of clearing *S. pneumoniae in vitro* and protecting mice from pathogen challenge *in vivo*. We believe our vaccine approach is promising to be expanded to more pneumococcal serotypes and other respiratory pathogens.

This study still has several limitations that we can address in the future before progressing to clinical evaluation. Firstly, capsular polysaccharides of more serotypes can be loaded in the liposomes, and a wider range of cationic lipids can be tried. GMP compliance and cost control can be taken

into consideration during the vaccine fabrication. Secondly, the vaccine *in vitro* study can be more comprehensive and include the components degradation monitoring, the morphology characterization, and the stability under various temperature conditions. Thirdly, to better analyze the iBALT immune responses, bronchoalveolar lavage fluids (BALF) can be tested, and lung samples from different time points after vaccination can be immunohistochemistry assessed. Lastly, a hybridoma can be established for a more detailed evaluation of the antibody.

A

Other Unpublished Works

During my Ph.D. study, I also contributed to the below research, which had not been published by the time I finished this thesis.

1. Chemical Synthesis and Immunological Evaluation of Cancer Vaccines Based on Ganglioside Antigens and α-Galactosylceramide: preparation, characterization, and quantification of liposomal vaccines; mice vaccination, cytokine quantification, cell phenotyping, iNKTs and BMDCs harvest, and data analysis.

2. Synthesis of a SulfoCy7/5 – αGalCer Probe as a Chemical Tool for Investigating the Uptake of Liposomal αGalCer Conjugates by Antigen Presenting Cells: preparation, characterization, and quantification of liposomes; uptake evaluation by flow cytometry.

References

[1] Agence de presse Meurisse, Portrait du prince valdemar de danemark.
URL https://gallica.bnf.fr/ark:/12148/btv1b9045537q

[2] Georgia Cooper, Carolyn Rosenstein, Annabel Walter, Lenore Peizer, The further separation of types among the pneumococci hitherto included in group IV and the development of therapeutic antisera for these types 55 (4) 531–554. doi:10.1084/jem.55.4.531.

[3] B. Vammen, Serological variants of pneumococcus types 9 and 10 37 (4) 359–365. doi:10.4049/jimmunol.37.4.359.

[4] Public Health Image Library, #2113.
URL https://phil.cdc.gov/details.aspx?pid=2113

[5] Sven Hammerschmidt, Manfred Rohde, Electron microscopy to study the fine structure of the pneumococcal cell, in: Federico Iovino (Ed.), *Streptococcus pneumoniae*: Methods and Protocols, Methods in Molecular Biology, Springer, pp. 13–33. doi:10.1007/978-1-4939-9199-0_2.

[6] Centers for Disease Control and Prevention, Resources related to identifying streptococcus pneumoniae and its serotypes or serogroups.
URL https://www.cdc.gov/streplab/pneumococcus/resources.html

[7] Global Pneumococcal Sequencing Project, Serotype.
URL https://www.pneumogen.net/gps/serotypes.html

[8] SSI Diagnostica, *Streptococcus pneumoniae*: Textbook in diagnosis, serotyping, virulence factors and enzyme-linked immunosorbent assay (ELISA) for measuring pneumococcal antibodies.
URL https://ssidiagnostica.com/wp-content/uploads/2021/03/BROCHURE-Streptococcus-pneumoniae-book-89567-5.pdf

[9] K. Aaron Geno, Gwendolyn L. Gilbert, Joon Young Song, Ian C. Skovsted, Keith P. Klugman, Christopher Jones, Helle B. Konradsen, Moon H. Nahm, Pneumococcal capsules and their types: Past, present, and future 28 (3) 871–899. doi:10.1128/CMR.00024-15.

[10] David H. Dockrell, Moira K. B. Whyte, Timothy J. Mitchell, Pneumococcal pneumonia: Mechanisms of infection and resolution 142 (2) 482–491. doi:10.1378/chest.12-0210.

[11] Ryan Gierke, Patricia Wodi, Miwako Kobayashi, Chapter 17: Pneumococcal disease, in: Centers for Disease Control and Prevention - Epidemiology and Prevention of Vaccine-Preventable Diseases, 14th Edition, pp. 255–274.
URL https://www.cdc.gov/vaccines/pubs/pinkbook/downloads/pneumo.pdf

[12] European Centre for Disease Prevention and Control, Factsheet about pneumococcal disease.
URL https://www.ecdc.europa.eu/en/pneumococcal-disease/facts

[13] Our World in Data, What are children dying from and what can we do about it?
URL https://ourworldindata.org/what-are-children-dying-from-and-what-can-we-do-about-it

[14] World Health Organization, Pneumococcal disease.
URL https://www.who.int/teams/health-product-policy-and-standards/standards-and-specifications/vaccine-standardization/pneumococcal-disease

[15] Our World in Data, Death rate from pneumonia for children vs. GDP per capita, 2019.
URL https://ourworldindata.org/grapher/death-rates-from-pneumonia-and-other-lower-respiratory-infections-vs-gdp-per-capita

[16] Catia Cillóniz, Carolina Garcia-Vidal, Adrian Ceccato, Antoni Torres, Antimicrobial resistance among *Streptococcus pneumoniae*, in: I. W. Fong, David Shlaes, Karl Drlica (Eds.), Antimicrobial Resistance in the 21st Century, Emerging Infectious Diseases of the 21st Century, Springer International Publishing, pp. 13–38. doi:10.1007/978-3-319-78538-7_2.

[17] R. Austrian, Prevention of pneumococcal infection by immunization with capsular polysaccharides of *Streptococcus pneumoniae*: Current status of polyvalent vaccines 136 Suppl S38–42. doi:10.1093/infdis/136.supplement.s38.

[18] Shannon L. Haughney, Latrisha K. Petersen, Amy D. Schoofs, Amanda E. Ramer-Tait, Janice D. King, David E. Briles, Michael J. Wannemuehler, Balaji Narasimhan, Retention of structure, antigenicity, and biological function of pneumococcal surface protein A (PspA) released from polyanhydride nanoparticles 9 (9) 8262–8271. doi:10.1016/j.actbio.2013.06.006.

[19] Marco Tamborrini, Nina Geib, Aniebrys Marrero-Nodarse, Maja Jud, Julia Hauser, Celestine Aho, Araceli Lamelas, Armando Zuniga, Gerd Pluschke, Arin Ghasparian, John A. Robinson, A synthetic virus-like particle streptococcal vaccine candidate using B-cell epitopes from the proline-rich region of pneumococcal surface protein A 3 (4) 850–874. doi:10.3390/vaccines3040850.

[20] Y. Fukuyama, Y. Yuki, Y. Katakai, N. Harada, H. Takahashi, S. Takeda, M. Mejima, S. Joo, S. Kurokawa, S. Sawada, H. Shibata, E. J. Park, K. Fujihashi, D. E. Briles, Y. Yasutomi, H. Tsukada, K. Akiyoshi, H. Kiyono, Nanogel-based pneumococcal surface protein A nasal vaccine induces microRNA-associated Th17 cell responses with neutralizing antibodies against *Streptococcus pneumoniae* in macaques 8 (5) 1144–1153. doi:10.1038/mi.2015.5.

[21] Danielle A. Wagner-Muñiz, Shannon L. Haughney, Sean M. Kelly, Michael J. Wannemuehler, Balaji Narasimhan, Room temperature stable PspA-based nanovaccine induces protective immunity 9 325. doi:10.3389/fimmu.2018.00325.

[22] Yoon-Chul Kye, Sung-Moo Park, Byoung-Shik Shim, Jannatul Firdous, Girak Kim, Han Wool Kim, Young-Jun Ju, Cheol Gyun Kim, Chong-Su Cho, Dong Wook Kim, Jae Ho Cho, Man Ki Song, Seung Hyun Han, Cheol-Heui Yun, Intranasal immunization with pneumococcal surface protein A in the presence of nanoparticle forming polysorbitol transporter adjuvant induces protective immunity against the *Streptococcus pneumonia* infection 90 362–372. doi:10.1016/j.actbio.2019.03.049.

[23] Elnaz Afshari, Reza Ahangari Cohan, Fattah Sotoodehnejadnematalahi, Seyed Fazlollah Mousavi, In-silico design and evaluation of an epitope-based serotype-independent promising vaccine candidate for highly cross-reactive regions of pneumococcal surface protein A 21 (1) 13. doi:10.1186/s12967-022-03864-z.

[24] Merck, Pneumovax®23 - highlights of prescribing information.
URL https://www.merck.com/product/usa/pi_circulars/p/pneumovax_23/pneumovax_pi.pdf

[25] Merck, Effectiveness data for Pneumovax®23 (pneumococcal vaccine polyvalent).
URL https://www.merckvaccines.com/pneumovax23/pneumococcal-vaccine-efficacy

[26] Rena D. Astronomo, Dennis R. Burton, Carbohydrate vaccines: Developing sweet solutions to sticky situations? 9 (4) 308–324. doi:10.1038/nrd3012.

[27] Pfizer, Pneumococcal 7-valent conjugate vaccine (diphtheria CRM197 protein) prevnar® FOR PEDIATRIC USE ONLY.
URL https://labeling.pfizer.com/showlabeling.aspx?id=134

[28] Pfizer, Prevnar®13 - highlights of prescribing information.
URL https://labeling.pfizer.com/ShowLabeling.aspx?id=501

[29] Pfizer, Prevnar®20 - highlights of prescribing information.
URL https://labeling.pfizer.com/ShowLabeling.aspx?id=15428

[30] Merck, Vaxneuvance™ - highlights of prescribing information.
URL https://www.merck.com/product/usa/pi_circulars/v/vaxneuvance/vaxneuvance_pi.pdf

[31] Madhu Emmadi, Naeem Khan, Lennart Lykke, Katrin Reppe, Sharavathi G. Parameswarappa, Marilda P. Lisboa, Sandra-Maria Wienhold, Martin Witzenrath, Claney L. Pereira, Peter H. Seeberger, A *streptococcus pneumoniae* type 2 oligosaccharide glycoconjugate elicits opsonic antibodies and is protective in an animal model of invasive pneumococcal disease 139 (41) 14783–14791. doi:10.1021/jacs.7b07836.

[32] Benjamin Schumann, Heung Sik Hahm, Sharavathi G. Parameswarappa, Katrin Reppe, Annette Wahlbrink, Subramanian Govindan, Paulina Kaplonek, Liise-anne Pirofski, Martin Witzenrath, Chakkumkal Anish, Claney L. Pereira, Peter H. Seeberger, A semisynthetic *Streptococcus pneumoniae* serotype 8 glycoconjugate vaccine 9 (380) eaaf5347. doi:10.1126/scitranslmed.aaf5347.

[33] Benjamin Schumann, Katrin Reppe, Paulina Kaplonek, Annette Wahlbrink, Chakkumkal Anish, Martin Witzenrath, Claney L. Pereira, Peter H. Seeberger, Development of an efficacious, semisynthetic glycoconjugate vaccine candidate against *Streptococcus pneumoniae* serotype 1 4 (3) 357–361. doi:10.1021/acscentsci.7b00504.

[34] Andrew B. Hill, Marie Beitelshees, Roozbeh Nayerhoda, Blaine A. Pfeifer, Charles H. Jones, Engineering a next-generation glycoconjugate-like *Streptococcus pneumoniae* vaccine 4 (11) 1553–1563. doi:10.1021/acsinfecdis.8b00100.

[35] Maruthi Prasanna, Daphnée Soulard, Emilie Camberlein, Nicolas Ruffier, Annie Lambert, François Trottein, Noemi Csaba, Cyrille Grandjean, Semisynthetic glycoconjugate based on dual role protein/PsaA as a pneumococcal vaccine 129 31–41. doi:10.1016/j.ejps.2018.12.013.

[36] Paulina Kaplonek, Ling Yao, Katrin Reppe, Franziska Voß, Thomas Kohler, Friederike Ebner, Alexander Schäfer, Ulrike Blohm, Patricia Priegue, Maria Bräutigam, Claney L. Pereira, Sharavathi G. Parameswarappa, Madhu Emmadi, Petra Ménová, Martin Witzenrath, Sven Hammerschmidt, Susanne Hartmann, Leif E. Sander, Peter H. Seeberger, A semisynthetic glycoconjugate provides expanded cross-serotype protection against *Streptococcus pneumoniae* 40 (7) 1038–1046. doi:10.1016/j.vaccine.2021.12.068.

[37] Pfizer, CAPiTA: Community-acquired pneumonia immunization trial in adults.
URL https://prevnar20adult.pfizerpro.com/clinical-studies/capita

[38] Catherine M. Crosby, Mitchell Kronenberg, Tissue-specific functions of invariant natural killer T cells 18 (9) 559–574. doi:10.1038/s41577-018-0034-2.

[39] L. Mori, M. Lepore, G. De Libero, The immunology of CD1- and MR1-restricted T cells 34 479–510. doi:10.1146/annurev-immunol-032414-112008.

[40] J. L. Matsuda, T. Mallevaey, J. Scott-Browne, L. Gapin, CD1d-restricted iNKT cells, the 'swiss-army knife' of the immune system 20 (3) 358–368. doi:10.1016/j.coi.2008.03.018.

[41] L. Brossay, M. Chioda, N. Burdin, Y. Koezuka, G. Casorati, P. Dellabona, M. Kronenberg, CD1d-mediated recognition of an α-galactosylceramide by natural killer T cells is highly conserved through mammalian evolution 188 (8) 1521–1528. doi:10.1084/jem.188.8.1521.

[42] L. Bai, S. Deng, R. Reboulet, R. Mathew, L. Teyton, P. B. Savage, A. Bendelac, Natural killer T (NKT) – B-cell interactions promote prolonged antibody responses and long-term memory to pneumococcal capsular polysaccharides 110 (40) 16097–16102. doi:10.1073/pnas.1303218110.

[43] S. Deng, L. Bai, R. Reboulet, R. Matthew, D. A. Engler, L. Teyton, A. Bendelac, P. B. Savage, A peptide-free, liposome-based oligosaccharide vaccine, adjuvanted with a natural killer T cell antigen, generates robust antibody responses *in vivo* 5 (4) 1437–1441. doi:10.1039/C3SC53471E.

[44] M. Cavallari, P. Stallforth, A. Kalinichenko, D. C. K. Rathwell, T. M. A. Gronewold, A. Adibekian, L. Mori, R. Landmann, P. H. Seeberger, G. De Libero, A semisynthetic carbohydrate-lipid vaccine that protects against *S. pneumoniae* in mice 10 (11) 950–956. doi:10.1038/nchembio.1650.

[45] T. Shute, E. Amiel, N. Alam, J. L. Yates, K. Mohrs, E. Dudley, B. Salas, C. Mesa, A. Serrata, D. Angel, B. K. Vincent, A. Weyers, P. A. Lanthier, E. Vomhof-Dekrey, R. Fromme, M. Laughlin, O. Durham, J. Miao, D. Shipp, R. J. Linhardt, K. Nash, E. A. Leadbetter, Glycolipid-containing nanoparticle vaccine engages invariant NKT cells to enhance humoral protection against systemic bacterial infection but abrogates T-independent vaccine responses 206 (8) 1806–1816. doi:10.4049/jimmunol.2001283.

[46] P. H. Seeberger, Discovery of semi- and fully-synthetic carbohydrate vaccines against bacterial infections using a medicinal chemistry approach 121 (7) 3598–3626. doi:10.1021/acs.chemrev.0c01210.

[47] Chung Truong Nguyen, Soo Young Kim, Myoung Suk Kim, Shee Eun Lee, Joon Haeng Rhee, Intranasal immunization with recombinant PspA fused with a flagellin enhances cross-protective immunity against *Streptococcus pneumoniae* infection in mice 29 (34) 5731–5739. doi:10.1016/j.vaccine.2011.05.095.

[48] Zhu Qing Yuan, Zhi Yue Lv, Hui Quan Gan, Mo Xian, Kou Xing Zhang, Jing Ying Mai, Xin Bing Yu, Zhong Dao Wu, Intranasal immunization with autolysin (LytA) in mice model induced protection against five prevalent *Streptococcus pneumoniae* serotypes in China 51 (1) 108–115. doi:10.1007/s12026-011-8234-x.

[49] Danielle Salha, Jason Szeto, Lisa Myers, Carol Claus, Anthony Sheung, Mei Tang, Belma Ljutic, David Hanwell, Karen Ogilvie, Marin Ming, Benjamin Messham, Germie van den Dobbelsteen, Robert Hopfer, Martina M. Ochs, Scott Gallichan, Neutralizing antibodies elicited by a novel detoxified pneumolysin derivative, PlyD1,

provide protection against both pneumococcal infection and lung injury 80 (6) 2212–2220. doi:10.1128/iai.06348-11.

[50] Hidehiko Suzuki, Akihiro Watari, Eri Hashimoto, Miki Yonemitsu, Hiroshi Kiyono, Kiyohito Yagi, Masuo Kondoh, Jun Kunisawa, C-terminal clostridium perfringens enterotoxin-mediated antigen delivery for nasal pneumococcal vaccine 10 (5) e0126352. doi:10.1371/journal.pone.0126352.

[51] J.-H. Xu, W.-J. Dai, B. Chen, X.-Y. Fan, Mucosal immunization with PsaA protein, using chitosan as a delivery system, increases protection against acute otitis media and invasive infection by *Streptococcus pneumoniae* 81 (3) 177–185. doi:10.1111/sji.12267.

[52] Rui Tada, Hidehiko Suzuki, Saeko Takahashi, Yoichi Negishi, Hiroshi Kiyono, Jun Kunisawa, Yukihiko Aramaki, Nasal vaccination with pneumococcal surface protein A in combination with cationic liposomes consisting of dotap and dc-chol confers antigen-mediated protective immunity against *Streptococcus pneumoniae* infections in mice 61 385–393. doi:10.1016/j.intimp.2018.06.027.

[53] Tasson C. Rodrigues, Maria Leonor S. Oliveira, Alessandra Soares-Schanoski, Stefanni L. Chavez-Rico, Douglas B. Figueiredo, Viviane M. Gonçalves, Daniela M. Ferreira, Nitesh K. Kunda, Imran Y. Saleem, Eliane N. Miyaji, Mucosal immunization with PspA (pneumococcal surface protein A)-adsorbed nanoparticles targeting the lungs for protection against pneumococcal infection 13 (1) e0191692. doi:10.1371/journal.pone.0191692.

[54] Sudhanshu Shekhar, Rabia Khan, Karl Schenck, Fernanda Cristina Petersen, Intranasal immunization with the commensal *Streptococcus mitis* confers protective immunity against pneumococcal lung infection 85 (6) e02235–18. doi:10.1128/AEM.02235-18.

[55] William Walkowski, Justin Bassett, Manmeet Bhalla, Blaine A. Pfeifer, Elsa N. Bou Ghanem, Intranasal vaccine delivery technology for respiratory tract disease application with a special emphasis on pneumococcal disease 9 (6) 589. doi:10.3390/vaccines9060589.

[56] T. Ikuse, R. Habuka, Y. Wakamatsu, T. Nakajima, N. Saitoh, H. Yoshida, B. Chang, M. Morita, M. Ohnishi, K. Oishi, A. Saitoh, Local outbreak of *Streptococcus pneumoniae* serotype 12F caused high morbidity and mortality among children and adults 146 (14) 1793–1796. doi:10.1017/S0950268818002133.

[57] A. Rokney, S. Ben-Shimol, Z. Korenman, N. Porat, Z. Gorodnitzky, N. Givon-Lavi, M. Ron, V. Agmon, R. Dagan, L. Valinsky, Emergence of *Streptococcus pneumoniae* serotype 12F after sequential introduction of 7- and 13-valent vaccines, Israel 24 (3) 453–461. doi:10.3201/eid2403.170769.

[58] S. Gregory, C. Whitney, An increase in *Streptococcus pneumoniae* serotype 12F.
URL https://www2c.cdc.gov/podcasts/media/pdf/EID_3-18_StreptococcusPneumoniae.pdf

[59] D. W. Cleary, J. Jones, R. A. Gladstone, K. L. Osman, V. T. Devine, J. M. Jefferies, S. D. Bentley, S. N. Faust, S. C. Clarke, Changes in serotype prevalence of *Streptococcus pneumoniae* in Southampton, UK between 2006 and 2018 12 (1) 13332. doi:10.1038/s41598-022-17600-6.

[60] Ulf Nobbmann, Refractive index increment dn/dc values - materials talks.
URL https://www.materials-talks.com/refractive-index-increment-dndc-values/

[61] Avanti Polar Lipids, Liposome preparation.
URL https://www.sigmaaldrich.com/DK/en/technical-documents/protocol/cell-culture-and-cell-culture-analysis/transfection-and-gene-editing/liposome-preparation

[62] Avanti Polar Lipids, Mini-extruder extrusion technique.
URL https://avantilipids.com/divisions/equipment-products/mini-extruder-extrusion-technique

[63] Ajeet Kumar, Chandra Kumar Dixit, 3 - methods for characterization of nanoparticles, in: Surendra Nimesh, Ramesh Chandra, Nidhi Gupta (Eds.), Advances in Nanomedicine for the Delivery of Therapeutic Nucleic Acids, Woodhead Publishing, pp. 43–58. doi:10.1016/B978-0-08-100557-6.00003-1.

[64] Avanti Polar Lipids, Phase transition temperatures for glycerophospholipids.
URL https://avantilipids.com/tech-support/physical-properties/phase-transition-temps

[65] Anne E. Regelin, Stefan Fankhaenel, Laura Gürtesch, Claudia Prinz, Günter von Kiedrowski, Ulrich Massing, Biophysical and lipofection studies of DOTAP analogs 1464 (1) 151–164. doi:10.1016/S0005-2736(00)00126-7.

[66] Avanti Polar Lipids, Mini-extruder assembly instructions.

URL https://avantilipids.com/divisions/equipment-products/mini-extruder-assembly-instructions

[67] Paul P. Van Veldhoven, Guy P. Mannaerts, Inorganic and organic phosphate measurements in the nanomolar range 161 (1) 45–48. doi:10.1016/0003-2697(87)90649-X.

[68] Sigma-Aldrich, Malachite green phosphate assay kit_technical bulletin.

URL https://www.sigmaaldrich.com/deepweb/assets/sigmaaldrich/product/documents/171/212/mak307bul.pdf

[69] Sigma-Aldrich, Cholesterol quantification assay kit_technical bulletin.

URL https://www.sigmaaldrich.com/deepweb/assets/sigmaaldrich/product/documents/175/601/cs0005bul-mk.pdf

[70] M. Viel, F. Collet, C. Lanos, Chemical and multi-physical characterization of agroresources' by-product as a possible raw building material 120 214–237. doi:10.1016/j.indcrop.2018.04.025.

[71] Michel. DuBois, K. A. Gilles, J. K. Hamilton, P. A. Rebers, Fred. Smith, Colorimetric method for determination of sugars and related substances 28 (3) 350–356. doi:10.1021/ac60111a017.

[72] Wyatt, FFF separation.

URL https://www.wyatt.com/solutions/techniques/fff-mals-separation.html

[73] Wyatt, MALS.

URL https://www.wyatt.com/library/theory/multi-angle-light-scattering-theory.html

[74] Pfizer, Pfizer-Biontech COVID-19 vaccine: Highlights of emergency use authorization.

URL https://labeling.pfizer.com/ShowLabeling.aspx?id=19542

[75] UCSF IACUC, IACUC standard procedure: Intranasal instillation in rodents.

URL https://iacuc.ucsf.edu/sites/g/files/tkssra751/f/wysiwyg/STDPROCEDURE-MiscRodentProcedures-IntranasalInstillationinRodents.pdf

[76] M. A. Miller, J. M. Stabenow, J. Parvathareddy, A. J. Wodowski, T. P. Fabrizio, X. R. Bina, L. Zalduondo, J. E. Bina, Visualization of murine intranasal dosing efficiency using luminescent *Francisella tularensis*: Effect of instillation volume and form of anesthesia 7 (2) e31359. doi:10.1371/journal.pone.0031359.

[77] K. Zubeidat, Y. Saba, O. Barel, F. L. Shoukair, A.-H. Hovav, Protocol for parotidectomy and saliva analysis in mice 3 (1) 101048. doi:10.1016/j.xpro.2021.101048.

[78] Alicja Puchta, Chris P. Verschoor, Tanja Thurn, Dawn M. E. Bowdish, Characterization of inflammatory responses during intranasal colonization with *Streptococcus pneumoniae* (83) e50490. doi:10.3791/50490.

[79] National Centre for the Replacement Refinement & Reduction of Animals in Research, Blood sampling: Mouse.
URL https://nc3rs.org.uk/3rs-resources/blood-sampling/blood-sampling-mouse

[80] Danish Animal Experiments Inspectorate, Guidelines for taking blood samples from mice and rats.
URL https://www.foedevarestyrelsen.dk/SiteCollectionDocuments/Dyrevelfaerdogveterinaermedicin/Dyrevelfærd/Forsøgsdyr/Dyreforsøgstilsynet/Guidelines-engelsk/Guidelinesfortakingbloodsamplesfrommiceandrats.pdf

[81] SARSTEDT, Centrifugation conditions.
URL https://www.sarstedt.com/fileadmin/user_upload/99_Broschueren/NEU/725/15_725_0000_142_Zentrifugationsbed_DE_EN_0219.pdf

[82] BD Biosciences, BD cytometric bead array (CBA) mouse enhanced sensitivity master buffer kit instruction manual.

[83] BD Biosciences, BD LSRFortessa cell analyzer user's guide.
URL https://www.bdbiosciences.com/content/dam/bdb/marketing-documents/BD_LSRFortessa_cell_analyzer_user_guide.pdf

[84] L. Van Kaer, V. V. Parekh, L. Wu, The response of CD1d-restricted invariant NKT cells to microbial pathogens and their products 6. doi:10.3389/fimmu.2015.00226.

[85] K. T. Mincham, J. D. Young, D. H. Strickland, OMIP 076: High-dimensional immunophenotyping of murine T-cell, B-cell, and antibody secreting cell subsets 99 (9) 888–892. doi:10.1002/cyto.a.24474.

[86] Thermo Fisher Scientific Inc., Mouse spleen cell isolation protocol.
URL https://www.thermofisher.com/uk/en/home/life-science/cell-analysis/
cell-analysis-learning-center/immunology-at-work/immunology-protocols/
mouse-spleen-cell-isolation-protocol.html

[87] Anni Skovbo, FACS core facility guidelines: Titration of antibody concentration in
flow cytometry.
URL https://facs.au.dk/fileadmin/ingen_mappe_valgt/Titration.pdf

[88] Thermo Fisher Scientific Inc., TECH TIP #65 - ELISA technical guide and proto-
cols.
URL http://tools.thermofisher.com/content/sfs/brochures/
TR0065-ELISA-guide.pdf

[89] P. Martineau, Affinity measurements by competition ELISA, in: R. Kontermann,
S. Dübel (Eds.), Antibody Engineering, Springer Protocols Handbooks, Springer,
pp. 657–665. doi:10.1007/978-3-642-01144-3_41.

[90] Moon H. Nahm, Robert L. Burton, Protocol for multiplexed opsonophagocytic
killing assay (UAB-MOPA) for antibodies against *Streptococcus pneumoniae*.
URL https://www.vaccine.uab.edu/uab-mopa.pdf

[91] Jeeseong C. Hwang, NIST's integrated colony enumerator.
URL https://doi.org/10.18434/M32073

[92] BD Biosciences, BD cytometric bead array solution.
URL https://www.bdbiosciences.com/en-dk/products/reagents/
immunoassays/cba

[93] A. M. Collins, IgG subclass co-expression brings harmony to the quartet model of
murine IgG function 94 (10) 949–954. doi:10.1038/icb.2016.65.

[94] FluoroFinder, Fluorofinder experiment design platform.
URL https://fluorofinder.com/

[95] Morten Løbner, Unleash the full potential of 5 laser flow cytometry - let's venture
beyond the visible spectrum of light.
URL https://1drv.ms/b/s!AjWJXaSTFnzujPQv3WzJ-y1wjU5kjQ

[96] Corine H. GeurtsvanKessel, Monique A.M. Willart, Ingrid M. Bergen, Leonie S. van Rijt, Femke Muskens, Dirk Elewaut, Albert D.M.E. Osterhaus, Rudi Hendriks, Guus F. Rimmelzwaan, Bart N. Lambrecht, Dendritic cells are crucial for maintenance of tertiary lymphoid structures in the lung of influenza virus-infected mice 206 (11) 2339–2349. doi:10.1084/jem.20090410.

[97] Kenneth Murphy, Casey Weaver, Janeway's Immunobiology, 9th Edition, Garland Science.

[98] Y. Kurono, The mucosal immune system of the upper respiratory tract and recent progress in mucosal vaccines 49 (1) 1–10. doi:10.1016/j.anl.2021.07.003.

[99] R. Stewart, S. A. Hammond, M. Oberst, R. W. Wilkinson, The role of Fc gamma receptors in the activity of immunomodulatory antibodies for cancer 2 (1) 29. doi:10.1186/s40425-014-0029-x.

[100] F. F. Gonzalez-Galarza, A. McCabe, E. J. Melo dos Santos, A. R. Jones, D. Middleton, A snapshot of human leukocyte antigen (HLA) diversity using data from the allele frequency net database 82 (7) 496–504. doi:10.1016/j.humimm.2020.10.004.